Does hepatic fibrosis accelerate orthotopic HCC tumor growth in a novel liver fibrosis model in the C3H/He mice?

Dissertation

zur

Erlangung des Doktorgrades (Dr. rer. nat.)

der

Mathematisch-Naturwissenschaftlichen Fakultät

der

Rheinische Friedrich-Wilhelms-Universität Bonn

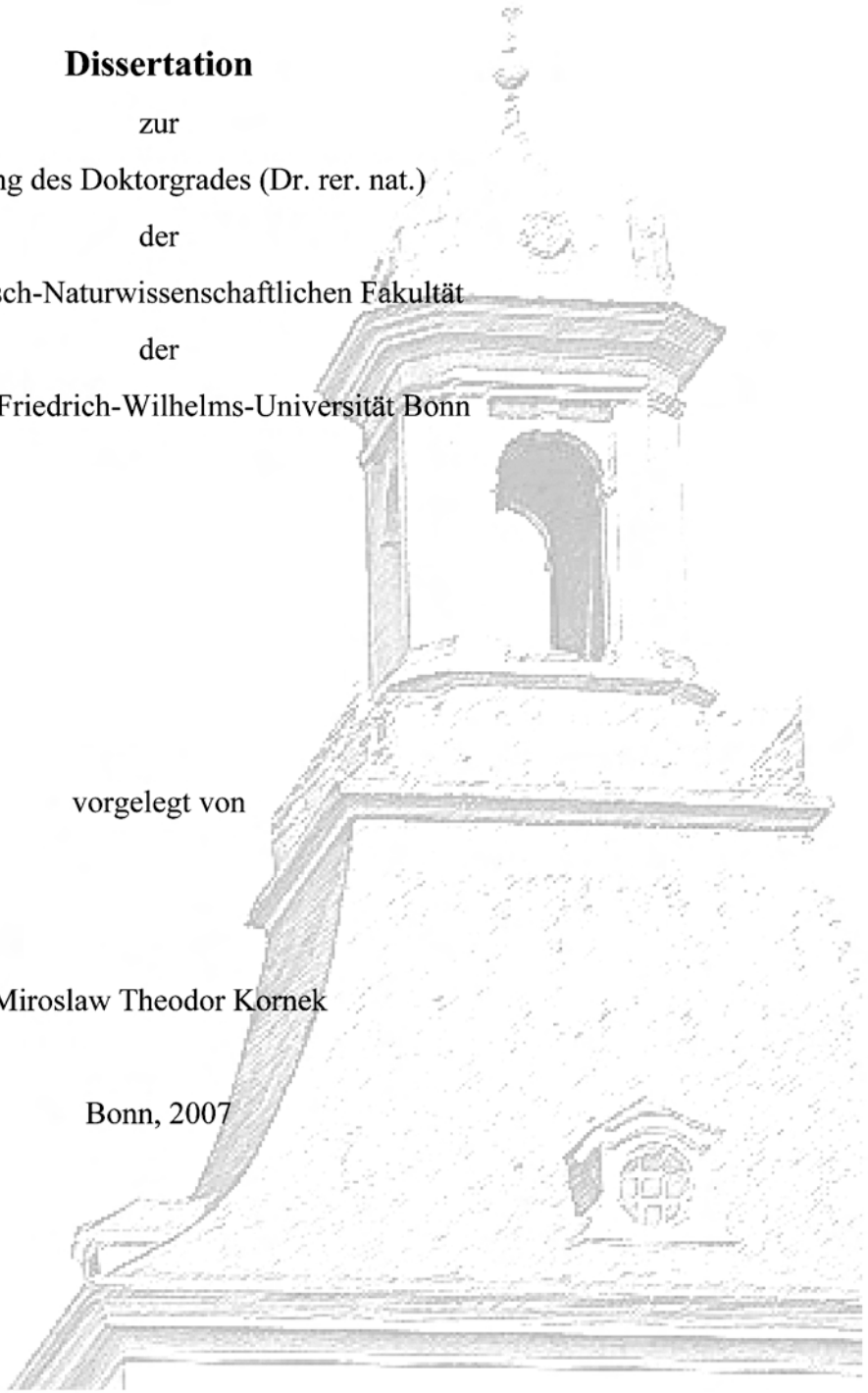

vorgelegt von

Miroslaw Theodor Kornek

Bonn, 2007

Angefertigt mit Genehmigung der Mathematisch-Naturwissenschaftlichen Fakultät
der Rheinischen Friedrich-Wilhelms-Universität Bonn.

1. Referent: PD Dr. med. V. Schmitz
2. Referent: Prof. Dr. V. Herzog

Tag der Promotion: 20.12.2007

Abgabejahr: 2007
Erscheinungsjahr: 2008

Does hepatic fibrosis accelerate orthotopic HCC tumor growth in a novel liver fibrosis model in the C3H/He mice?

Department of Internal Medicine I

University Hospital Bonn

For completion of the Doctorate degree in Natural Sciences at the

Rheinische Friedrich-Wilhelms University of Bonn

Miroslaw Theodor Kornek

Born on July 18th, 1975

in Oppeln, Poland

Bonn, August 2007

Declaration

I hereby declare that the submitted dissertation was completed exclusively by myself. I have not used any sources or materials other than those described.

Moreover I declare that the following dissertation has not been submitted elsewhere in this form or any other form, and has not been used to obtain any other equivalent qualifications at any other organization/institution.

Additionally, I have not applied for, nor will I attempt to apply for any other degree or qualification in relation to this work.

Bonn, August 2007

Miroslaw Theodor Kornek

Acknowledgements

First of all, I would like to thank to the most precious human being on earth, to my wife Veronika. She is the woman at my side who supported me, built me up and was always there for me; even she had enough to do with her own doctorial thesis and with the little daily problems of life.

I am especially grateful for my parents, who made in the past an important, risky step to settle over here, to let everything behind them and thereby giving me a better chance to reach everything which would have been limited under the communistic dictatorship.

I also would like to thank to PD Dr. med. Volker Schmitz, who gave me the chance to become a valuable member of the scientific community and provided me always with great supervision and inspiration to develop good scientific skills. Furthermore I would like to thank Prof. Dr. med. Christian Kurts (IMMEI) and Sabine Dentler for proof reading and correction my PhD thesis. Ecspecially I thank Prof. Dr.med. Cristian Kurts, for guiding my wife, Dr. med. Dr. rer. nat. Veronika Lukacs-Kornek trough her PhD time and final exam at the same time point.

For the assistances over and beyond the call of duty, I would like especially thank to Ursula (Uschi), Becker and Maren Klöckner.

I would also like to express my thanks to the other colleagues/students: Dr. rer. nat. Esther Raskopf, Dr. med. Maria Gonzalez-Carmona, Dierk Berger, Martin Hennenberg, Annabelle Vogt, Sebastian Stehl.

Table of contents

1 Introduction

1.1 Epidemiology of Hepatocellular Carcinoma (HCC)

On a global scale, intrahepatic cancers are the fifth most frequent cause of lethal cancer. Approximately, HCC accounts for more than ½ million deaths every year world wide and current data indicate that its incidence is steadily increasing in the Western-World (Parkin 2001). In Germany one percent of all cancer cases are identified as HCC and the incidenc is rising as proposed for the Western World. 1999 in Germany the incidence rate for men was approximately 4.7 cases per 100 thousand and for women 2.1 per 100 thousand, which indicating a ratio of 2.2:1 (Caselmann, Blum et al. 1999). World wide the ratio of male to female is currently 2.7:1 and in Western-Europe 3.6:1 (Llovet, Burroughs et al. 2003). These numbers suggest that women in general are less likely to be affected by HCC than men. Already in the nineties it was hypothezized that the fact that in general women might have a lower tendency to abuse alcohol and to smoke heavily could lead to this incidences (Lai, Gregory et al. 1987).

The outlook for HCC incidence does not expect any reduction, if the world population growth and ageing still increase progressivly in the cancer burden -15 million new cases and 10 million new deaths are expected in 2020, even if current rates remain unchanged suggested the founding members of the International Liver Cancer Assosiation (ILCA); Jordi Bruix, M.D. (President) and Josep M Llovet, M.D. (Executive Secretary) (Llovet, Burroughs et al. 2003).

1.2 Hepatocellular carcinogenesis factors

Hepatocarcinogenesis is supposed to be a slowly unfolding long term process which accumulates neoplastic phenotypes in one or more cells resulting in uncontrolled, autonomous growth and metastatic spread (Coleman 2003). This malignant transformation of hepatocytes is induced by chronic inflammation in the liver, characterized by a shortened half-life for these cells and as a response to the

ongoing inflammation a higher proliferation rate associated with regeneration (Guo, Zhou et al. 2000). In some cases, this leads to increased accumulation of mutations in the genome and to genomic instability and alterations. To date, the stage of no return for this cell process remains unknown (Liang and Heller 2004). For that reason, HCC is strongly associated with chronic liver diseases, including chronic hepatitis and cirrhosis (figure1). In fact, on a global scale, most cases of HCC, approximately 80%, occur in combination with cirrhosis world wide (Johnson 1997; Llovet, Burroughs et al. 2003). Only less than 10% are observed in non-cirrhotic livers and even without hepatitis. These observations derive from livers of patients without well established risk factors (Bluteau, Jeannot et al. 2002). Typically, chronic liver diseases are based on infections with hepatitis virus B (HBV) or C (HCV), as well as alcohol abuse and exposure to aflatoxin (Kountouras and Lygidakis 2000; Okuda 2000).

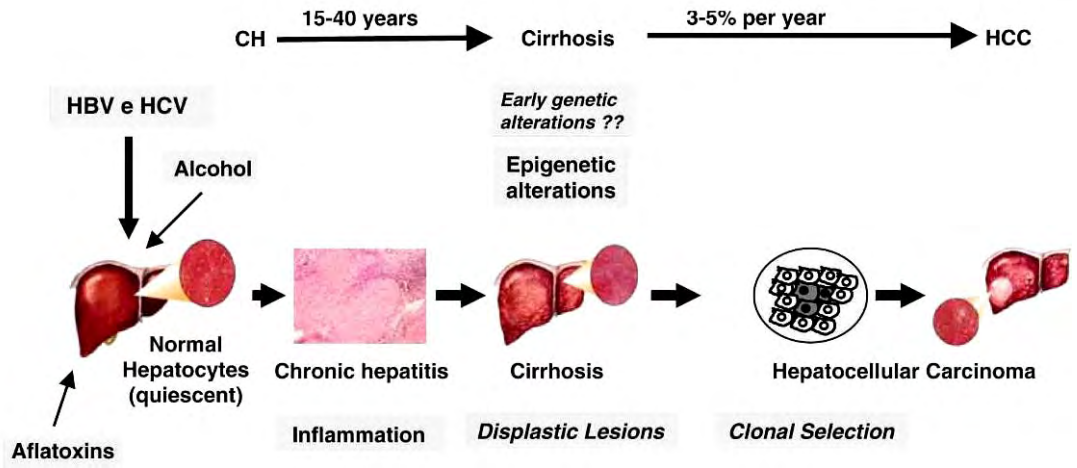

Figure 1 Pathogenesis of human hepatocellular carcinoma (HCC). Chronically, hepatitis B and C, associated with liver cirrhosis represent major risk factors for HCC development, being implicated in over 70% of HCC cases globally (original figure from Levrero M., Oncogene, 2006 (Levrero 2006) modified).

1.2.1 Chronic hepatitis

In general, chronic hepatitis is accurately defined as a long term ongoing liver inflammation which has been continuously present for a period of more then six months at least and which is characterized by inflammatory cell infiltration, death of

hepatocytes and enhanced proliferation of hepatocytes (Ishak 1994; Simpson, Lukacs et al. 1997). Known causes for the above described symptoms, apart from other factors, include an infection with members of the hepatitis virus family. The genome of the hepatic virus is mainly organized on single stranded RNA or, in case of the hepatitis B virus, as double stranded DNA. The main hepatitis virus families are represented by the hepatitis A virus, -B virus und -C virus. Also, two other hepatitis types have been isolated, namely hepatitis D virus and hepatitis E virus (table1).

Several studies have shown a correlation between hepatitis B virus infection and an increased incidence of HCC. In humans, an even stronger association between chronic hepatitis C viruses and HCC is known (Beasley and Hwang 1984; Brechot, Gozuacik et al. 2000; Inoue and Seitz 2001). An infection with these two hepatitis viruses lead to a 100 to 200-fold increased risk of malignant transformation of hepatocytes and finally to lethal HCC by setting up conditions predisposing to chronic hepatic inflammation.

Disease	Virus	Virus Family	Genomic-organization
Hepatitis A	Hepatitis A Virus	Picornavirus	single stranded RNA
Hepatitis B	Hepatitis B Virus	Hepadnavirus	double stranded DNA-RT
Hepatitis C	Hepatitis C Virus	Flavivirus	single stranded RNA
Hepatitis D	Hepatitis D Virus	Deltavirus	single stranded RNA
Hepatitis E	Hepatitis E Virus	Calicivirus	single stranded RNA

Table 1 Overview of genomic organization of various members of the hepatitis virus forms and their virus family classification (RT: reverse transcripted genome, data summarized from Dictionary by LaborLawTalk, www.dictionary.laborlawtalk.com/virus_classification).

1.2.1.1 Hepatitis B (HBV)

Serum HBV DNA levels have been identified as predictive factors for HCC, considerating the fact that serum HBV DNA levels have significantly declined by the time HCC develops. This is probably because, during HCC progression, hepatic tumor cells no longer allow viral DNA replication (Chen, Yang et al. 2006).

Furthermore, it has been statistically proven that an infection with hepatitis B virus in combination with cirrhosis induces HCC in up to 12% - 55% of HBV patients (Fattovich, Stroffolini et al. 2004). The hepatitis B virus results from the genomic organization in double stranded DNA, the only hepatic virus with the ability to randomly integrate into the host genome. Thus, HBV integration may occur in non-coding or encoding host sequences. It has been shown by others that this integration could happen at the genome locus encoding proteins for cell cycle, cell cycle regulation, proliferation and viability (Horikawa and Barrett 2001; Ferber, Montoya et al. 2003; Paterlini-Brechot, Saigo et al. 2003). Integration has been verified for patients with chronic HBV infection (Brechot, Gozuacik et al. 2000; Minami, Daimon et al. 2005). Several viral DNA rearrangements due to host integration can be detected during long term inflammation apart from chromosomal deletion at the site of integration (Wang, Lau et al. 2004; Hessein, Saad el et al. 2005). Also, indirect induction of HCC, another direct product induction by viral gene, such as the HBx protein has been described (Rabe and Caselmann 2000). Investigations of intratumoral integrated viral DNA sequences show a large proportion which encodes HBx besides others. HBx itself may act as pro- or antiapoptotic protein. Additionally, HBx may contribute to tumor angiogenesis in HCC through modulation of the angiogenesis pathway. Evidence for induced upregulation of vascular endothelial growth factor (VEGF) transcription or stabilization of hypoxia inducible factor HIF-1 by HBx have been described (Lee, Lee et al. 2000; Yoo, Oh et al. 2003; Yoo and Lee 2004).

1.2.1.2 Hepatitis C (HCV)

In 1999, the World Health Organization (WHO) estimated that about 170 million people were HCV positive world-wide. At that time, this represented approximately 3% of the world population (1999). Statistically, in Europe and the United States, hepatitis C virus (HCV) infection in combination with cirrhosis causes HCC in 27% - 73% of cases (Fattovich, Stroffolini et al. 2004). Since the discovery of HCV in 1989, the typical road map for chronic hepatitis C leads from mild hepatitis,

fibrosis and cirrhosis to HCC. Several studies describe the HCV virus as a single stranded RNA virus with a short half-life of only several days and with no proof-reading function of the viral RNA-dependent RNA polymerase. This suggest that the high rate of virus replication could lead to the genetic variability of HCV (Moradpour, Cerny et al. 2001). Six HCV genotypes have been isolated to date: genotypes 1-3 with global distribution, genotypes 4 and 5 found mainly in Africa and genotype 6 located in Asia (Simmonds, Alberti et al. 1994). HCV infection does not induce a protective immunity, but allows persistence of the virus in the host organism. Liver inflammation and damage is supposed to be a reaction by the host immune system against HCV infected cells and is not due to the viral infection itself or HCV replication in the host cell. How HCV triggers HCC development is poorly understood. Two major possibilities have been considered: The HCV virus proteins, e.g. the virus core protein, may act directly on general pathways to increase cell proliferation and enhance malignant transformation of hepatocytes or it may act by accumulation of genetic alterations in the host genome (Cerny and Chisari 1999; El-Serag and Mason 2000).

1.2.2 Cirrhosis

In 1978, cirrhosis was defined by the World Health Organization *as a diffuse process characterized by fibrosis and the conversion of normal liver architecture into structurally abnormal nodules* (Anthony, Ishak et al. 1978).

The most common cause of hepatic fibrosis is alcohol abuse, which leads to repeated liver injury/damage and degeneration of liver parenchymal tissue. Apart from alcohol abuse, other factors have the potential to induce hepatic fibrogenesis. The following factors are recognized by the World Health Organization (WHO): viral hepatitis (HCV), metabolic disorders, biliary disease, venous outflow obstruction, toxins and therapeutic drugs (Anthony, Ishak et al. 1978). All these liver damaging mechanisms have the potential to trigger fibrogenesis by a common general mechanism or to induce liver inflammation by direct or indirect mechanisms. During an ongoing liver injury, the host immune system becomes activated and Kupfer

cells/macrophages, apart from other APCs (antigen presenting cells) or inflammatory cells, infiltrate the damaged liver (Duffield 2003; Duffield, Forbes et al. 2005). Under such circumstances, Kupfer cells can activate quiescent hepatic stellate cells (HSCs) and induce fibrogenesis (Friedman 2005).

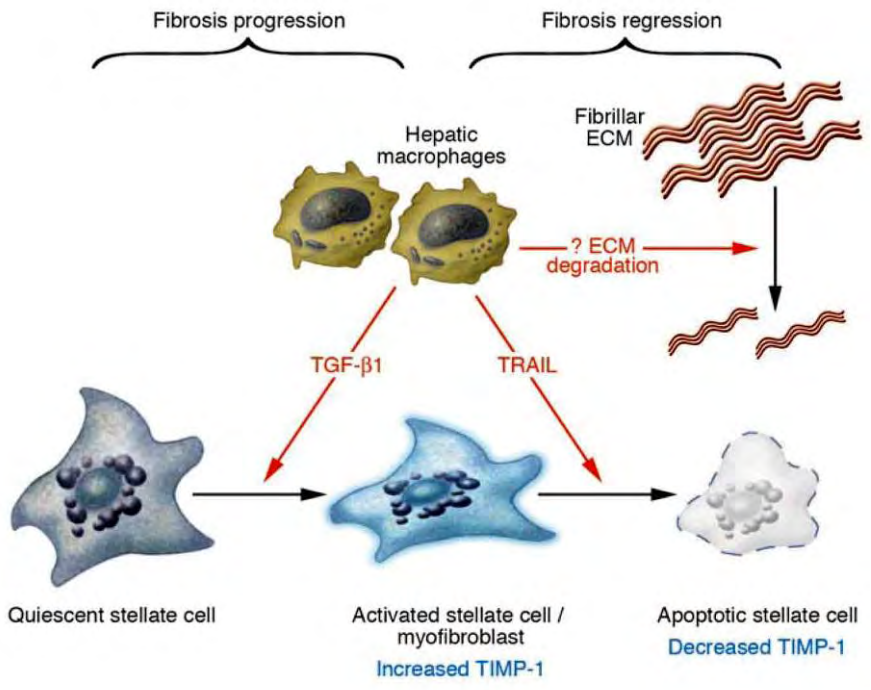

Figure 2 Overview of the known macrophage dualism in hepatic fibrogenesis (original figure from Friedman S.L., J. Clin. Invest. 2005 (Friedman 2005)).

These HSCs, activated by Kupfer cells/macrophages, migrate to the site of liver injury/inflammation and produce large amounts of extra cellular matrix (ECM) resulting in substitution of the normal hepatocytes alignment by deposition of predominantly type 1 collagen which results in formation of fibrotic septa (Bataller and Brenner 2005). Once fibrogenesis advances, collagen deposition ends up in forming collagen bands which form porto-porto, porto-central or central-central bridging septae and therefore disrupt the normal radial liver cell alignment (Anthony, Ishak et al. 1978). New evidence suggested that Kupfer cells/macrophages may contribute to the HSC activation through release of paracrine factors such as TGF-ß1. However, it has been postulated that macrophages may also provoke HSC apoptosis by a TNF-related apoptosis-inducing ligand, TRAIL (figure2; (Friedman 2005)). It

has been controversially discussed whether end stage liver fibrosis (cirrhosis) is reversible and if it may be resolved to restore tissue integrity (Desmet and Roskams 2004).

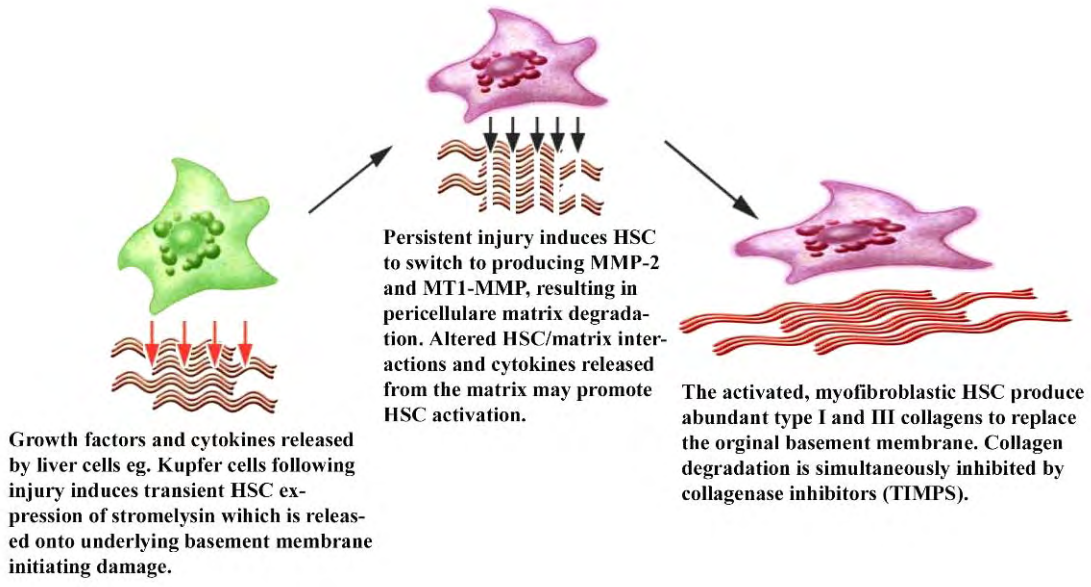

Figure 3 A proposed model showing the role of HSCs cell derived MMP-2 and TIMPs in regulating the hepatic ECM during fibrogenesis, (This figure is an adaptation of the figure from Friedman S.L., J. Clin. Invest. 2005 (Friedman 2005)).

Ongoing hepatic fibrogenesis is associated with proteolytic mechanisms of matrix degradation. It has been reported that activated HCS upregulates the expression of MMP-2 (gelatinase A) and MT1-MMP, which serve as cell membrane receptors for proMMP-2 and TIMP-2 (tissue inhibitor of metalloproteinases-2) together with TIMP-1 (Li and Friedman 1999). One substrate for MMP-2 is collagen IV. This is a ubiquitous part of the normal liver matrix, which is degraded during disease progression and substituted by abundant collagen type I and III. Simultaneously, TIMP-2 inhibits collagen type I and type III degradation. In activated HCS, MMP-2 upregulation is also mediated by the presence of collagen type I. Furthermore, MMP-2 has a pro-proliferation effect on activated HCS. Therefore, active MMP-2 is regulated via a positive feedback loop during hepatic fibrosis progression (Westermarck and Kahari 1999; Benyon and Arthur 2001).

Fibrosis staging and grading is usually performed on the results of a liver biopsy. Several scales (table2) are used by pathologists and scientists such as the one suggested by Metavir, (Paradis, Dargere et al. 1999), the scoring system proposed by Desmet & Scheuer (Desmet, Gerber et al. 1994) and the one by Ishak (Ishak, Baptista et al. 1995).

Stage	Metavir	Desmet & Scheuer	Ishak
0	No fibrosis	No fibrosis	No fibrosis
1	Periportal fibrosis expansion	Enlarge, fibrotic portal tracts	Fibrous expansion of some portal areas, with or without short fibrous septa
2	Portal-portal septae (>1 septum)	Periportal or portal-portal septa with intact architecture	Fibrous expansion of some portal areas, with or without short fibrous septae
3	Porto-central septae	Fibrosis with architec-tural distortion but no obvious cirrhosis	Fibrous expansion of most portal areas with occasional porto-porto bridging
4	Cirrhosis	Probable or definite cirrhosis	Fibrous expansion of portal areas with marked bridging (portal-portal or portal-central)
5	-	-	Marked bridging (portal-portal or portal-central) with occasional nodules (incomeplete cirrhosis
6	-	-	Cirrhosis

Table 2 Histological scoring systems

1.2.2.1 Intrahepatic microcirculation and portal hypertension

Cirrhosis is the main cause, apart from others, inducing portal hypertension (PHT) through fibrotic septa formation resulting in decreased intrahepatic

microcirculation. More than 90% of patients with PHT in Europe and the USA also have a positive diagnosis for cirrhosis (Wongcharatrawee and Groszmann 2000). PHT is the result of alterations in portal blood flow and vascular resistance opposing that flow. This relationship is defined by Ohm's law in the equation:

$$\Delta P = Q \times R$$

Where **ΔP** is the portal pressure gradient, **Q** is blood flow within the entire portal venous system and **R** is the vascular resistance of the entire portal venous system (Groszmann and Abraldes 2005).

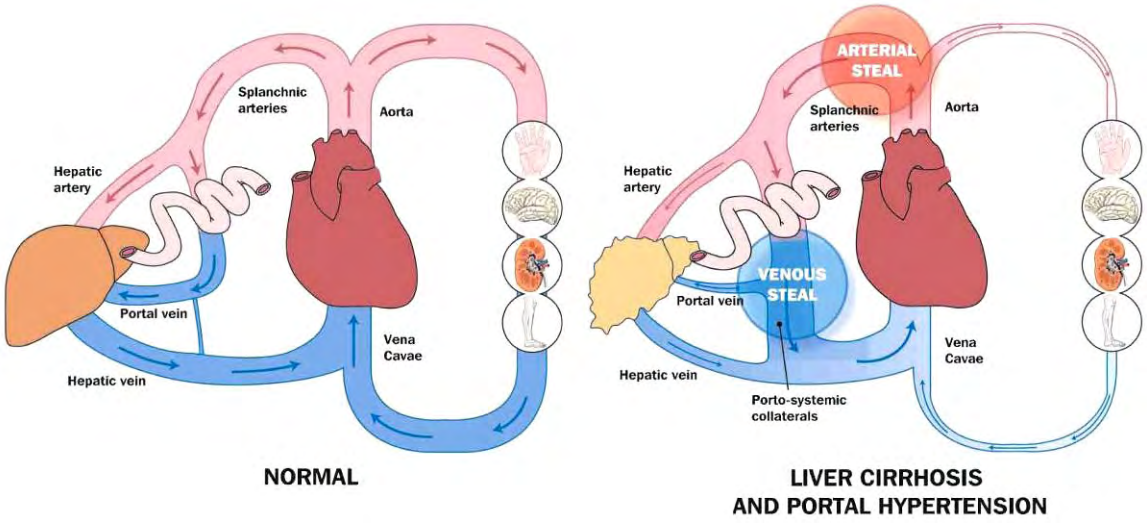

Figure 4 Schematic overview of the hemodynamic blood flow situation before and after fibrosis/cirrhosis in humans (original figure from Newby D.E. and Hayes P.C. , Q J Med, 2002 (Newby and Hayes 2002)).

In cirrhosis, intrahepatic vascular resistance is significantly increased due to liver fibrosis as a response to persistent liver injury. Additionally, portal pressure and portal blood flow are elevated. This results in shunting of the portal blood into the liver via porto systemic collateral anastamoses (figure4), creating a situation termed venous steal (Newby and Hayes 2002). In other words, the blood flow towards the liver is bypassed. Elevated intrahepatic vascular resistances (IHVR), or **R**, as a consequence of alteration in the hepatic microcirculation due to fibrogenesis can also

be influenced by other abnormal liver functions (e.g. thrombosis) (Laleman, Landeghem et al. 2005). A possible indicator of disturbed hepatic vascular resistance is the measurement of hepatic microcirculation (HM, equals liver perfusion) by non-invasive laser Doppler flowmeter method. Application of HM measurement has been validated in animal models (Wheatley, Almond et al. 1993; Seifalian, Chidambaram et al. 1998; Jiao, Seifalian et al. 1999).

1.2.3 Molecular hepatocellular carcinoma pathogenesis-hepatocarcinoma genesis

The malignant transformation of hepatocytes is the origin of hepatocellular carcinoma. Necrosis and proliferation of hepatocytes and infiltration of inflammatory cells in the development of either chronic hepatitis or cirrhosis are well investigated. The entire organ is affected, especially the matrix compounds and the microenvironment. The influence of the microenvironment is mediated by bidirectional interactions between epithelial tumor cells and neighboring stromal cells, such as endothelial and immune cells (Bosch, Ribes et al. 1999; Buendia 2000). In general, the initial phase of HCC is divided into three major steps: first, initiation (start of the malignant transformation), second, promotion (clonal expansion and formation of foci) and third, progression (tumor growth) (Dragan and Pitot 1992; Durr and Caselmann 2000).

Malignant transformation may be caused by exposure to chemical or physical agents or viruses (e.g. HBV/HCV) resulting in accumulation of DNA mutations. This acquisition of mutations is generally considered to be irreversible. Apart from this accumulation, malfunction of growth factors might lead to a malignant transformation. It was shown *in vitro* and *in vivo* that several growth factors, such as IGF-2 (insulin-like growth factor-2), TGF-α (transforming factor-α), TGF-β, EGF (epidermal growth factor) aFGF (acidic fibroblast growth factor) and HGF (hepatocytes growth factor), play a role in carcinogenesis (Caselmann 1998; Durr and Caselmann 2000; Okuda 2000). The promotion phase includes clonal expansion and focus formation of abnormal hepatocytes. This step may be reversible depending on the continued exposure to a tumor promoting agent. Only a portion of these initiated

hepatocytes will become dysplastic nodules. The following tumor progression will depend on whether these dysplastic nodules will die or survive, whether the survivors will grow further and whether the accumulated DNA alterations have occurred in DNA sequences which code oncogene activation or inactivation tumor suppressor genes.

1.2.3.1 Tumor metastasis

Metastasis is generally the major cause of death in cancer patients, especially highly metastatic carcinoma types, e.g. cervix carcinoma (Fidler 1990). Interestingly 57% of HCC patients with unresectable HCC died as a direct result of cancer progression. But 43% HCC patients died actually dieing from complications of their cirrhosis, including sepsis, GI bleeds, and renal failure (Couto, Dvorchik et al. 2007). Spread of cancer cells from the primary tumor site and the establishment of *de novo* cancer satellites require several previous steps. The development of metastasis is therefore a complex series of linked, sequential steps. Each step needs a successfully accomplished previous step to be initiated: 1, the disconnection of intercellular adhesions and separation of single cell from the solid tumor, 2, the escape from anoikis, 3, proteolysis of extracellular matrix, 4, locomotion of tumor cells in the extracellular matrix, 5, invasion of lymph-and blood vessels, 6, immunological escape into the circulation, 7, adhesion to endothelial cells, 8, extravasations from lymph- and blood vessels and 9, proliferation and induction of angiogenesis (Bohle and Kalthoff 1999).

1.2.3.2 Role of matrix metalloproteinase in tumor invasion

As explained above, tumor cells take part in several interactions with the extracellular matrix during ongoing metastasis. Matrix metalloproteinases are assumed to play an assisting role in the promotion of tumor cells to undergo metastasis (Lynch and Matrisian 2002; Fingleton 2006). Recent publications underline the role of two members of the matrix metalloproteinase family, MMP-2

and MMP-9. These two MMPs are abundantly expressed in various malignant tumors (Heppner, Matrisian et al. 1996; Liabakk, Talbot et al. 1996; Basset, Okada et al. 1997; Johnsen, Lund et al. 1998).

The MMP family currently consists of about 24 members. All are collectively capable of degrading ECM components. According to their substrate, structure and catalytical activity, the MMP family is classified into subgroups of collagenases, stromelysins, gelatinases, membrane-type MMPs and other MMPs. A functional MMP subgroup member contains a signal peptide, a propeptide, a catalytic domain with the highly conserved zinc motive, and a hemopexin-like domain linked to the catalytic domain by a hinge region. Gelatinases (MMP-2 and MMP-9) additionally contain a fibronectin type II insert. Moreover, the membrane-type MMPs, the MT-MMPs, contain a transmembrane domain at the carboxyl-terminal end of the hemopexin-like domain. The smallest MMPs known to date are MMP-7 and MMP-26, without the MMP characteristic, hemopexin-like domain (figure5).

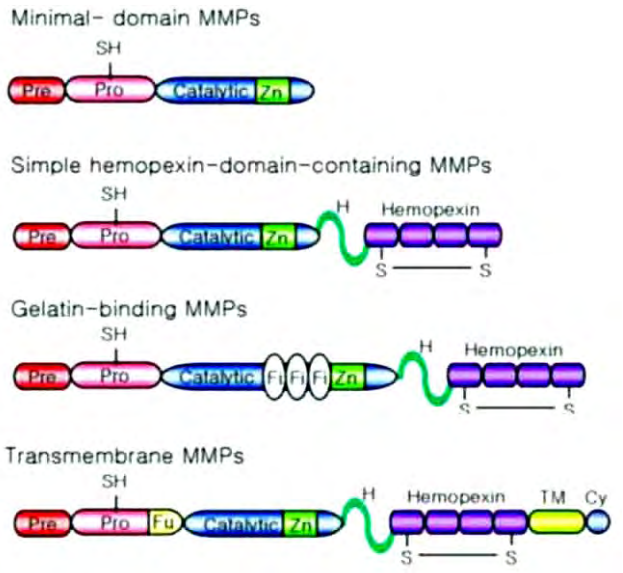

Figure 5 Structure of selected human matrix metalloproteinases; Pre, signal peptide; Pro, propeptide; Catalytic, catalytic domain; Zn, highly conserved zinc motive; H, hinge region; hemopexin, hemopexin-like domain (original figure from Sang-Oh Yoon et al., J Biol Chem, 2002 (Yoon, Park et al. 2002)).

MMP-2 (72 kDa) and MMP-9 (92 kDa) are both capable of degrading ECM components such as gelatin, laminin and nidogen. MMP-9 is also capable of degrading native collagen type I proteolytically and it can activate MMP-9 and MMP-13. Interestingly, active MT1-MMP serves as a cell membrane receptor for proMMP-2 and TIMP-2. This binding provides the proteolytic activation of proMMP-2 at the cell surface. MT1-MMP also has an additional catalytic function, it is capable of degrading grade collagen type I, II and III, apart from gelatin, fibronectin, laminin, vitronectin and aggrecan.

As described above, tumor metastasis is a multistage process. During this process malignant cells detach themselves from the primary tumor site and migrate through the tumor surrounding parenchyma, then cross structural barriers (cell-cell attachment or cell-matrix attachment) and reach the blood vessel or lymph vessel to circulate in the host organism. Recently formed MMPs (e.g. MMP-2) are released by various tumor cells and adjacent tissue to cleave the ECM, consisting of collagens, laminins, fibronectin, vitronectin and heparin sulphate proteoglycans, or to ensure cooperation between tumor cells and environment. Active MMP-2 binds to cell surface of invasive melanoma and endothelial cells via αvβ3 integrin (Westermarck and Kahari 1999; Yoon, Park et al. 2002). These findings were supported by high-level expression of distinct MMPs in invasive malignant tumors. It has to be mentioned that MMP-9 is required for the release of sVEGF (vascular endothelial growth factor) during long bone development. Interestingly, MMP-2 deficient mice show reduced angiogenesis and tumor progression (Itoh, Tanioka et al. 1998; Masson, Lefebvre et al. 1998; Itoh, Tanioka et al. 1999). Taken together, regulation of MMP expression and activity are crucial factors in further investigation and understanding of the mechanism of MMPs in tumor cell invasion.

1.2.4 Tumor angiogenesis

Tumor growth greater than a distinct diameter (2-3mm), is restricted by angiogenesis. Without ongoing angiogenesis, adequate supplies of oxygen and nutrients are limited. New blood vessels are formed by two distinct processes,

vasculogenesis and angiogenesis. Ongoing angiogenesis is restricted to vasculogenesis, which is thought to occur first and is therefore essential for angiogenesis. In vasculogenesis, endothelial cells are differentiated from mesodermal precursor cells only during embryonic development (Hanahan 1997; Ferrara and Alitalo 1999; Saaristo, Karpanen et al. 2000; Poole, Finkelstein et al. 2001). These precursors are the angioblasts, which differentiate into endothelial cells to form the blood vessel wall. The blood vessel lumen is formed by precursors of the hematopoietic cells (Risau and Flamme 1995). In contrast, in angiogenesis, new blood vessels are generated from pre-existing ones by sprouting, splitting and fusion in the adult organism (Hanahan 1997; Ferrara and Alitalo 1999; Saaristo, Karpanen et al. 2000; Poole, Finkelstein et al. 2001), i.e. quiescent endothelial cells become active once again and turn on their cell cycle, migrate and dissolve the basal membrane to form *de novo* blood vessels (Yancopoulos, Davis et al. 2000; Bhushan, Young et al. 2002).

Angiogenesis plays a major role in a wide range of biological processes, such as wound healing or organ regeneration. Under normal conditions, angiogenesis does not occur in an adult organism, except for wound healing and female reproduction cycle. The formation of *de novo* blood vessels is regulated by a stringent control mechanism involving selected endogenous pro- and anti-angiogenic factors. The imbalance between these factors which leads towards angiogenesis is the so-called angiogenic switch and is the result of the acquisition of pro-angiogenic factors. Through these accumulations of stimulatory factors, quiescent endothelial cells become active again. The so-called angiogenic switch is supposed to be a rate-limiting step in tumor development (Hanahan and Folkman 1996; Distler, Neidhart et al. 2002; Tonini, Rossi et al. 2003).

Angiogenesis depends on strictly regulated interactions between endothelial cells and ECM. These interactions are partially arranged by integral membrane proteins, e.g. integrin and MMPs and their inhibitors TIMPs (Eliceiri 2001; Eliceiri and Cheresh 2001; Pepper 2001). A wide range of growth factors are capable of stimulating angiogenesis *in vitro* and *in vivo*. The two most potent growth factors are represented by the FGF (fibroblast growth factor) family and VEGF (vascular endothelial growth factor). VEGF, an endothelial cell specific mitogen, is currently

the most intensively investigated angiogenic factor in HCC (Ferrara 1999; Eliceiri 2001; Eliceiri and Cheresh 2001).

1.2.4.1 Role of vascular endothelial growth factor and its receptors in tumor angiogenesis

In 1983, a protein was discovered which induces vascular leakage, the so-called tumor vascular permeability factor (VPF). Later, it was shown by others that VPF and VEGF were in fact the same molecule. In 1992, first results indicated that expression of VEGF mRNA correlated with vascularization in the developing murine embryo. This finding was the leading link to the idea that VEGF was an angiogenic factor (Senger, Galli et al. 1983; Keck, Hauser et al. 1989; Leung, Cachianes et al. 1989; Breier, Albrecht et al. 1992). To date, the role of VEGF has been well described in vasculogenesis and angiogenesis. Moreover, VEGF is considered to be one of the main factors in tumor angiogenesis. Therefore, the VEGF/VEGFR pathway is of central interest in basic research.

Structurally, VEGF belongs to the VEGF/PDGF (platelet-derived growth factor) family characterized by eight conserved cysteine residues in their VEGF homology domain. Currently, the murine and human isoforms are VEGF-A, -B, -C, -D, and –E. VEGF-A, VEGF-B and VEGF-E are linked to angiogenesis, while VEGF-C and VEGF-D are predominantly involved in lymph angiogenesis. Other relevant findings suggest a specific major role for VEGF-C and its receptor (VEGFR-3/Flt-4) in tumor metastasis. Several reports indicate a pathophysiological link between elevated VEGF-C expression levels and the risk of tumor metastasis (Stacker, Baldwin et al. 2002; Dadras, Lange-Asschenfeldt et al. 2005; Shibuya 2006; Hirakawa, Brown et al. 2007). The role of VEGF-B seems to be controversial. Some reports mentioned that VEGF-B takes part in angiogenesis and some suggested a role in lymph angiogenesis (Neufeld, Cohen et al. 1999). Interestingly, VEGF-E has been described as a non-mammalian or non-human VEGF-A homologue encoded by the parapoxvirus ORF (Ogawa, Oku et al. 1998).

The human VEGF-A ORF is organized into eight exons and through ongoing splicing, five different isoforms have been reported, consisting of 121, 145, 165, 189, 206 amino acids. Meanwhile, other isoforms have been reported containing 148, 162 and 183 amino acids. Also, another variant of $VEGF_{165}$, termed $VEGF_{165}$b, has been identified (Ogawa, Oku et al. 1998).

VEGF-A promotes angiogenesis by stimulating vascular endothelial cell proliferation and migration and it is required for the survival of endothelial cells in newly formed blood vessels. VEGF-A itself has a ubiquitous tissue distribution and is expressed by a wide variety of cell types (e.g. hepatocytes). VEGF-A expression is regulated by a wide range of different stimuli such as growth factors, hormones, transformation, p53 mutation, tumor promoters and nitric oxide. The most interesting stimulus is hypoxia. The key mediator of hypoxia response is HIF-1 alpha (hypoxia inducible factor 1). Under hypoxia conditions, HIF-1 alpha regulates the VEGF-A transcription and post transcriptionally the stability of VEGF-A mRNA.

The crucial step of angiogenesis induction *via* VEGF is the interaction between paracrine released VEGF and VEGF-binding to their relevant receptors which are mainly expressed in endothelial cells. VEGF is an antiparallel dimer, covalently linked by two disulfide bonds with receptor binding sites at each pole. All VEGF isoforms are capable of binding and activating the VEGF receptors with different affinities. VEGF-A is able to bind to all three receptor tyrosine kinases: VEGFR-1, also known as Flt-1 (Fms-like tyrosine kinase 1), VEGF-2, also known as Flk-1 (fetal liver kinase 1) in mice and as KDR (kinase insert domain containing receptor) in humans and VEGFR-3, also described in the literature as Flt-4. VEGFR-1 and VEGFR-2 are primarily located in the vascular endothelium, whereas VEGFR-3 is found in the lymphatic endothelium. The affinity of VEGFR-1 for VEGF-A is ten-fold higher than that of VEGFR-2, but the tyrosine kinase activity of VEGFR-1 is weaker than that of VEGFR-2. Apparently, VEGFR-1 can act as a decoy receptor preventing VEGF-A binding to VEGFR-2, apart from other possible mechanisms. VEGF-C and its receptor VEGFR-3 are essential for lymph angiogenesis (Shibuya, Yamaguchi et al. 1990; Terman, Carrion et al. 1991; Park, Keller et al. 1993; Wey, Fan et al. 2005). Interestingly, VEGFR-3 has a distinct structure compared to the other known VEGFRs. It is proteolytically cleaved in its fifth Ig homology domain

but the disulfide bridge keeps the aminoterminal part connected with the rest of the molecule.

The role of VEGF-VEGFR interaction in tumor angiogenesis has been well described. Further studies suggest an additional, more direct role in cancer genesis by stimulation of VEGFs on tumor cells. To date, the presence of VEGFRs has been reported in the following tumor cells: non-small-cell lung carcinoma, melanoma, prostate carcinoma, leukemia, mesothelioma, breast cancer and in a murine implanted hepatocellular carcinoma, based on immunohistochemical stainings (Meister, Grunebach et al. 1999; Neufeld, Cohen et al. 1999; Ishida, Murray et al. 2001; Price, Miralem et al. 2001; Tian, Song et al. 2001). *In vitro* studies pronounced the involvement of VEGFR-1 activation by VEGF-A or VEGF-B in the MAPK pathway in tumor cells, which is observed together with increased cell migration and invasion (Fan, Wey et al. 2005). Additionally, an anti-tumor effect was reported by down-regulating VEGFR2 expression in tumor endothelial cells via tumor necrosis factor-alpha (TNF-α) (Menon, Iyer et al. 2003). Other recent data showed that binding to its receptors in the pre-existing endothelium triggered endothelial cell proliferation and migration into the tumor, resulting in vascular angiogenesis. VEGF-A and -B are secreted by tumor cells themselves and by infiltrating immune cells such as monocytes. An additional role is described in recruiting endothelial cells from the bone marrow for endothelial vessel formation (Dvorak, Detmar et al. 1995).

1.2.4.2 Role of VEGF-C in tumor metastasis

Most recent published data on VEGF-C (or VEGF related protein, VRP) presented strong evidences for another unrecognized role of VEGF-C and its receptor VEGFR-3 (Flt-4) in lymph angiogenesis. *In vitro*, it was shown that VEGF-C acts synergistically with VEGF-A to induce tube formation of bovine aortic endothelial cells. It is thought that VEGF-C induced effects are most likely mediated by the interaction with VEGFR-2 in blood vascular endothelium and primarily by VEGFR-3 in the lymphatic endothelium. Furthermore, VEGF-C is considered to influence ongoing metastasis (see discussion). Several recent publications suggested a

correlation between lymph metastasis progression and VEGF-C (Su, Yang et al. 2006; Su, Yen et al. 2007).

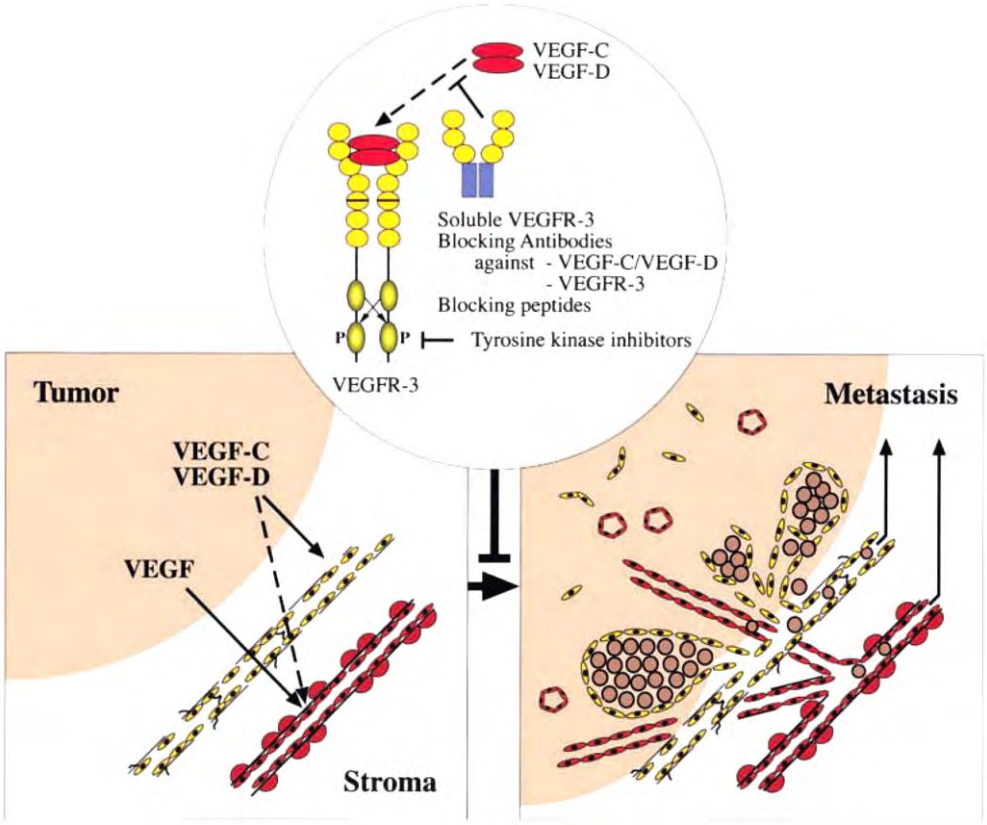

Figure 6 VEGF-C and –D secreted by tumor cells infiltrated inflammatory cells or other stromal cells stimulate tumor associated lymph angiogenesis and may contribute to tumor angiogenesis. Blocking the VEGFR-3 pathway can be used as one target for anti tumor lymph angiogenesis and lymphatic metastic intervention studies (Original figure from Karpanen and Alitalo (Karpanen and Alitalo 2001)).

All these findings (table 3) lead to the assumption that VEGF-C takes part in tumor metastasis *via* the lymphatic system by inducing growth of tumor associated lymphatic vessels and by promoting tumor cell invasion into and growth inside the lymphatic vasculature (figure 6). Other groups reported that an over-expression of VEGF-C/-D in transgenic mice induced not only tumor lymph angiogenesis but also resulted in increased lymphatic metastasis (Mandriota, Jussila et al. 2001; Skobe, Hawighorst et al. 2001; Stacker, Caesar et al. 2001; Padera, Stoll et al. 2002; Kawakami, Yanai et al. 2005). Yet, only one study could show a positive correlation of VEGF-C expression and metastasis in human HCC (Yamaguchi, Yano et al. 2006).

Tumor type	positive correlation between VEGF-C and metastasis	Reference
breast cancer	yes	(Kurebayashi, Otsuki et al. 1999) (Hashimoto, Kodama et al. 2001)
cervical cancer	yes	(Ueda, Terai et al. 2001) (Van Trappen, Ryan et al. 2002) (Gombos, Xu et al. 2005)
colorectal cancer	yes	(Akagi, Ikeda et al. 2000) (Kaio, Tanaka et al. 2003) (Kawakami, Furuhata et al. 2003)
endometrial cancer	yes	(Hirai, Nakagawara et al. 2001)
esophagus cancer	yes	(Kitadai, Amioka et al. 2001)
gallbladder cancer	yes	(Nakashima, Kondoh et al. 2003)
melanoma	**no**, but increased LVD	(Straume and Akslen 2003)
neuroblastoma	no	(Komuro, Kaneko et al. 2001)
oral Cancer	yes	(Wen, Yu et al. 2001)
ovarian carcinoma	yes	(Yokoyama, Sakamoto et al. 2003)
pancreatic cancer	yes	(Tang, Itakura et al. 2001)
prostate cancer	**no**	(Tsurusaki, Kanda et al. 1999)
thyroid cancer	yes	(Tanaka, Kurebayashi et al. 2002)

Table 3 Overview of published data indicating a positive correlation between VEGF-C and metastasis; (modified from (Stacker, Baldwin et al. 2002; Pepper, Tille et al. 2003; He, Karpanen et al. 2004); LVD: lymph vessel density.

In blood vessel angiogenesis, an active role for VEGF-C has also been reported. In this publication, the neutralization of VEGFR-3 with a blocking antibody against VEGFR-3 in a murine tumor model lead to reduced tumor growth. Thus, this

observation was associated with reduction in the number of intratumoral *de novo* blood vessels (Laakkonen, Waltari et al. 2007). Furthermore, the disruption of the interaction between VEGF-C and its receptor VEGFR-3 (Flt-4) leads to decreased levels of metastasis in several murine tumor models. The efficiency of using soluble Flt-4-Ig in blocking tumor lymph angiogenesis and metastasis was confirmed by others as reported in several recent publications (Shimizu, Kubo et al. 2004; Roberts, Kloos et al. 2006). Additionally, the disruption of the VEGFR-3 receptor pathway using small interfering RNA against VEGF-C (Chen, Varney et al. 2005) or the use of neutralizing VEGF-D antibodies (Stacker, Caesar et al. 2001) resulted both in inhibition of tumor lymph angiogenesis and metastasis.

These latest findings raise the question whether VEGF-C could be an even more valuable target for cancer research, anti tumor growth and anti metastasis strategies (Su, Yang et al. 2006).

1.2.5 HCC tumor markers

Several molecular biomarkers for HCC might provide an indication for HCC growth, metastasis or recurrence before application of an invasive diagnostic method. Currently, histopathology obtained from biopsy or surgery is serving as the gold standard to confirm HCC diagnosis. Only a few HCC markers exist, such as AFP (alpha-fetoprotein), a tumor associated protein (Korn 2001). It has been reported that patients with high AFP levels tend to have a larger HCC tumor size (Tangkijvanich, Anukulkarnkusol et al. 2000). Additionally, all patients with elevated AFP mRNA values died within one year. However, patients with a negative AFP mRNA rate have better survival rates than those with positive or elevated ones (Wong, Lau et al. 1999; Wong, Lau et al. 2000; Ijichi, Takayama et al. 2002). Most current results showed that approximately 54% of HCC patients are negative for AFP. Other markers, such as elevated ALT levels, indicate an ongoing liver injury and are also predictive HCC markers in combination with further evaluative methods. In this context, it should be mentioned that the presence of nodules elucidated during a routine radiological

investigation is one of the first indications for HCC (Bruix and Sherman 2005; Farinati, Marino et al. 2006; Suruki, Hayashi et al. 2006).

Other molecular biomarkers, such as adhesion molecules, especially ICAM-1 (intracellular adhesion molecule-1) and laminin-5, provide further indication of metastasis and tumor recurrence (Qin and Tang 2004). In contrast to AFP, which has been well investigated in the past and is now considered not to be a very predictable HCC marker, ICAM-1 could be another possible marker closely associated with HCC progression and prognosis. To date, higher levels of soluble ICAM-1 are found more frequently in patients with multiple lesions, intrahepatic metastasis and an overall poorer prognosis. Laminin-5 is also strongly associated with HCC occurrence, metastasis and poor prognosis (Sun, Zhou et al. 1999). As described in previous chapters, proteinases, such as MMPs, as well as angiogenesis regulators, such as VEGF, have been validated as potential HCC predictors due to their function and role in HCC carcinogenesis (Qin and Tang 2004).

1.3 Murine HCC tumor models

To understand the molecular role and function of distinct genes in novel and challenging human anti cancer therapies, first a murine model must be developed, which sufficiently mimics the human disease, before any clinical approach becomes possible. In general, the murine tumor bearing model seems to be suitable due to its easy handling. The feasibility of murine tumor bearing models has been proven and accepted. Wild type mice from various mouse lines together with rats are used for implantation with syngenic tumor cells (Schmitz, Barajas et al. 2001; Melero, Gabari et al. 2003; Raskopf, Dzienisowicz et al. 2005; Schmitz, Kornek et al. 2005). Also, knock-out mice (Nakau, Miyoshi et al. 2002) or knock-in/transgenic mice (Shiota and Kawasaki 1998) are used in investigations besides others, e.g. nude mice (Sun, Zhou et al. 1999). Currently, the following four most common murine tumor models are available and in use: the implantation model, sub-cutaneously or orthotopic (Schmitz, Barajas et al. 2001; Melero, Gabari et al. 2003; Schmitz, Tirado-Ledo et al. 2004; Raskopf, Dzienisowicz et al. 2005; Schmitz, Kornek et al. 2005; Schmitz, Raskopf et

al. 2006; Schmitz, Vilanueva et al. 2006), the metastasis model tumor cell seeding via implantation into the spleen and locomotion of tumor cells to the liver (Gnant, Puhlmann et al. 1999) or controlled by oncogenes associated with oncogene over expression (Shachaf, Kopelman et al. 2004). However, all of the above cited murine mice models are lacking one important feature, which reflects the patient's diseases history prior to HCC occurrence, namely long term liver injury finally manifested in cirrhosis as described in the first chapters. Several observations in HCC patients with or without cirrhosis suggest that cirrhosis has a major impact on HCC occurrence and patients' survival. A recent cohort study indicates that HCC currently represents the major cause of liver-related death in patients with compensated cirrhosis. Additionally, cirrhosis underlies HCC in approximately 80%–90% of cases worldwide. Furthermore, it has been reported that activity of the liver disease, characterized by inflammation, necrosis, and regeneration, plays an important role in HCC progression (Tsukuma, Hiyama et al. 1993; Fattovich, Stroffolini et al. 2004). Evidently, these complications and circumstances might limit transferability and interpretation of experimental data regarding clinical relevance. Therefore, a novel murine tumor model which includes this certain obstacle is warranted.

1.4 Overview of murine models of hepatic fibrosis/cirrhosis

The pathogenesis of hepatic fibrosis is only partially understood in certain aspects and in the context of hepatic carcinogenesis, no well characterized fibrosis HCC models are available. Therefore, novel and highly reproducible fibrosis models are required for further investigations and intervention studies. Several animal fibrosis models have been developed, mainly in small rodents such as the rat or mouse. Compared to the wide spectrum of etiological backgrounds, various fibrosis models were established using completely different approaches, to remodel the genesis of hepatic fibrosis.

Here, the three most widely used models are briefly introduced: First, the cholestatic fibrosis model induced by bile duct ligation. This model is usually applied in rats as here the bile duct is surgically ligated, resulting in cholestasis and

subsequent hepatic fibrosis and cirrhosis. In general, bile duct-ligated animals induce fibrosis as early as after 12 days and hepatic cirrhosis occurs in almost all animals within four to eight weeks. Second, the chemically fibrosis model induced by using different hepatotoxins leading to degeneration of hepatocytes and activation of the immune system and finally to hepatic fibrosis. Two different chemical agents, both classified as carcinogens, have been in use for fibrogenesis initialization, TAA (thioacetamide) and CCL_4 (carbon tetrachloride) (Weiler-Normann, Herkel et al. 2007). A marked strain difference in the susceptibility to fibrosis induction is known. The CCL_4 application to C3H/He mice is associated with an intolerably high mortality rate of 60% (Hillebrandt, Goos et al. 2002). The combination of TAA intra peritoneal and ethanol feeding has been proven to accelerate fibrosis induction (Kornek, Raskopf et al. 2005; Kornek, Raskopf et al. 2006). Both hepatotoxins result in oxidative stress in the liver and intrahepatic injury. Third, transgenic animals over expressing mediators or regulators are involved in fibrosis, e.g. TGF-β.

1.5 Designated doctoral thesis goals

First aim of this PhD thesis is the establishment of a reliable method to induce fibrosis in the C3H/He mice strain with a lower mortality rate than observed with CCL_4 (60%) and to provide evidence for its use as a novel model by characterization of common fibrosis bio markers extended with the use of a novel non-invasive approach to demonstrate first time hepatic microcirculation (HM) consequences and functional relevance *in vivo*.

Second aim is to combine this novel fibrosis induction approach with the intrahepatic implantation of syngenic HEPA129 tumor cells and to analyze tumor growth under these conditions.

Third aim is to focus the study on angiogenesis and metastasis related gene transcription in this novel C3H/He fibrotic HCC model.

The data obtained from this study will provide new insights in cancer genesis under pre-fibrotic conditions achieved by the combination of pre-damaged liver with implanted intrahepatic syngenic tumor cells. It might bring this novel model closer to HCC patient's disease history and will thus be reliable tool to mimic future human anti cancer therapies under fibrotic/cirrhotic circumstances.

2 Materials

2.1 Hardware and manufacturer

Cell culture incubator	Hereaus Sepatech (Osterode)
Cell culture microscope	Olympus (Hamburg)
ELISA-Reader	Dynatech Laboratories (Frankfurt)
Microtome	Leica (Wetzlar)
Mini-shaker	IKA, Sigma-Aldrich (Taufkirchen)
LightCycler	Roche Diagnostics (Mannheim)
Laser Doppler flowmetry	LEA Medizintechnik GmbH
pH-meter	Hannah Instruments (Kehl am Rhein)
Photometer	Gene Quant, Pharmacia (Freiburg)
Shaker	ProMax 2000, Heidolph (Kelheim)
Cell culture Hood	Hereaus Sepatech (Osterode)
Thermocycler	Eppendorf GmbH (Hamburg)
Table centrifuge	Beckman (Palo Alto, CA, USA)
Water bath	Köttermann (Uetze-Hänningen)
Sorvall RC-5B centrifuge	DuPont (Bad Homburg)
Sorvall GSA (rotor)	DuPont (Bad Homburg)
Sorvall SS34 (rotor)	DuPont (Bad Homburg)
Vortex	Scientific Industries Genie-2
Scale	BP2100S, BP310S, Sartorius
Fine-scale	Scaltec SBC 21

2.2 General materials

Reaction-tubes	Eppendorf (Hamburg)
(0.5 mL - 2 mL)	

Cryo-tubes (2 ml)	Greiner Labortechnik GmbH (Frickenhausen)
Reaction-tubes (large) (15 ml, 50 ml)	Greiner Labortechnik GmbH (Frickenhausen)
Cell culture bottles ($25\ cm^2$, $75\ cm^2$, $175\ cm^2$)	Greiner Labortechnik GmbH (Frickenhausen)
Neubauer counting chamber	Brand (Wertheim)
Injection needle (20G x 1½)	Terumo Deutschland GmbH (Eschborn)
Suture material- absorbable Maxon HR13 (1m, USP 5/0)	Aesculap (Tuttlingen)
Dako Pen	Dako Cytomation GmbH (Hamburg)
Chirurgic instruments	Martin, Tuttlingen
Object slides	Engelbrecht (Edermünde)
Cover slip (18 x 18 mm)	Menzel Gläser (Braunschweig)

2.3 Antibodies

Rat anti mouse CD31	Cedarlane (Hornby, Ontario, Canada)
Rabbit anti rat (Biotin)	Dako Cytomation GmbH (Hamburg)
Rabbit anti-von Willebrand factor	Dako Cytomation GmbH (Hamburg)
Rat anti-mouse ICAM-1 (CD54)	BD Pharmingen
Anti Armenian and Syrian hamster IgG antibody cocktail	BD Pharmingen
Pig anti rabbit immunoglobin G	Dako Cytomation GmbH (Hamburg)

2.4 Kits

Biorad DC Protein Assay kit	Biorad, Munich
GPTransaminase kit	Roche Diagnostics, Mannheim
Dako ChemMate™ detection kit	Dako Cytomation GmbH (Hamburg)
Quantikine murine sICAM ELISA	R & D Systems, Wiesbaden-Nordenstadt
Quantikine human/murine MMP-2 ELISA	“
Quantikine murine VEGF ELISA	“
GenElute Total Mammalian RNA Kit	Sigma, Taufkirchen
HighPure RNA Isolation Tissue Kit	Roche Diagnostics, Mannheim
Transkriptor cDNA Synthesis Kit	Roche Diagnostics, Mannheim

2.5 Tumor cell line and animals

C3H/He female mice were obtained from Charles River and housed under SPF conditions in the animal facility of the University Hospital. Animal procedures were performed in accordance with approved protocols of the responsible local governmental administration and followed recommendations for proper care and use of laboratory animals. The C3H/He mice strain is syngenic to the Hepa129 tumor cell line.

The origin of this mice strain goes back to the crossing of a Bagg albino female and a DBA male mouse by Strong in 1920. The litter was sent to Andervont in 1930, then to Heston at F35. To NIH in 1951 from Heston at F57. To Charles River in 1974 from NIH.

Hepa129 cells (Hepatoma 129 originating from C3H mice, obtained from NCI-Frederick Cancer Research And Development Center (DCT Tumor Repository)

as tumor samples and were maintained in RPMI 1640 supplemented with 10% FCS, 200 mM glutamine and penicillin/streptomycin.

2.6 Reagents

2.6.1 General reagents for histology

Aquatex	Merck (Darmstadt)
Antibody Diluent	Dako Cytomation GmbH (Hamburg)
Biotin blocking solution	Dako Cytomation GmbH (Hamburg)
Mayers Hämalaun	Sigma (Taufkirchen)
Streptavidin-Biotin HRP/AEC	Dako Cytomation GmbH (Hamburg)

2.6.2 Buffers and solutions

Phosphate buffered saline (PBS)

NaH_2PO_4 ..... 20 mM

NaCl ..... 50 mM

pH 7.4

2.6.3 Solutions for cell culture

DMEM (4,5 g Glucose, mit Glutamax)	Sigma (Taufkirchen)
RPMI 1640 (mit Glutamax)	PAA (Cölbe)

FCS	PAA (Cölbe)
Penicillin/Streptomycin	Sigma (Taufkirchen)
Trypsin-EDTA solution	Sigma (Taufkirchen

2.6.4 Solutions for animals

Ketamin	Pharmacia GmbH, Karlsruhe
Rompun	aniMedica GmbH, Senden-Boesensell
NaCl (0.9 %)	B. Braun (Melsungen)
Thioacetamide	Sigma-Aldrich (Taufkirchen)
Ethanol (absolute)	B. Braun (Melsungen)

2.7 LightCycler primers and probes

Target gene	5'-primer	Probe	3'-primer
18sRNA	aaa tca gtt atg gtt cct ttg gtc	tcc tct cc	gct cta gaa tta cca cag tta tcc aa
VEGF-A	gca gct tga gtt aaa cga acg	cca ggc tg	ggt tcc cga aac cct gag
VEGF-C	cag aca agt tca ttc aat tat tag acg	ctc tgc ca	cat gtc ttg tta gct gcc tga
Flk-1/KDR	gat gga ggc ctc tac acc tg	tgg ctg tg	tct ttt cct ggg cac ctt c
Flt-1	cca ctc cct tga aca cga g	gac ctg ga	cgc ctt acg gaa gct ctc t
Flt-4	tga tga tag tcc acc cag ca	cag cct gg	cca gga aag gac aca cag ttg
MMP-2	gtg gga caa gaa cca gat cac	gac ctg ga	gca tca tcc acg gtt tca g
MMP-9	acg aca tag acg gca tcc a	ctc cag cc	gct gtg gtt cag ttg tgg tg
HIF-1 alpha	cat gat ggc tcc ctt ttt ca	cag cag ga	gtc acc tgg ttg ctg caa ta

Table 4 Specific primer oligonucleotides and oligonucleotide probes for qPCR

3 Methods

The methods described in this section are all based upon today's standard molecular and cellular biology techniques.

3.1 Fibrosis induction trough administration of thioacetamide (TAA) with or without ethanol feeding

For the fibrosis induction protocol establishment, induction of fibrosis was studied in C3H/He mice using either i.p. injections of TAA (0.15 mg/g body weight solved in sterile PBS) three times per week for 15 weeks alone (n=12) or in combination with alcohol feeding. Each time drinking water was prepared fresh and ethanol was diluted in sweetened drinking water (10% v/v, n=21). For the implantation and tumor growth study in pre-fibrotic mice, fibrosis was induced in C3H/He mice by the TAA and ethanol protocol, which was established before. For this purpose, fibrosis was induced for 19 weeks by i.p. TAA injections in combination with ethanol feeding.

3.2 Functional effects of fibrosis induction on hepatic microcirculation (HM) measured with Laser Doppler technique

In order to verify functional effects of fibrosis on hepatic microcirculation (HM), relative absorption units (AU) were measured on tissue surface by using laser Doppler flowmetry (O2C, LEA Medizintechnik GmbH). Its use for measurement of the HM has been validated in animal models by others (Wheatley and Zhao 1993; Jiao, Seifalian et al. 1999). Before HM measurement, mice were anaesthetized by i.p. application of a combination which consists of ketamin (0.1 mg/g bodyweight) and rompun (2% 0.01 mg/g bodyweight), then HM measurement was performed. Laparotomy was closed in two layers by continuous suture with absorbable material.

3.3 Hepa129 tumor cell line implantation

3.3.1 Fibrotic-Orthotopic Hepa129 tumor model

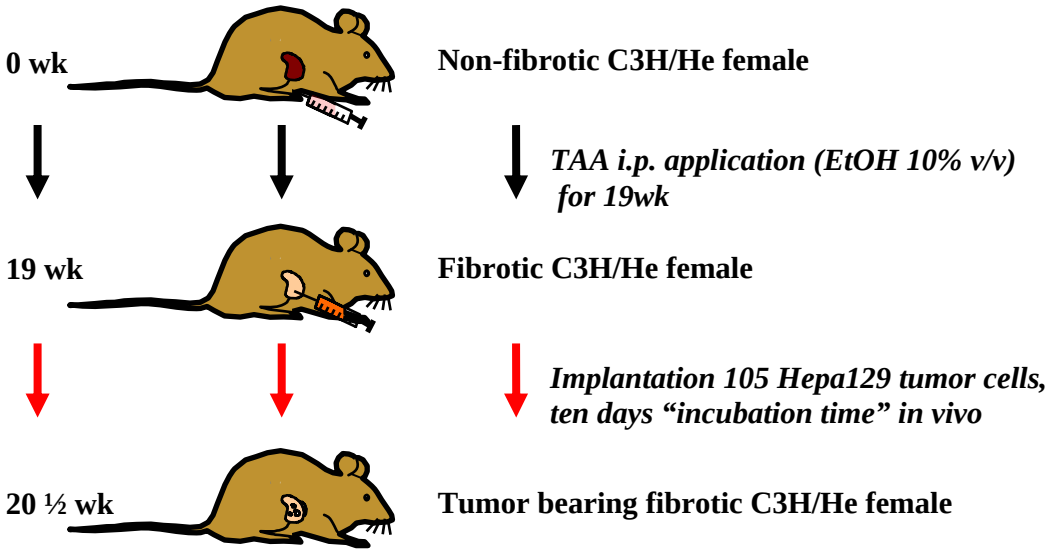

Figure 7 Schematic overview of the current fibrosis induction and implantation protocol.

Fibrotic or non-fibrotic mice were anaesthetized via an i.p. injection of ketamin and rompun anesthetic mix (ketamin 0.1 mg/g bodyweight and rompun 2% 0.01 mg/g bodyweight). After anesthesia, laparotomy for tumor cell implantation was performed. Mice were laparotomized and orthotopic HCC was established by intrahepatic injection of 10^5 hepatoma cells (Hepa129) suspended in 50 µL RPMI into the left liver lobe in a total of 14 mice (fibrotic n = 7, non-fibrotic n = 7). Post injection bleeding and tumor cell escape were avoided by local compression. Laparotomy was closed in two layers by continuous suture with absorbable material. To allow comparative, statistical analysis of the data arithmetic mean tumor diameters were calculated from tumor width (a) and length (b) by caliper measurement after laparotomy at day 10 after tumor cell implantation. TAA injections were not stopped after tumor cell implantation.

3.3.2 Fibrotic-Metastatic Hepa129 tumor model

To establish intrahepatic HCC metastases in pre-damaged fibrotic mice and healthy control mice, animals received an intrasplenic injection of 7 x 10^5 Hepa129 cells in 100 µl RPMI1640. Before laparotomy and tumor cell injection with a 27 G syringe subcapsular into the spleen animals were narcotized by i.p. injection of a ketamin and rompun anesthetic mix (0.1 mg/g ketamin and 2% 0.01 mg/g rompun). Twelve days after tumor cell implantation, animals were sacrificed trough a cervical dislocation and the livers were explanted and tumor and metastasis growth were documented.

3.4 Blood sera preparation and alanine transaminase (ALT) assay

After cervical dislocation, the blood was pipetted out of the thorax after aortal incision. After 30 min of co-agulation blood samples were centrifuged down two times (1200 rpm for 5min) to separate the blood serum from blood aggregates. Blood serum levels of ALT activity were measured using the GPTransaminase kit (Roche Diagnostics, Germany) according to the manufacturer's instructions.

3.5 Protein extraction and protein Elisa

Liver damage and fibrosis induction was characterized by determination of ALT, VEGF-A, ICAM-1, TIMP-1 and MMP-2 concentrations, respectively, in liver samples at week 5, 10 and 15. To extract protein, liver tissue samples were homogenized in 500 µl PBS with proteinase inhibitor (Complete Mini, Roche Applied Sciences). Separated cells were broken up by repeated freeze thaw cycles and debris was pelleted by centrifugation. Protein concentrations were determined using the Biorad DC Protein Assay kit (Biorad) according to the manufacturer's protocol. 2.5 mg of protein was used in each test (VEGF-A, MMP-2, ICAM-1 ELISA Quantikine murine VEGF-A ELISA, Quantikine murine sICAM-1 ELISA, Quantikine human/murine MMP-2 ELISA, R & D Systems).

3.6 mRNA extraction and cDNA preparation

RNA from liver tissue samples of TAA/EtOH treated or control mice was neither isolated by using the GenElute Total Mammalian RNA Kit (Sigma) according to the manufacturers' protocol. RNA was then digested with RQ1 DNase (Promega). RNA concentrations were determined and 1µg RNA was used in the RT-Reaction with random primers (Promega) and MMLV-Reverse Transcriptase (Promega, Mannheim, Germany). Alternatively murine RNA was isolated from liver tissue or tumor samples using the HighPure RNA Isolation Tissue Kit (Roche) according to the manufacturers' protocol. RNA concentrations were determined and 10 µL RNA was used in the following RT-reaction with random primers (Transkriptor cDNA Synthesis Kit, Roche).

3.7 Quantitative real time PCR (polymerase chain reaction)

Transcript levels of VEGF-A/-C, Flk-1/KDR, Flt-1, Flt-4, ICAM-1, MMP-2 and MMP-9 were determined in relation to 18sRNA mRNA levels by semiquantitative real time PCR (LightCycler, Roche Diagnostics). Primers were obtained from Invitrogen GmbH and probes from Roche Diagnostic. Sequences are given in Table 3.

3.8 Histology

Paraffin liver sections were treated with proteinase K (DAKO) for 10 min at room temperature. Samples were then blocked with 5% pig serum in PBS, followed by incubation with rabbit anti-von Willebrand factor (factor VIII-related antigen, 1:1500, DAKO) for 60 min at RT. Endogenous peroxidase activity was quenched by H_2O_2-treatment (DAKO) for 10 min. After washing with PBS, sections were incubated with a secondary antibody dilution of biotinylated pig anti rabbit immunoglobin G (1:300) and streptavidin conjugated to horseradish peroxidase (DAKO). Sections were visualized by using the Dako ChemMate™ detection kit and

counter-stained with hematoxylin (DAKO). Areas presenting highest vascularization were identified and blood vessels were counted in high power fields (HPF, x40 magnification), 5 HPF were evaluated in each section.

To determine ICAM-1 expression, cryopreserved liver sample sections were immune-stained with rat anti-mouse ICAM-1 (CD54) (1:50, BD Pharmingen) and incubated with a biotinylated anti Armenian and Syrian hamster IgG antibody cocktail (BD Pharmingen) and streptavidine peroxidase. Enzymatic activity was developed using AEC (Dako) as substrate and sections were counter-stained with Mayer hematoxylin.

For hematoxylin-eosin (H.E.) and van Gieson staining, 4% formaldehyde-fixed liver samples were paraffin embedded and sections of 5 µm thickness were stained according to standard procedures. Fibrosis was assessed according to the fibrosis proposed by Ishak et al. (Ishak, Baptista et al. 1995).

To determine cell proliferation, cryopreserved liver sample sections were immune-stained with rabbit anti-mouse Ki-67 (1:25, Dako) and incubated with a biotinylated anti rabbit swine IgG secondary antibody (Dako) and streptavidine peroxidase. Enzymatic activity was developed using AEC (Dako) as substrate and sections were counter-stained with Mayer hematoxylin.

3.9 Statistical analysis

All data are given as mean with SD or SEM, as mentioned in the corresponding figure legend. Differences between values of independent experimental groups were analyzed for statistical significance by Mann-Whitney t-test or by unpaired student’s t-test. An error level (p) < 0.05 was supposed to indicate significance.

4 Results

4.1 Experimental murine fibrosis model in the C3H/He mice

4.1.1 The establishment of a hepatic fibrosis model via thioacetamide (TAA)

The most common method to induce fibrosis in mammals is use of CCL_4. TAA administration can be done in various ways. Adding it as a food supply to the drinking water has turned out to be sufficient to induce weak fibrosis. Addition to the oxygen gas which the animal has to inhale was also considered to induce sufficient fibrosis (Cremonese, Pereira-Filho et al. 2001). However, the most widely used application of CCL_4 is to inject it i.p. over several weeks and months (Constandinou, Henderson et al. 2005; Weiler-Normann, Herkel et al. 2007).

Here, a different chemical compound was chosen. Apart from CCL_4, TAA also showed in mammals a potency for liver fibrosis induction, but it was considered to be weaker. However, for future plans, the author was restricted to the C3H/He mice strain, since a syngenic HCC cell line is available (HEPA129) only for this mice strain and the next step was to combine the existing HCC orthotopic model (Schmitz, Tirado-Ledo et al. 2004) with the novel fibrosis C3H/He model. The observation that in this particular mice strain, the CCL_4 method for fibrosis induction showed a surprisingly high mortality rate of about 60% has already been published. Therefore, another method with an acceptably lower mortality rate was considered to show positive results. A first attempt was done with TAA i.p. alone resulting in a mild unconvincing F2 fibrosis. However, a second attempt showed that combination of TAA i.p. with additional ethanol feeding in drinking water (TAA i.p. and EtOH) resulted in F4 fibrosis (F4).

4.1.1.1 Comparison of the TAA i.p. and TAA i.p. and EtOH scoring results

In both study groups, the TAA i.p. cohort without additional ethanol feeding and the cohort with additional ethanol supplement, the TAA administration period for fibrosis induction was limited to 15 weeks in order to obtain comparable results for these two groups. Interestingly but not surprisingly, fibrosis induction was low in mice that were exposed only to TAA (i.p.). In this setting, only an F2 fibrosis score out of a maximum of F6 was reached after 15 weeks of fibrosis induction initiation. Combination of TAA i.p. with EtOH considerably accelerated the development of fibrosis resulting in score F4 out of a maximum score of F6, according to the Ishak scoring/grading system (Ishak, Baptista et al. 1995). For a more detailed presentation of this result, please see chapter 4.1.1.4.

4.1.1.2 Mortality overview

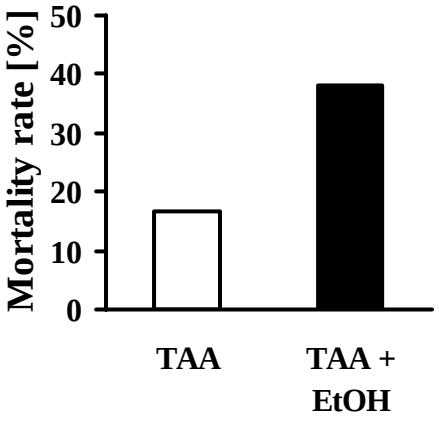

Figure 8 Mortality overview in C3H/He mice, mice received TAA i.p. alone or a combination of TAA i.p. and EtOH in the drinking water for fibrosis induction. During the first period of fibrosis induction 17% vs. 38% animals died in the TAA i.p. vs. TAA i.p. and EtOH treatment group, within two weeks.

Fibrosis induction by TAA i.p. alone was associated with a 17% mortality rate, but in the combination group of mice receiving TAA i.p. and EtOH in the drinking water, mortality increased by almost 50% to 38% (figure 8). Mortality was

almost completely restricted to the first two treatment weeks and all animals which survived the first two weeks had long-term survival.

4.1.1.3 Macro morphological changes after TAA i.p. and EtOH combined treatment

Macroscopically, after 10 weeks of treatment with TAA i.p. in combination with EtOH, the murine livers were slightly enlarged with an irregular nodular liver surface compared to a liver from healthy non-treated control mice (figure 9).

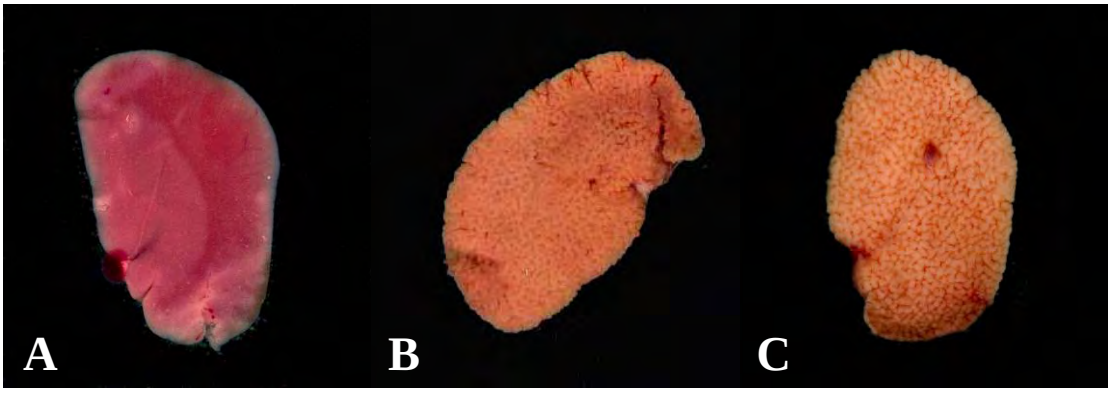

Figure 9 Representative photographs of murine left liver lobes taken from non-treated control C3H/He mice (**A**) and from mice treated with the TAA i.p. and EtOH combination after ten weeks of fibrosis induction (**B**). At week 10, a micronodular organ surface could already be noted and was obvious after 15 weeks (**C**) of TAA i.p. and EtOH treatment.

The macroscopically changes of the liver surface are identified as micro-nodular (< 3mm). However, it is questionable whether the human classification, which has been validated for Homo sapiens, is suitable for small rodents.

4.1.1.4 Histological changes of the murine liver during fibrosis induction

For fibrotic remodeling documentation, a van Gieson staining was used to show the position of intrahepatic ECM extracellularly. At the onset of fibrosis

induction and at week 5, 10 and 15, liver samples were taken, embedded in paraffin, cut and stained for van Gieson, HE and von Willebrand factor. The van Gieson staining colors connective tissue, in this case the ECM fibers, light red and the intracellular cytoplasm yellow to light brown. Figure 10 shows van Gieson staining performed in an untreated healthy control mouse (figure 10A). Figure 10A represents a close-up picture of a portal field in a healthy liver. Figures 10B and C show structural changes due to fibrosis induction via TAA i.p. monotherapy or by TAA i.p. and EtOH combination. The typical organization structure of a regular portal field is as follows: the central vein is located in the center with five portal tracts surrounding it. A normal portal tract is composed of a branch of the hepatic artery and the interlobular bile duct of approximately the same diameter and a branch of the portal vein of more than three times the diameter of the artery (Roskams, Baptista et al. 2003). In contrast to these regular portal fields in healthy mice, the architecture in liver from treated mice shows remarkable changes which are more or lest manifested. After 15 weeks of combined treatment with TAA i.p. and EtOH in drinking water, a remarkable change in the liver architecture was observed. Here, fibrosis was characterized by fibrotic septa, traversing the lobular liver parenchyma by porto-porto bridging resulting in a nodular pattern formed by so-called pseudolobuli (figure 10C). The majority of bridging was porto-porto bridging. Almost no porto-central bridging was observed at this time point of fibrosis induction.

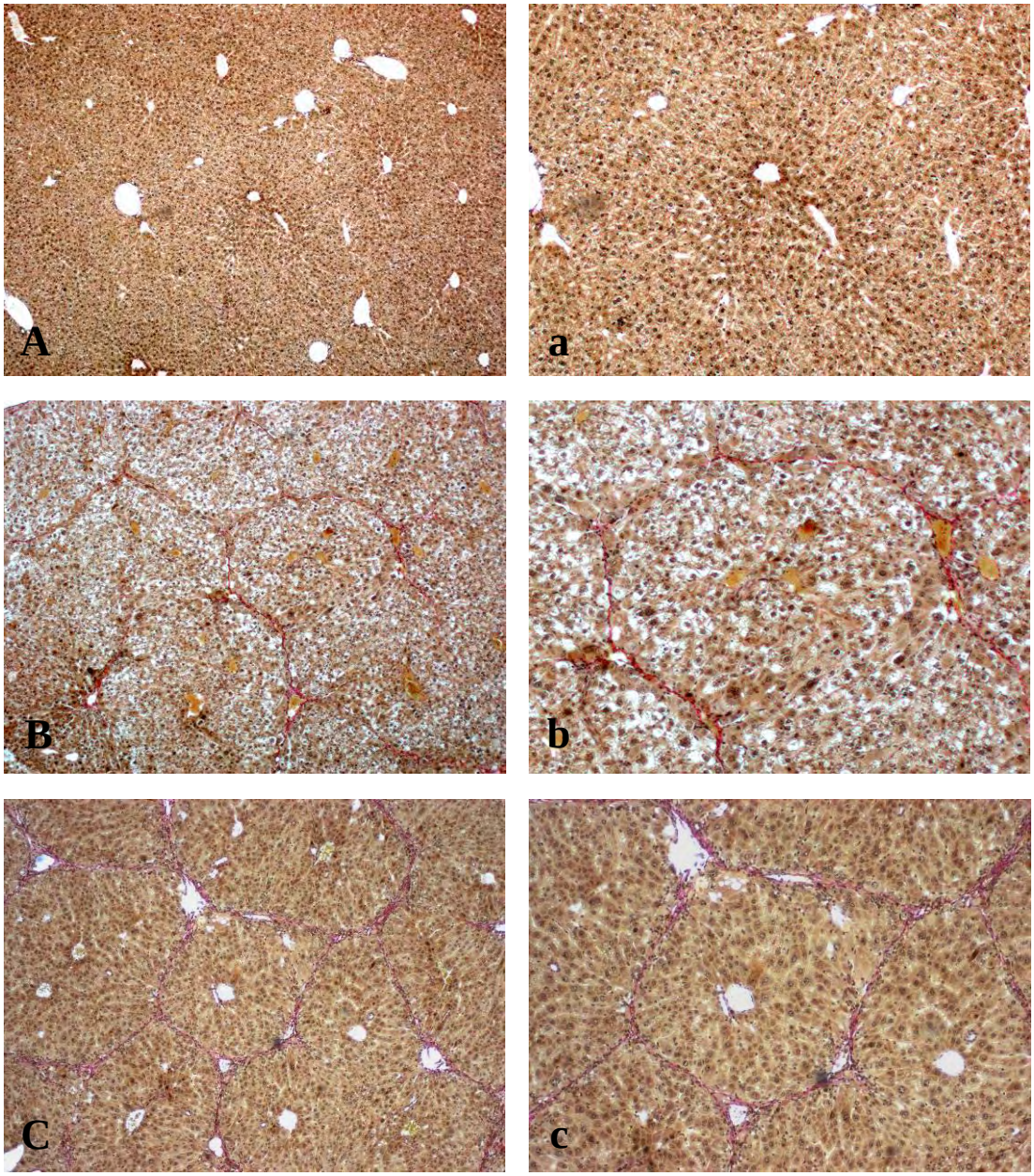

Figure 10 Progression of liver fibrosis in C3H/He mice. Liver fibrosis was assessed by van Gieson staining 15 weeks after treatment onset with TAA i.p. monotherapy or TAA i.p. and EtOH combination. Scoring of fibrosis was performed according to the score system proposed by Ishak et al. (Ishak, Baptista et al. 1995): **A/a** Untreated liver, liver-cell alignment (score F0); **B/b** 15th week of TAA i.p. monotreatment, fibrous septa areas were less defined and discontinuous (score F2); **C/c** 15th week of TAA i.p. and EtOH feeding, obvious pseudolobuli appearance and liver parenchyma regeneration (score F4). Original magnification 40x (A-D) or 64x (a-d).

In comparison to mice treated with the combined treatment of TAA and EtOH in the drinking water, the group which was only treated with the TAA i.p. monotherapy, demonstrated an increase in fibrotic fibers, resulting in incomplete

septal bridging with vague modularity of the parenchyma and mainly formation of incomplete, blind ending septa, resulting in portal fibrosis after 15 weeks (score F2, figure 10B).

Interestingly, at week ten after fibrosis induction by TAA i.p. and EtOH co-administration, an ongoing inflammation was observed around the developing fibrotic septal areas. Additionally, a dense mix of infiltrate lymphocytes could be identified around these areas. These changes concerning architecture and inflammation were visualized with HE staining at week ten (figure 11). For verification and validation purposes, the observed inflammation was additionally mirrored in elevated ALT blood serum values (see paragraphs below).

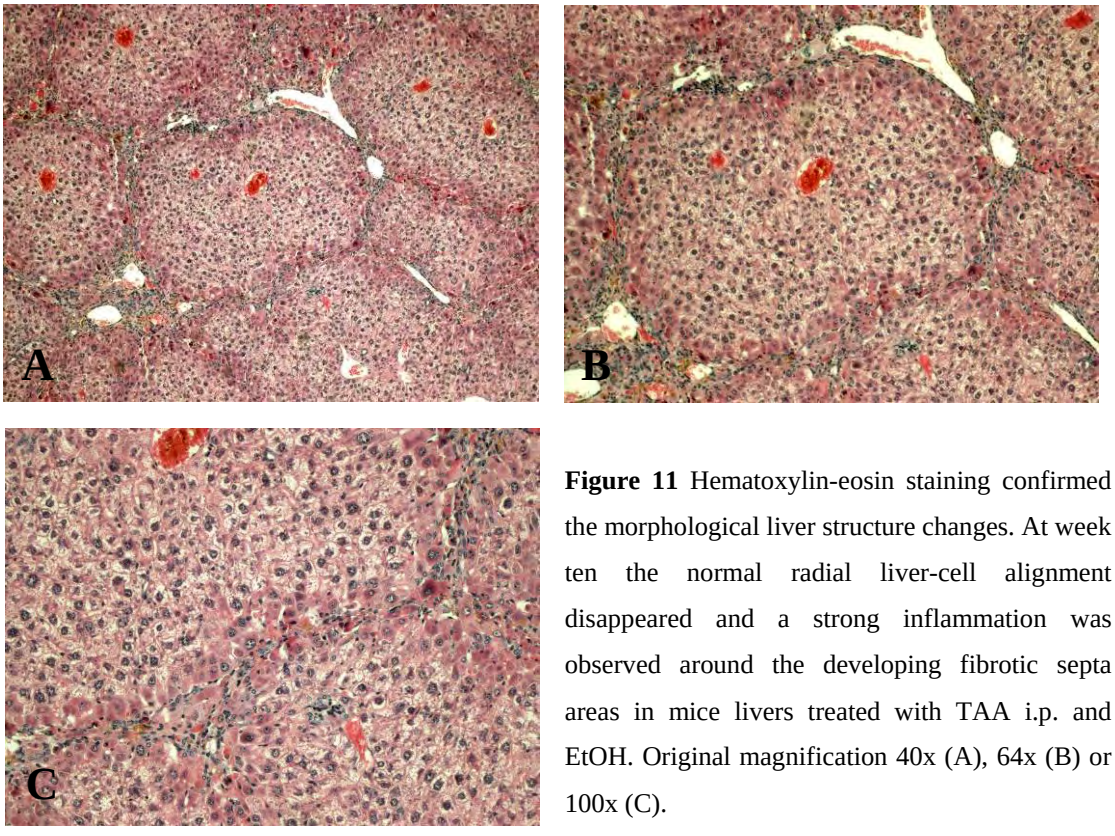

Figure 11 Hematoxylin-eosin staining confirmed the morphological liver structure changes. At week ten the normal radial liver-cell alignment disappeared and a strong inflammation was observed around the developing fibrotic septa areas in mice livers treated with TAA i.p. and EtOH. Original magnification 40x (A), 64x (B) or 100x (C).

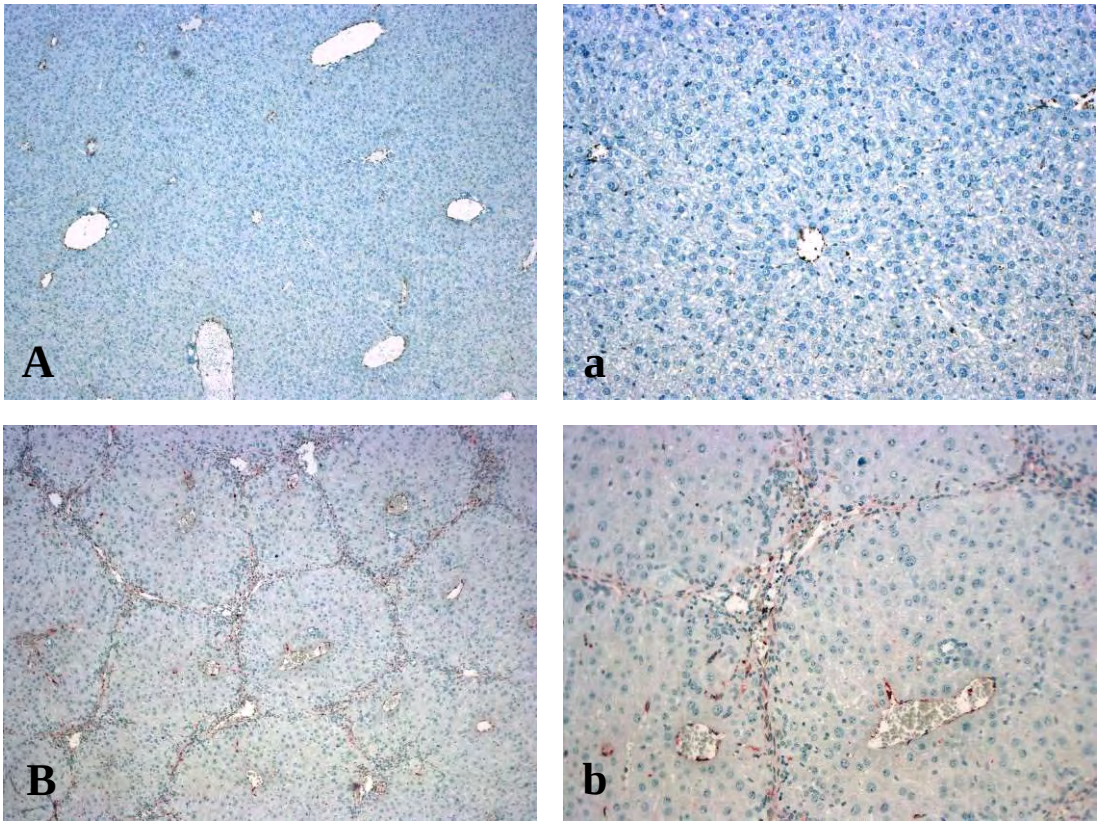

Figure 12 Appearance of von Willebrand factor positive structures in fibrotic C3H/He mice. Vascular sections were detected by vWF immunolabeling on liver sections (A/a and B/b). **A/a** Untreated liver, vWF expression was restricted to the endothelium of central veins and of portal veins; **B/b** 15th weeks of TAA i.p and EtOH feeding, vWF-labeled endothelial cells were observed within most of the septa in fibrotic liver samples. Original magnification 40x (A/B) or 64x (a/b).

To investigate effects on liver angiogenesis, the blood vessel density was quantified using vWF staining. The von Willebrand factor is one of the most useful markers to identify endothelial cells which form the blood vessels and it is therefore considered to be useful in measuring angiogenesis.

Although the overall number of major blood vessels was not significantly influenced (control 18.6/HPF vs. TAA/EtOH 21.5/HPF at week 15, p=0.1338 figure 13), vWF-labeled structures (≈ capillary vessels) were increased within fibrotic bridges (figure 12).

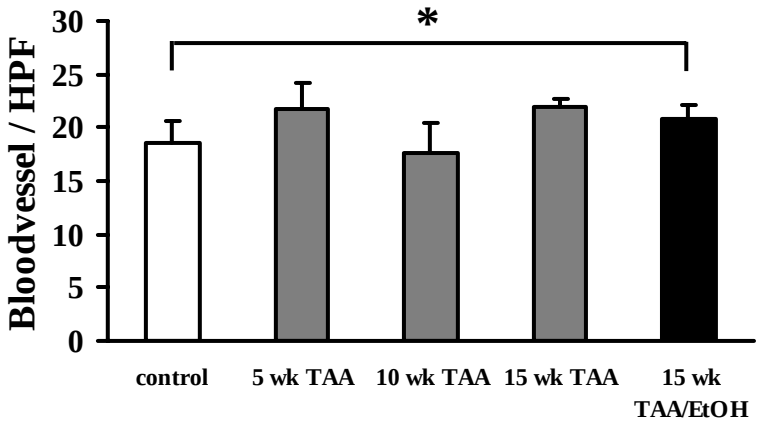

Figure 13 Hepatic blood vessel density in fibrotic C3H/He mice at different time points of fibrosis induction with the TAA i.p. monotherapy or TAA i.p. and EtOH co-administration. vWF stained liver sections were divided into high power fields and major blood vessel numbers were analyzed The data represent mean ± SEM; *p=0.13.

It has been known that fibrosis-cirrhosis is associated with an increase in microvascularization, as a result of the reduced hepatic microcirculation due to the septal shunt. However, vWF staining is limited to larger vessels rather than microvenues or single endothelial cells and LSECs (liver sinusoid endothelial cells).

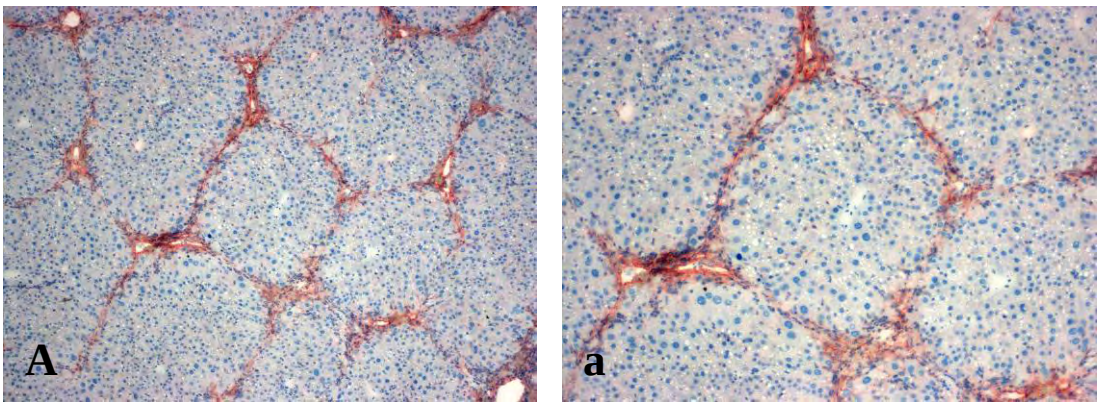

Figure 14 Representative ICAM-1 staining in samples taken from fibrotic C3H/He mice treated with the TAA i.p. and EtOH co-administration at week 15. ICAM-1 (CD54) was dominantly expressed in fibrotic septa area and not in the liver parenchyma. Original magnification 40x (A) or 64x (a).

In view of this limitation, additional anti-ICAM-1 immunohistochemistry was done to verify the previous vWF data. ICAM-1 is also supposed to be a marker of activated endothelial cells which are able to migrate (Janeway, Travers et al. 2005). The ICAM-1 staining results showed a denser liver ICAM-1 staining in fibrotic liver samples in septal areas (figure 14). This observation was quantitatively verified with ICAM-1 Elisa, performed in corresponding liver samples.

4.1.1.5 Expression changes in relevant fibrosis biomarkers during induction of fibrosis with the combination of TAA i.p. and EtOH

Development of liver fibrosis and cirrhosis can be characterized by the use of bio-markers. Among these, MMP-2 and alpha 1 procollagen (I) as two possible markers of fibrosis were selected to verify successful fibrosis induction (Kornek, Raskopf et al. 2006). In experimental studies, it has been shown that fibrosis is correlated with elevated VEGF levels. Other complementary supportive markers were chosen to verify histological findings and to quantify them, including ICAM-1 and TIMP-1 Elisa. To confirm ongoing hepatic inflammation, ALT measurement in serum was performed.

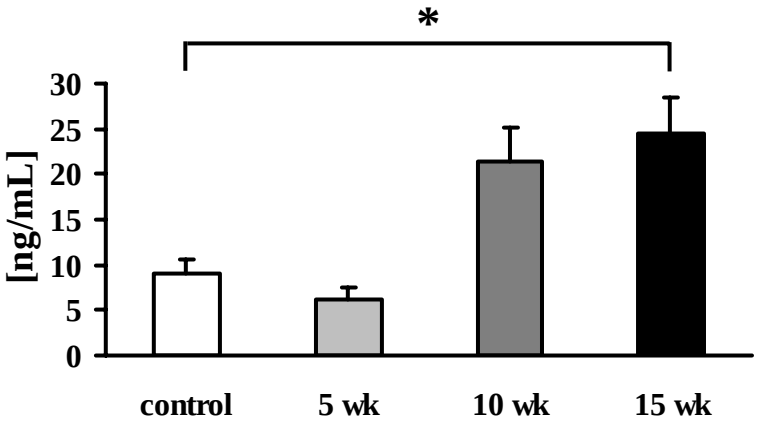

Figure 15 Hepatic MMP-2 levels were 2.7-fold increased during fibrosis development after 15 weeks of fibrosis induction with TAA i.p. and EtOH compared to control non-fibrotic mice. The data represent mean ± SEM; *$p<0.0001$.

To characterize known features of fibrosis induction in this model, MMP-2 expression was determined and evaluated and it showed a significant 2.7-fold increase during the course of fibrosis development after 15 weeks of TAA i.p. and EtOH feeding (control: 9 ng/mL, 15th wk TAA i.p. and EtOH: 24.5 ng/mL, $p<0.0001$; figure 15).

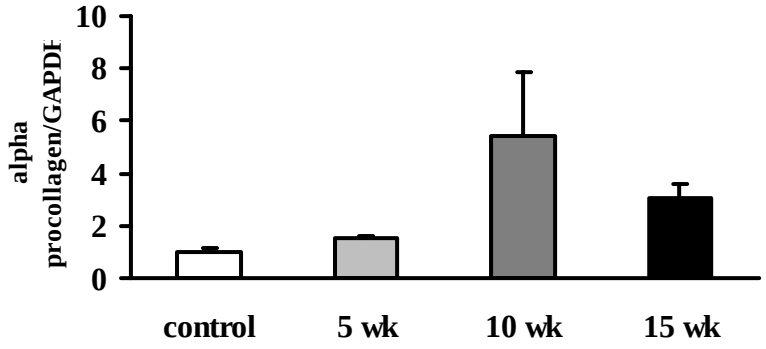

Figure 16 Hepatic transcript levels of alpha 1 procollagen (I) was determined relative to GAPDH mRNA levels by quantitative real time PCR, before and after combined TAA/EtOH treatment at week 5, 10 and 15. The data represent mean ± SEM.

Alpha 1 procollagen (I) transcript levels were quantitatively analyzed in mRNA samples taken from fibrotic livers at different time points after fibrosis induction with the TAA i.p. and EtOH combination and also as control before induction. Hepatic mRNA transcript levels were 3.9 and 2.2-fold higher at week 10 and 15 in fibrotic mice compared to untreated controls (figure 16) indicating enhanced collagen type I production associated with ongoing liver injury and fibrosis development.

In contrast to the previously described observations, no significant differences in the hepatic vascularization with larger blood vessels between control murine livers and fibrotic murine livers taken at different time point were recognized. Interestingly, fibrosis induction itself was associated with hepatic VEGF up regulation in protein level in TAA+EtOH treated mice. A high peak of intrahepatic VEGF were detectable

at week 10 of fibrosis induction with TAA i.p. and EtOH (261 pg/mL, 10th week: TAA+EtOH: 483 pg/mL, p=0.0015, figure 17).

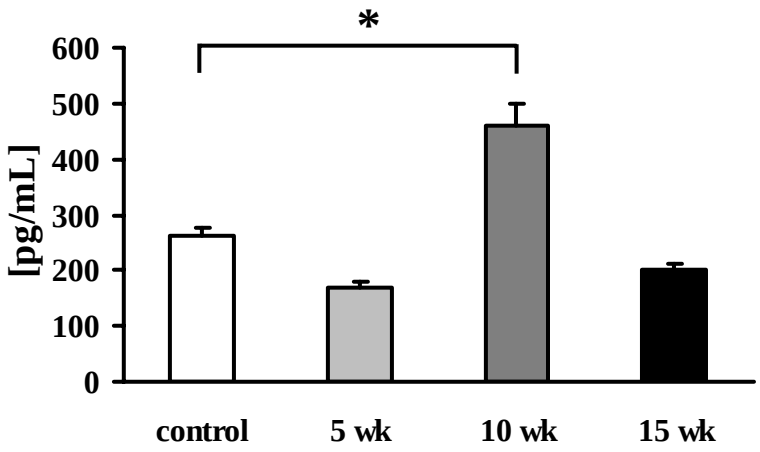

Figure 17 Hepatic VEGF protein levels in untreated C3H/He mice and after TAA+EtOH treatment at week 5, 10 and 15 of fibrosis induction. A hepatic VEGF up regulation in protein level has been monitored during liver fibrosis development at week 10. The data represent mean ± SEM; *p=0.0015.

To verify the previous ICAM-1 histology data with a second independent readout, an ICAM-1 Elisa was performed. In line with the ICAM-1 staining results, the ICAM-1 Elisa showed elevated hepatic ICAM-1 values in protein levels in homogenized fibrotic liver samples at different time points compared to control mice, up to 3.5-fold higher in cirrhotic mice at week 15 of treatment (score F4).

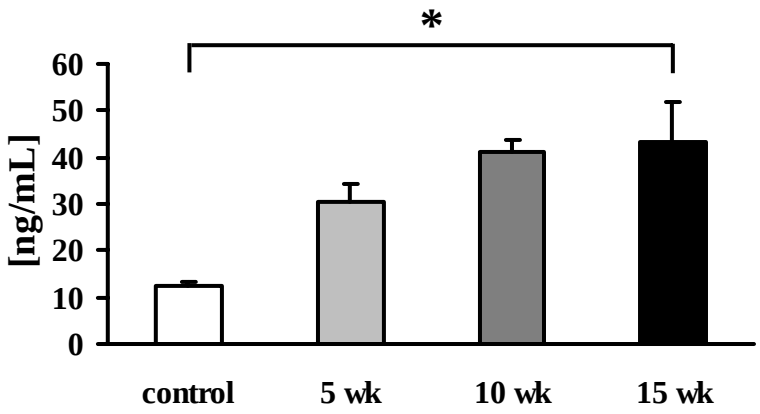

Figure 18 Hepatic ICAM-1 values were 3.5-fold higher than in control C3H/He mice at week 15 and the progression of fibrosis was paralleled by increased ICAM values. The data represent mean ± SEM; *p=0.0044.

Complementarily increased liver ICAM-1 levels correlated well to fibrosis progression as shown by van Gieson staining and fibrosis grading (control 12.24 ng/mL, at week 15, TAA+EtOH 43.28 ng/mL, p=0.0044; figure 18).

In contrast to the ICAM-1 and MMP-2 Elisa data, which indicate a relationship between fibrosis grade and hepatic ICAM-1 and MMP-2 proteins, TIMP-1, an inflammatory marker, was only slightly significantly elevated in fibrotic mice at stage F4 (control 0.476 ng/mL vs. TAA+EtOH 0.751 ng/mL, p<0.0001 at week 15), while a significant peak level was seen 10 weeks after treatment initiation with TAA i.p. and EtOH (control 0.476 ng/mL vs. TAA+EtOH 8.87 ng/mL, p<0.0001; figure 19).

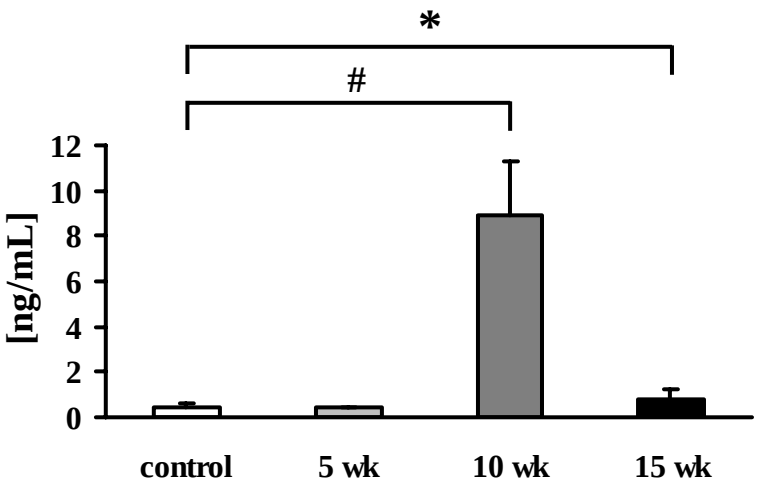

Figure19 At week 10, a high peak of hepatic TIMP-1 protein was monitored in homogenized liver samples from mice treated with TAA i.p. and EtOH, 18.5-fold higher than in control mice, otherwise no significant elevation was observed. The data represent mean ± SEM; *$p<0.0001$, $^{\#}p<0.0001$.

Hepatic damage by liver mediated inflammation as described by inflammatory reactions around fibrotic septa (figure 3) at week 10 (TAA+EtOH group) in HE histology samples were mirrored by increased systemic ALT levels of up to 2290 U/L (Figure 20) at the same time point of fibrosis induction with TAA i.p and ethanol. After 15 weeks, the ALT values decreased to almost normal levels of control mice (week 10, TAA+EtOH: 2290 U/L, week 15, TAA+EtOH: 89 U/L, p=0.0136].

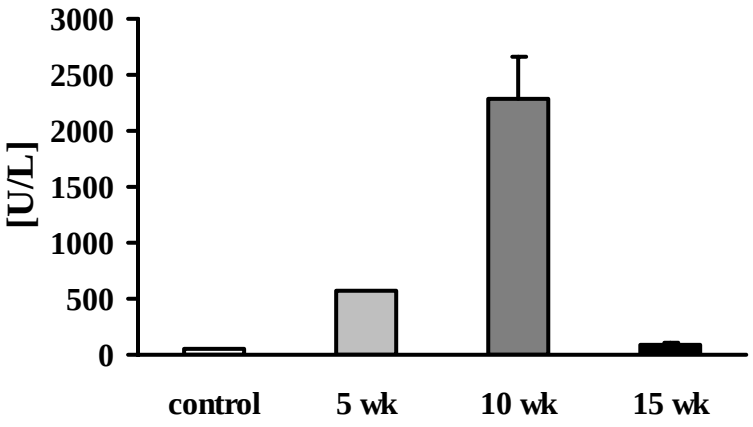

Figure 20 Blood serum ALT values evaluation during fibrosis development in TAA+EtOH treated C3H/He mice. ALT levels increased to 2290 U/L at week 10, and decreased to almost normal levels in control mice after 15 weeks.

4.2 Fibrotic HCC metastatic model establishment

To characterize the effect of liver fibrosis on hepatic metastatic tumor cell growth, an accepted and recognized method for metastatic tumor cell seeding was chosen. Syngenic HCC tumor cells were injected into the spleen to reach the liver *via* the blood stream, to adhere to and set off malign transformation of the liver. Since intrahepatic ICAM-1, an adhesion protein, was elevated in fibrotic mice, the efficiency of tumor cells, which arrive with the blood stream, might be more increased in a pre-damaged fibrotic liver than in healthy mice and therefore, more HCC satellites should be observed in a fibrotic liver.

Nine days after tumor implantation into spleens, operated control mice and fibrotic mice were examined after laparotomy for the presence of HCC satellites on the liver surface or for solid tumors (figure 21).

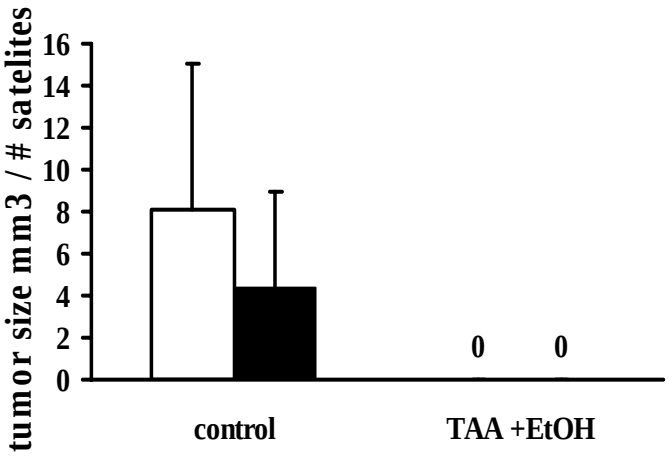

Figure 21 Metastatic HCC satellites count in pre-damaged liver in fibrotic mice (black bar) and in healthy non-fibrotic mice and tumor volume (white bar), nine days after tumor cell implantation into the spleen. The data represent mean ± SD.

No hepatic metastases were identified on the fibrotic liver surface, also no solid tumor growth. In contrast to this observation, on healthy non-fibrotic livers, taken from control mice, several HCC satellites and hepatic tumors, formed by HEPA129, cells were counted or measured on the liver surface. Tumor growth was evaluated by calculating tumor volume from visible tumor diameters on the liver surface.

To investigate possible intrahepatic metastasis appearance in fibrotic mice livers and to exclude misinterpretation of the previous findings, corresponding tumor samples were embedded in paraffin and stained for van Gieson to visualize intrahepatic HCC satellites, besides stained ECM (figure 22).

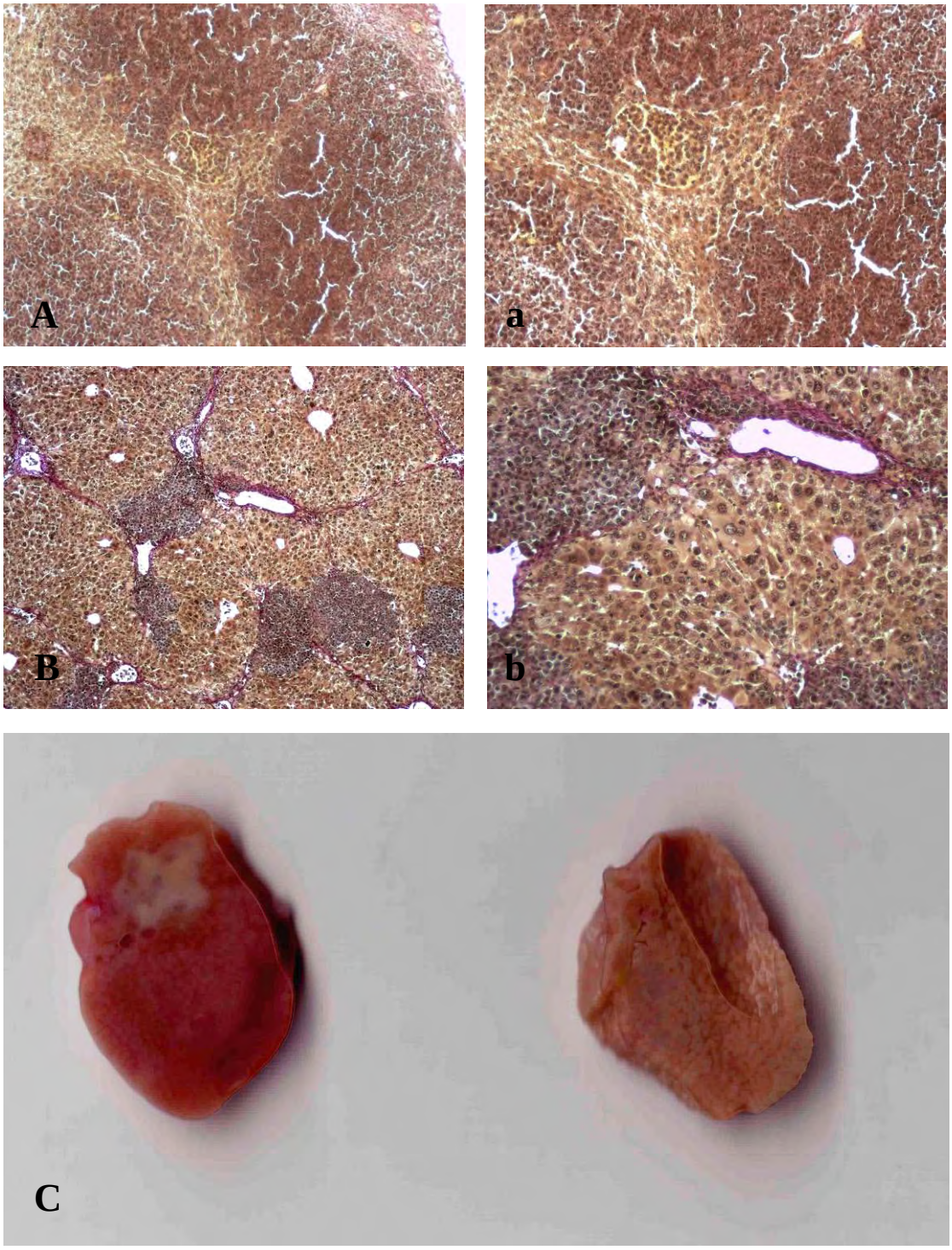

Figure 22 Intrahepatic HCC satellites appearance at fibrotic or non-fibrotic livers after intrasplenic tumor cell implantation was evaluated by van Gieson staining in healthy mice post surgically (**A**/**a**) and in fibrotic mice (**B**/**b**). Line up of murine left liver lobes, taken from healthy mice, shows a HCC tumor at the liver surface as a result of infiltrating tumor cells (**C**, left) or in case of fibrotic mice, a micronodular organ surface only due to fibrosis induction, but no HCC satellites or tumor appearance (**C**, right). Original magnification 40x (A/B) or 100x (a/b).

Interestingly, fibrotic mice livers showed no obvious surface HCC satellites or tumors nine days after implantation, but intrahepatically, presence of small tumor cell accumulations were observed in corresponding paraffin section after a van Gieson staining. In contrast to this finding, in healthy mice, migration of tumor cells from the spleen to the liver occurred, resulting in a visible liver surface tumor and surface HCC satellites nine days after implantation of tumor cells into the spleen. However, intrahepatically almost no further HCC tumor cells accumulations were observed in healthy mice as described in fibrotic mice (figure 22).

4.3 Characterization of a novel orthotopic HCC model in fibrotic C3H/He mice

Due to the misleading results of the previous attempt to combine the new murine fibrotic C3H/He model, induced by TAA i.p. and EtOH, with the metastasis model based on direct implantation of tumor cells into the spleen, another strategy was chosen to accomplish the establishment of a reliable and easy to analyze orthotopic HCC model in pre-fibrotic mice. The direct implantation of HCC tumor cells into the pre-damaged fibrotic liver was chosen as an alternative method and also as an accepted approach to generate intrahepatic tumor growth.

4.3.1 Validation of possible hypoxia induction by fibrosis and in the tumor by HM measurement and HIF-1 alpha determination

Fibrosis induction was verified with help of indirect hepatic microcirculation (HM) blood flow analysis, as described before, showing a relative reduction of relative absorption units (AU) in fibrotic mice, significant by about 55% at week 19 after induction of fibrosis (figure 23, $p<0.0001$).

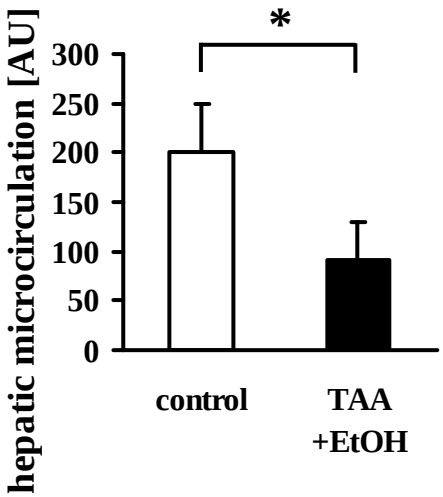

Figure 23 Hepatic microcirculation (HM) was measured in the left liver lobe during laparotomy under anesthesia one week before tumor cell implantation into non-fibrotic control mice (white bar) or fibrotic mice (black bar) showing a significant reduction by 55%. The data represent mean ± SD; *p<0.0001.

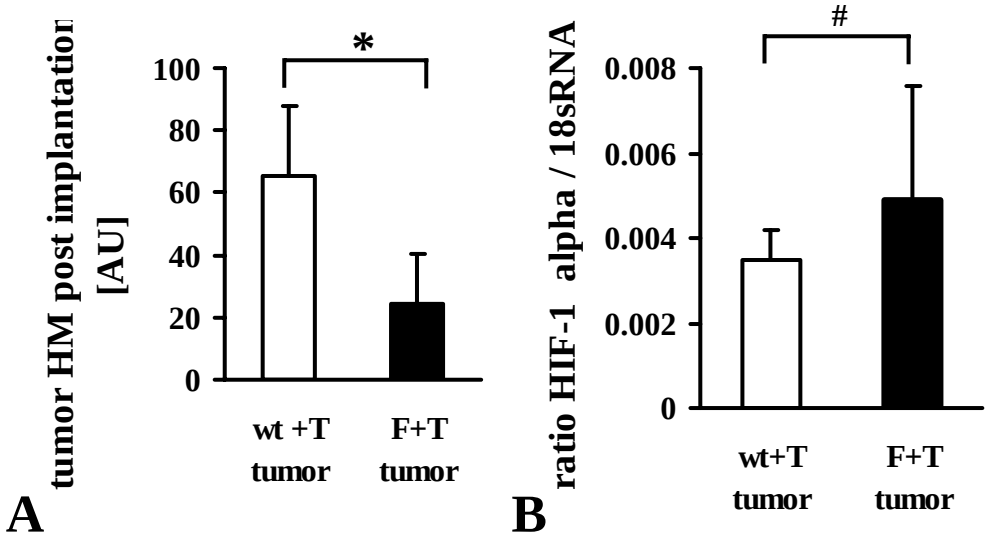

Figure 24 Intratumoral hepatic microcirculation (HM) was measured in hepatic tumors ten days after tumor cell implantation (**A**) and relative HIF-1 alpha mRNA transcription levels from intrahepatic tumor samples (**B**). Gene transcription is presented as ratio to 18sRNA housekeeping gene (n=5). The data represent mean ± SD; *p<0.0001, # p=0.0754.

Thus, ten days after implantation, a further HM measurement was performed in both cohorts. Additionally, HIF-1 alpha transcription was analyzed in tumor samples taken from non-fibrotic and fibrotic mice (figure24).

Reduced HM in fibrotic mice (figure 24) was mirrored by a similar intratumoral HM reduction which reached only about 63% of HM in fibrotic mice compared to non-fibrotic tumor bearing mice. It can be speculated that reduced HM in fibrosis results in a higher degree of intratumoral hypoxia in pre-damaged fibrotic mice (intratumoral HM 65.6 AU non-fibrotic vs. 24.2 AU fibrotic mice, $p<0.0001$, figure 24A). Correspondingly, hypoxia responsive transcription factor HIF-1 alpha was elevated in tumors of fibrotic mice (figure 24B), albeit not significantly so, but this indicates hypoxia in tumors taken from a fibrotic environment.

4.3.2 Orthotopic HCC tumor growth and metastasis in fibrotic mice

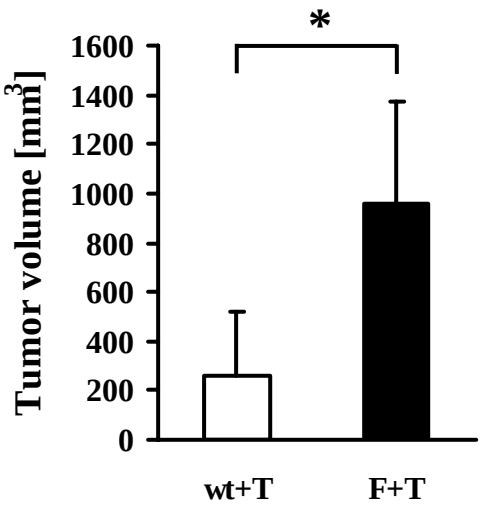

Figure 25 HCC tumor volume measurements in pre-damaged liver in fibrotic mice (black bar) and in healthy non-fibrotic mice (white bar) ten days after tumor cell implantation. The data represent mean tumor volumes ± SD; *p=0.009.

Tumor growth was evaluated by calculating tumor volume from visible tumor diameters on the liver surface (figure 25). Mean tumor sizes were 3.7-fold increased in fibrotic mice compared to non-fibrotic controls (956 mm^3 vs. 260 mm^3 in fibrotic and non-fibrotic mice, p=0.009, figure 25). Furthermore, the mean number of surface HCC satellites was markedly higher in fibrotic mice (mean 27) compared to non-fibrotic controls (mean 3.1, p=0.0006, figure 26).

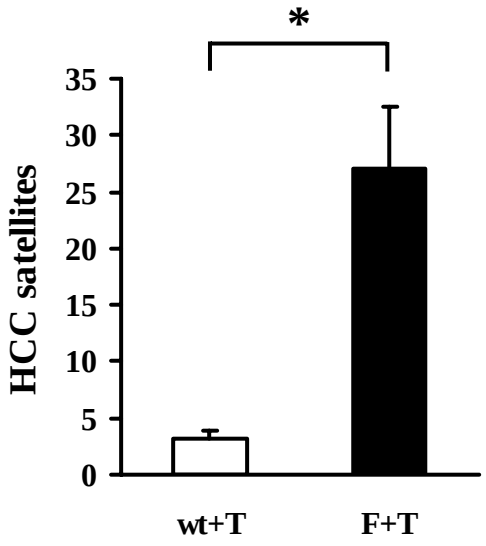

Figure 26 HCC satellites count in pre-damaged liver in fibrotic mice (black bar) and in healthy non-fibrotic mice (white bar) ten days after tumor cell implantation. The data represent mean amount of counted liver surface HCC satellites; ± SD; p=0.0006.

4.3.3 Histological and immuno-histological assessment of fibrosis

In order to verify fibrosis induction, a van Gieson staining was performed in paraffin sections from both, fibrotic and non-fibrotic groups. Similar to our previous publication (Kornek, Raskopf et al. 2006) livers of TAA i.p. and EtOH treated mice showed fibrotic septa with predominantly porto-porto bridging (figure 27A/a/B7b). When applying the Ishak scoring system (Ishak, Baptista et al. 1995), fibrosis was graded as F4 (maximum score F6) in the implanted mice.

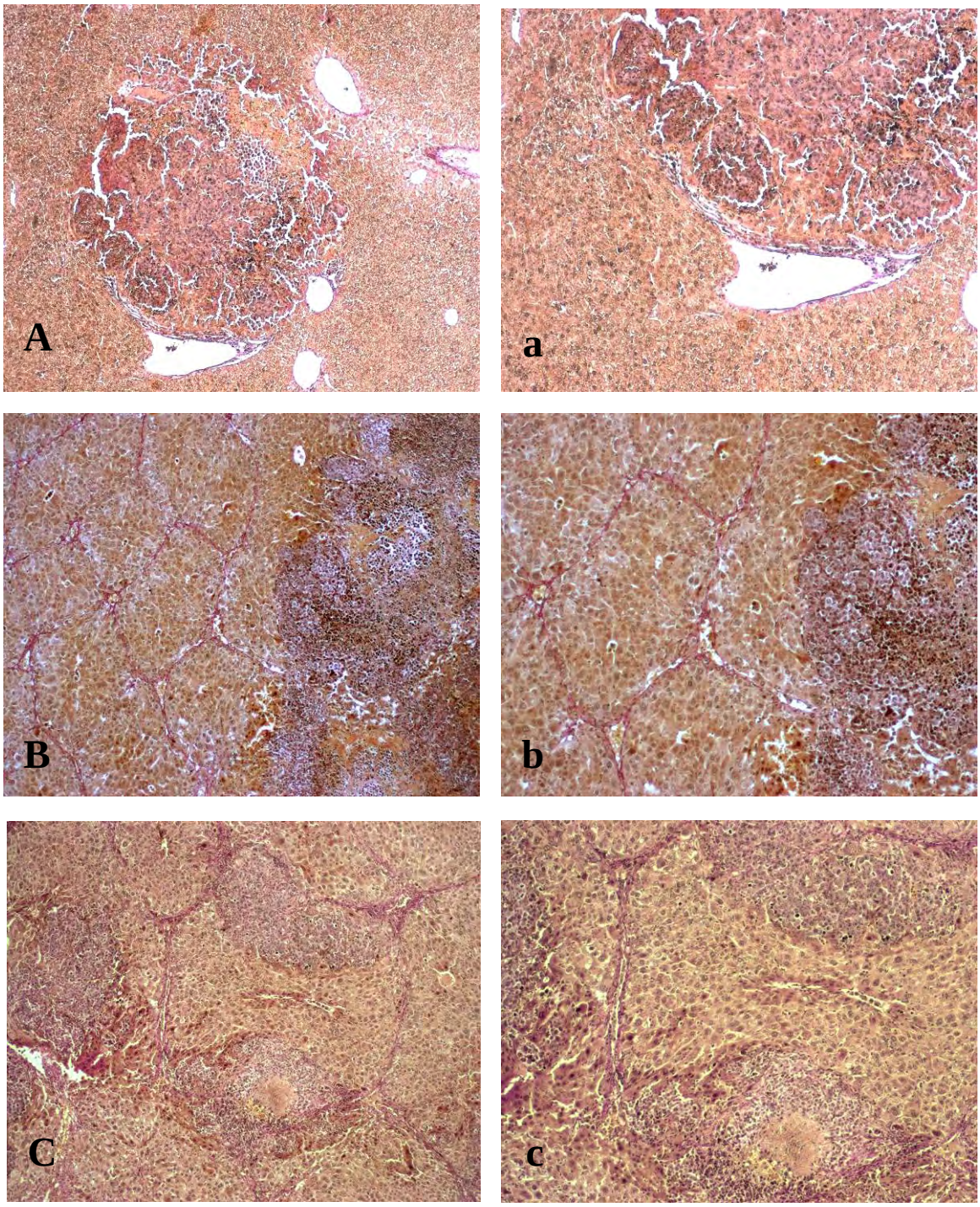

Figure 27 Representative van Gieson staining of paraffin sections taken from implanted non-fibrotic control liver (A/a) or fibrotic liver (B/b and C/c) ten days after HCC tumor implantation into livers. Scoring of fibrosis was performed according to the score system proposed by Ishak et al. (Ishak, Baptista et al. 1995). Original magnification 40x (A/B/C) or 100x (a/b/c).

Surprisingly, the tumor growth was restricted to the implantation site in the non-fibrotic controls. However, the tumors were larger at the primary injection site and tumor satellites were widely spread into the pre-damaged fibrotic livers (figure 27C/c).

As proof that the identified tumor satellites were still growing, proliferation of single tumor cells and major tumor front were demonstrated by Ki-67 staining on cryo section taken from tumor cell implanted fibrotic mice liver and as a control from implanted non-fibrotic mice (figure 28).

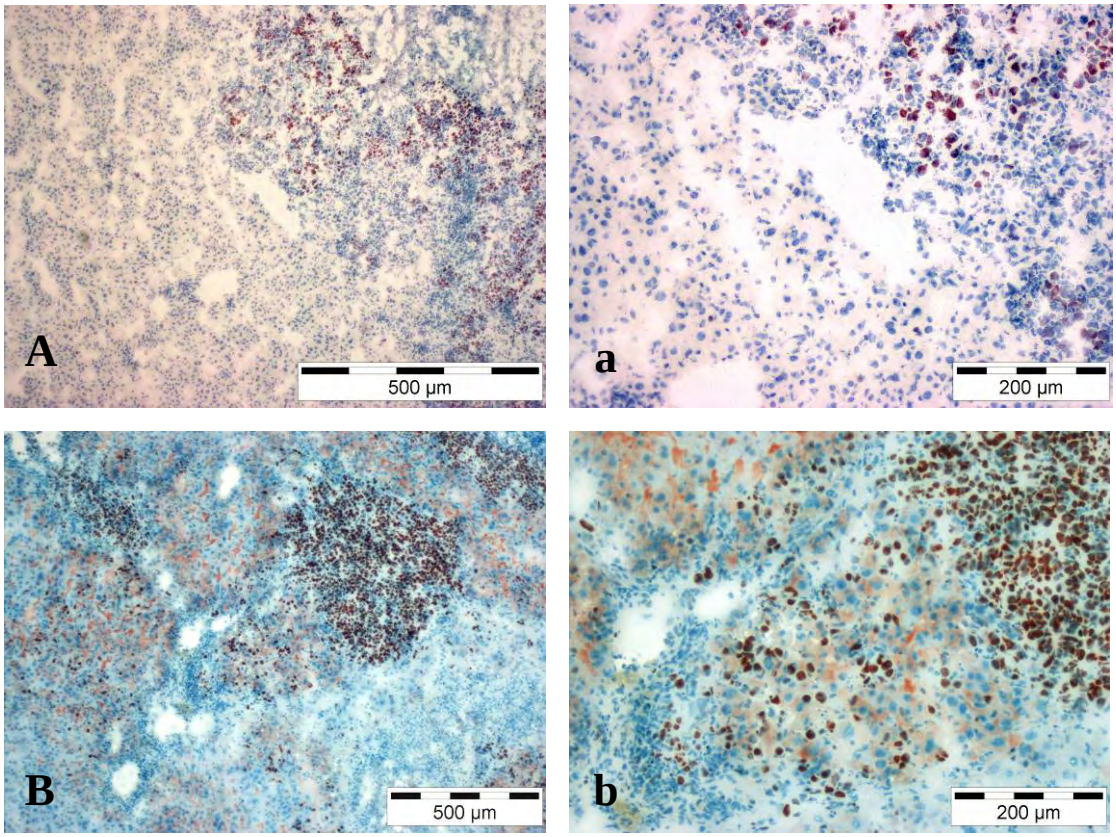

Figure 28 Representative photographs of cryo sections positive for Ki-67 proliferation marker for determination of proliferating cells intratumoral in non-fibrotic mice (A/a) show no infiltration of Ki-67 positive cells into the tumor surrounding, no fibrotic liver parenchyma and only a weak proliferation in the tumor itself. In pre-damaged fibrotic mice, tumor satellites were positive for Ki-67 and, additionally, single positive Ki-67 cells were observed infiltrating the fibrotic liver parenchyma (B/b). Original magnification 40x (A/B) or 100x (a/b).

4.3.4 Determination of serum sVEGF levels

To evaluate the impact of fibrosis and tumor presence on systemic serum VEGF levels, blood was taken to determine circulating VEGF-A. In tumor bearing mice, tumor cell implantation had been performed ten days before VEGF analysis. In agreement with previously published data, serum VEGF levels did not differ between fibrotic and non-fibrotic mice at this time point. Then, a VEGF incline had been observed at an earlier stage of fibrosis induction (week 10, (Kornek, Raskopf et al. 2006)). The establishment of intrahepatic Hepa129 tumors only slightly affected systemic VEGF levels in both groups, fibrotic and non-fibrotic tumor bearing mice, to a similar extent, with 1.3-fold (non-fibrotic, p=0.0013 and fibrotic, p=0.0048, figure 29) higher VEGF serum concentrations compared to the corresponding non-tumor bearing controls.

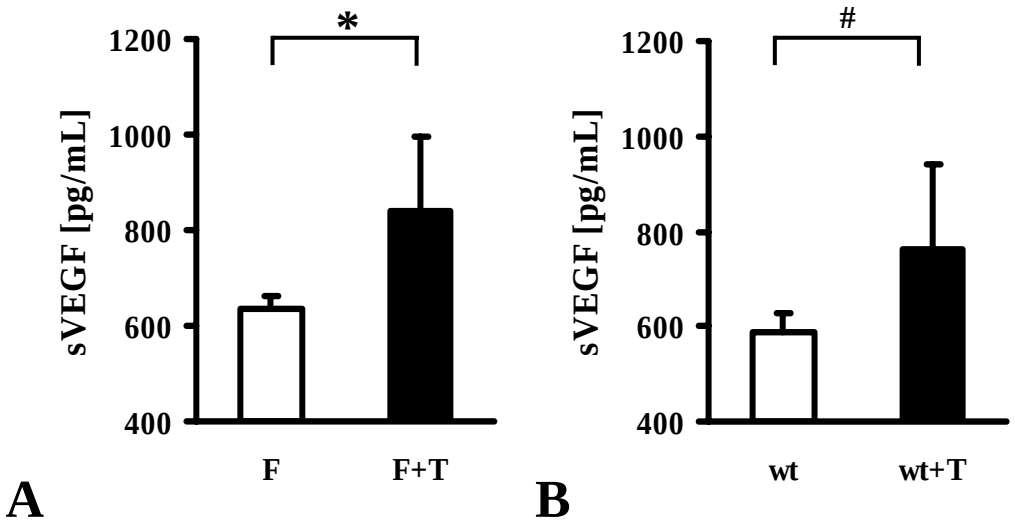

Figure 29 Serum soluble VEGF ELISA results taken from fibrotic mice before tumor cell implantation into pre-fibrotic livers (A; white bar) and ten days after implantation (black bar; A). And B, sVEGF serum results from healthy mice without tumor cell implantation (B; white bar) compared to sVEGF serum results from non-fibrotic tumor bearing mice (B; black bar) ten days after implantation. The data represent mean sVEGF values [pg/mL] ± SD; *p=0.0048, # p=0.0013.

4.3.5 Intratumoral VEGF-A and VEGF-C expression in fibrotic and non-fibrotic mice

To elucidate a possible role of tumoral VEGF-A transcription and to examine possible explanation of intrahepatic satellite formation induced trough tumoral VEGF-C transcript up regulation in this tumor model, the corresponding tumoral transcription levels were analyzed and presented as a ratio to 18sRNA housekeeping gene (figure 30). In respect to tumoral VEGF-A transcription, no significant difference (p=0.421) could be observed between fibrotic tumor tissue and non-fibrotic tumor tissue. Contrary to this finding, intratumoral VEGF-C transcription was significantly elevated (2.5-fold, p=0.0079) in fibrotic mice compared to tumor bearing healthy non-fibrotic mice. *In vitro*, VEGF-C was barely detectable, whereas VEGF-A was strongly expressed in cultured Hepa129 hepatoma cells (figure 33).

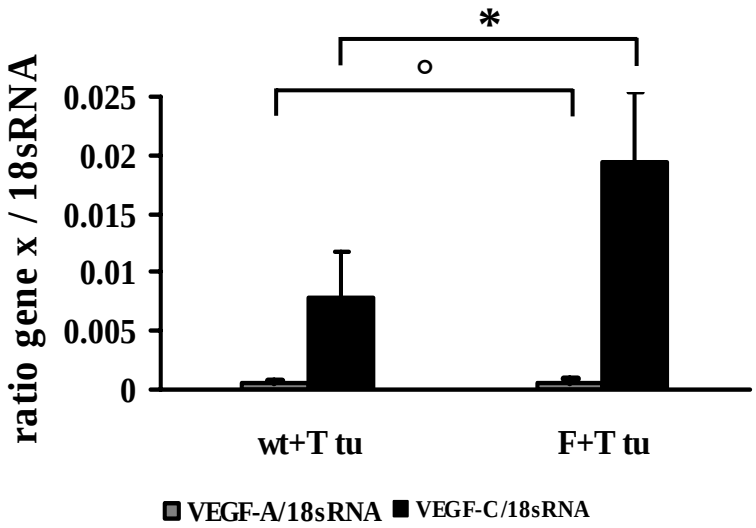

Figure 30 Semi-quantitative mRNA transcription levels were determined for tumoral VEGF-A mRNA and tumoral VEGF-C mRNA. Semi-quantitative gene transcription is presented as ratio to 18sRNA housekeeping gene (n=5). The data represent mean semi-quantitative transcript values ± SD; non-fibrotic intratumoral samples (wt+T tumor) or intratumoral samples of fibrotic mice (F+T tumor); *p=0.0079, °p=0.421**.**

4.3.6 Intratumoral VEGF-A receptor (KDR, Flt-1) and VEGF-C receptor (Flt-4) in fibrotic and non-fibrotic mice

To obtain a closer overview on the interplay between VEGF-A/-C and their main receptors, Flt-1 (KDR), Flk-1 and Flt-4 mRNA transcription levels were determined and presented as a ratio to 18sRNA as housekeeping gene (figure 31). Intratumoral Flt-1 and intratumoral Flk-1 (KDR) were 3.2-fold (p=0.0079) and 2.1-fold (p=0.004) increased, respectively, in fibrotic vs. non-fibrotic tumor bearing mice. Flt-4 was intratumorally up regulated to a similar extent in fibrotic mice compared to non- fibrotic mice (3.5-fold, p=0.0079).

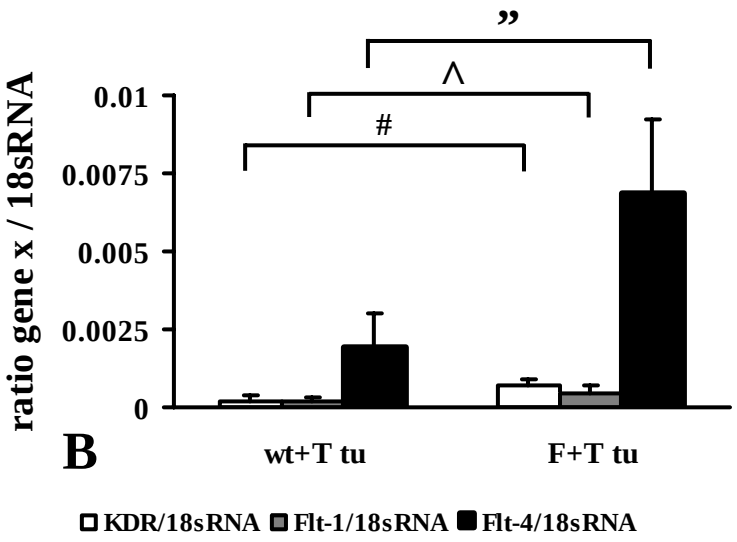

Figure 31 Semi-quantitative mRNA transcription levels were determined for intratumoral Flk-1/KDR, Flt-1 and Flt-4 transcripts. Tumoral gene transcription is presented as ratio to 18sRNA housekeeping gene (n=5). The data represent mean semi-quantitative transcript values± SD; non-fibrotic intratumoral samples (wt+T tumor) or intratumoral samples of fibrotic mice (F+T tumor); "p=0.0079, ^p=0.0079, #p=0.0004.

4.3.7 Intratumoral MMP-2 and MMP-9 transcription in fibrotic and non-fibrotic mice

MMP-2 and MMP-9 have been intensively studied as pro-tumoral and pro-metastatic markers. Particularly, MMP-2 and MMP-9 have been shown to bear an important pathophysiological role in tumor progression by degrading the ECM and vascular basal membrane. In this model, both markers were elevated in tumors of fibrotic mice compared to tumors of non-fibrotic mice with statistical significance. Intratumoral MMP-9 was 2.8-fold increased in fibrotic mice compared to intratumoral levels of non-fibrotic mice (p=0.0079, figure 32). In case of MMP-2, intratumoral transcription was 3 fold (p=0.004) up in fibrotic compared to non-fibrotic mice. Thus, these data further underline the tumor promoting role of fibrosis and particularly support the potential tumor promoting role of MMP-2 and also, to a lesser extent, of MMP-9.

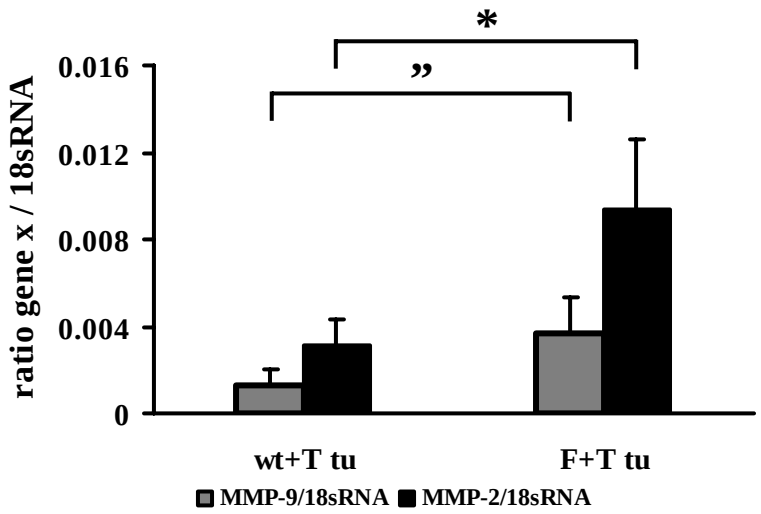

Figure 32 Semi-quantitative mRNA transcription levels were determined for intratumoral MMP-2 and intratumoral MMP-9 after tumor cell implantation into non-fibrotic or fibrotic mice. Intratumoral gene transcription is presented as ratio to 18sRNA housekeeping gene (n=5). The data represent mean semi-quantitative transcript values ± SD; non-fibrotic intratumoral samples (wt+T tumor) or intratumoral samples of fibrotic mice (F+T tumor); *p=0.004, “p=0.0079.

4.4 In vitro Hepa129 tumor cell line characterization before implantation on mRNA level

Surprisingly, Hepa129 *in vitro* data showed that in cultured tumor cells, almost no detectable VEGF-C transcription and its receptor Flt-4 occurred despite VEGF-A transcripts and these were on a higher level monitored compared to VEGF-C. Also, the transcription of KDR mRNA, the main VEGF-A receptor, occurred only on a very low level under *in vitro* conditions (figure 33). However *in vivo*, after implantation into a fibrotic mice liver or a non-fibrotic mice liver, the values of these important angiogenesis markers or metastasis bio markers change significantly as shown in previous chapters of this work.

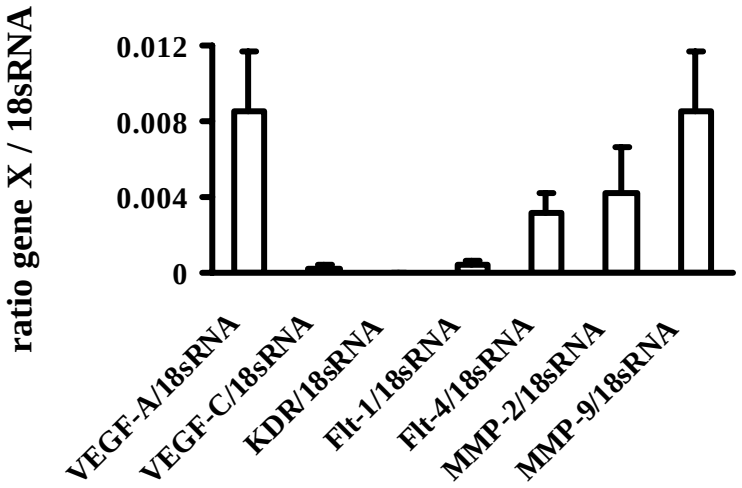

Figure 33 Summary of the *in vitro* characterizations of the applied Hepa129 hepatoma cells before implantation into fibrotic or non-fibrotic mice. Semi-quantitative gene transcription is presented as ratio to 18sRNA housekeeping gene (n=5). The data represent mean semi-quantitative transcript values± SD.

5 Discussion

5.1 Part I: The combination of systemic thioacetamide (TAA) injections with ethanol feeding accelerates hepatic fibrosis and is associated with intrahepatic up regulation of MMP-2, VEGF and ICAM-1

Treatment of HCC is challenging and improved animal models are needed for testing of innovative therapies. Hepa129 hepatoma cells have been demonstrated to be suitable for orthotopic tumor growth (Schmitz, Tirado-Ledo et al. 2004) and for therapeutic intervention studies in C3H mice (Raskopf, Dzienisowicz et al. 2005). The aim of the present thesis was to further enhance the transferability and relevance of the tumor cell implantation model to the clinical situation. For this purpose, it was intended to induce fibrosis with TAA, because CCl_4 application is known to be associated with high mortality in this mouse strain (Kuriyama, Yamazaki et al. 1999). Thus, the fibrotic potential of TAA was tested by injections alone and combined with ethanol (EtOH) feeding for fibrosis induction. Fibrosis was assessed by histology for van Gieson staining and by determining molecular fibrosis markers for MMP-2, sICAM-1 and alpha 1 procollagen (I). Inducing hepatic fibrosis by repetitive TAA (thioacetamide) injections and continuous EtOH feeding (10% v/v) in C3H/He mice led to a lower mortality rate than CCL_4 treatment in the same mouse strain. Interestingly TAA i.p. alone was not sufficient to induce liver fibrosis, whereas the combination of TAA i.p. and EtOH in the drinking water resulted in a considerably accelerated fibrosis induction. Fibrogenesis was characterized by typical histological changes besides protein level and steady state mRNA transcription measurement of alpha 1 procollagen (I) besides the quantification of typical fibrosis associated proteins as MMP-2, sVEGF and septal sICAM-1. All these biomarkers have been shown to be up regulated during fibrosis induction in small rodents and human.

Although in this TAA i.p. and EtOH fibrosis induction model the mortality was lower than in CCl_4 fibrosis (Hillebrandt, Goos et al. 2002), it was still considerably high in the combination group (TAA i.p. and EtOH), despite the fact that the TAA dose for i.p. injection (0.15 mg/g bodyweight) was lower than in previous publications. Based on TAA titration by others, three different doses were used , 0.2,

0.4 or 0.6 mg/g body weight twice a week, resulting in 30%, 70% or 80% mortality, respectively (Hillebrandt, Goos et al. 2002). In the present thesis, TAA (0.15 mg/g body weight three times a week) was applied i.p. in combination with EtOH in the drinking water. This combination led to a mortality rate of 38%, which was considered to be acceptable. When TAA was injected i.p. without additional EtOH feeding, the mortality was considerable lower (18%), but fibrosis induction was insufficient.

Combination of TAA/EtOH resulted in fibrosis stage F4 after 15 weeks, whereas TAA injection alone resulted in milder fibrosis (score F2), as measured by the Ishak scoring system (Ishak, Baptista et al. 1995). Liver fibrosis was characterized by fibrotic expansion of portal areas with marked porto-porto bridging disrupting the liver parenchyma. A similar finding was described by previous physiological studies of the liver, namely that the combination of CCL_4 and ethanol had the potential to enhance fibrogenesis in rat models (Siegers, Pauli et al. 1986; Bosma, Brouwer et al. 1988). One possible mechanism among others is that alcohol; here absolute EtOH diluted in sweetened drinking water (10% v/v), may have increased inflammation in the liver by induction of oxidative stress and thereby effectively have attenuated hepatocyte death, i.e., apoptosis and necrosis. (Higuchi, Kurose et al. 1996). Additionally it was reported that ethanol can be oxidized by liver microsomes. These microsomes, induced by EtOH, contributed to increased acetaldehyde generation. Acetaldehyde increased collagen transcription *in vivo* (Lieber 1993), as well as hepatic collagen expression *in vivo* (baboon model of alcoholic cirrhosis) and *in vitro* (cultured myofibroblasts and lipocytes) (Li, Kim et al. 1992; Lieber, Leo et al. 2003). Recent evidence provided a more detailed view on the relation between ethanol consumption and collagen expression (Holstege, Bedossa et al. 1994; Albano 2006; Kisseleva and Brenner 2006). It was shown that ethanol and/or its metabolites including acetaldehyde have direct effects on HSC activation. These effects might be mediated by ethanol/acetaldehyde and/or ethanol/acetaldehyde-induced oxidative stress and TGFβ1 expression, which activated signaling pathways leading to the binding of transcription factors to the type I collagen gene promoter (Wang, Batey et al. 2006). Therefore the marked acceleration of fibrogenesis in this setting was likely due to synergistic effect of TAA i.p. injections and EtOH feeding on the activation of HSCs.

Development of liver fibrosis and cirrhosis can be characterized by a large spectrum of molecular bio-markers. The most frequently applied, and therefore used in this study, are MMP-2 and alpha 1 procollagen (I). These are the two main parameters for fibrotic changes in the injured liver. During ongoing liver inflammation HSCs become activated and up regulate MMP-2 expression. One substrate for MMP-2 is collagen IV, a ubiquitous compound of normal liver matrix, which can be degraded during disease progression and substituted with collagen type I and III. This two collagen types are also produced by activated HSCs during inflammatory conditions, during which quiescent HSCs were converted to cells with a phenotype similar to myofibroblasts (figure 34).

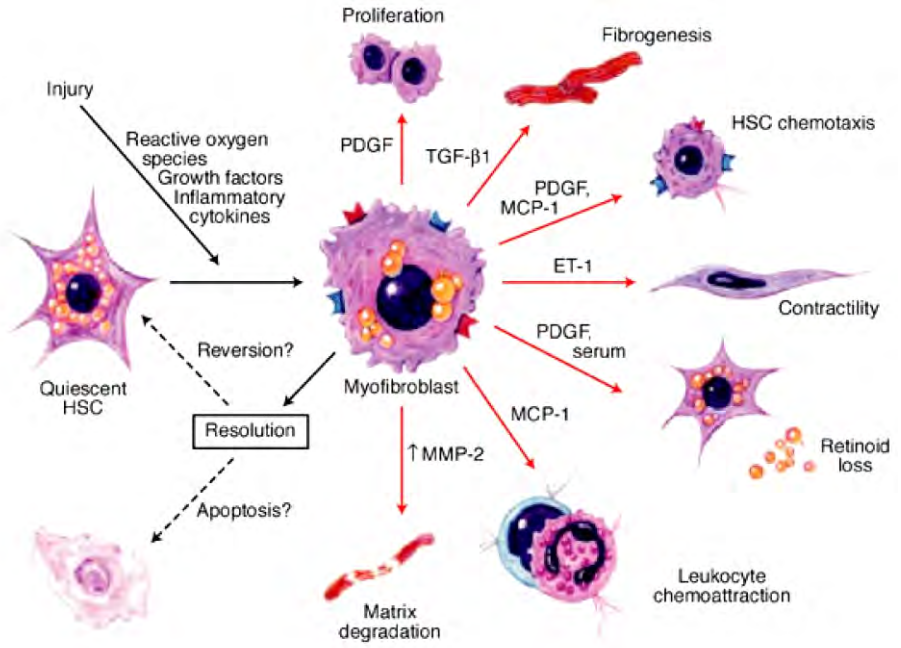

Figure 34 Phenotypic features of hepatic stellate cell activation during liver injury and resolution. Following liver injury, HSCs undergo activation mediated by reactive oxygen species, growth factors and inflammatory cytokines produced by hepatocytes, Kupfer cells, leukocytes, platelets and sinusoidal endothelial cells. This results in a transition from quiescent vitamin-A-rich HSCs into proliferative, fibrogenic, contractile myofibroblasts. The major phenotypic changes include proliferation, fibrogenesis, chemotaxis, contractility, retinoid loss, leukocyte chemoattraction and cytokine release, and matrix degradation (Original figure taken out from Friedman S.L. (Friedman 2000).

When activated, HSCs presented increased capacity for proliferation, mobility, contractility and synthesis of collagen type I and II besides other components of extracellular matrix (Friedman 2000; Bataller and Brenner 2005; Brandao, Ramalho et al. 2006; Kisseleva and Brenner 2006).

Consonant with this model of fibrosis progression and with published data in other models and in human, MMP-2 and alpha 1 procollagen (I) were significantly elevated at fibrosis week 10 to 15 (F4). A similar observation was made in a rat fibrosis model, showing increased expression levels of alpha 1 procollagen (I) mRNA in advanced fibrosis (Du, Zhang et al. 1997). The present findings of elevated MMP-2 and alpha 1 procollagen (I) levels are supported by previous publications indicating a correlation between progression of liver fibrosis and progelatinase A and gelatinase A (MMP-2) in a CCL_4 rat liver fibrosis model (Takahara, Furui et al. 1995; Du, Zhang et al. 1997; Zheng, Zhang et al. 2005).

In contrast to MMP-2 which showed a progressive increase following fibrosis induction, the tissue protective proteinase inhibitor TIMP-1 was strongly increased only at week 10. At this time point liver damage was dominated by a dense mixed lymphocytic periportal infiltrate. Presumably, TIMP-1 up regulation was secondary to the inflammatory reaction. TIMP-1 concentrations fully normalized until week 15, which was accompanied by an almost complete disappearance of any inflammatory periportal infiltrate. Collagenase activities were described to initially raise with liver injury and fall with continuous progression to cirrhosis (Carter, McCarron et al. 1982; Maruyama, Feinman et al. 1982; Perez-Tamayo, Montfort et al. 1987; Montfort, Perez-Tamayo et al. 1990; Murawaki, Yamada et al. 1990). Thus, TIMP-1 possibly bears regulatory functions in collagen degradation and in hepatic fibrosis in our model, which corresponds well with observations in human and rat liver fibrosis (Iredale, Goddard et al. 1995; Benyon, Iredale et al. 1996; Iredale, Benyon et al. 1996).

Corresponding to data on vWF and VEGF (Rosmorduc, Wendum et al. 1999; Corpechot, Barbu et al. 2002), formation of fibrotic septa was also characterized by increased staining against von-Willebrand factor (vWF) along these septa. Since anti-vWF staining was paralleled by up regulated VEGF expression, it is tempting to

assume that septal angiogenesis, at least partly, was VEGF dependent. Additionally, liver inflammation might have the potency to increase VEGF expression, because VEGF itself is capable of increasing alpha procollagen mRNA levels in activated hepatic stellate cells (Yoshiji, Kuriyama et al. 2003). Correspondingly, the highest alpha 1 procollagen (I)/GAPDH ratio values were observed in fibrotic liver samples at week 10. This might at least partly be attributed to elevated VEGF values at this time point.

The interplay between inflammation and angiogenesis affects extracellular matrix and various adhesive interactions on the level of endothelial cells and matrix substances. In this respect, up regulation of ICAM-1 was found in liver biopsies obtained from patients suffering from alcoholic hepatitis and cirrhosis (Gimbrone 1995; Gimbrone, Nagel et al. 1997; Sacanella and Estruch 2003). Interestingly, this trait of liver fibrosis was also reflected by a 3.5 fold incline in ICAM-1. ICAM-1 expression is known to be driven by VEGF via nuclear factor-κB activation in endothelial cells (Kim, Moon et al. 2001). Septal ICAM-1 up regulation strikingly fell in line with septal VEGF up regulation as shown by other groups (Rosmorduc, Wendum et al. 1999; Corpechot, Barbu et al. 2002). A similar correlation between fibrosis and ICAM expression had been also found in immunohistochemistry of fibrotic rat livers (Lu, Zeng et al. 1999).

5.2 Part II: Accelerated orthotopic HCC growth is linked with increased VEGF-A and VEGF-C receptors transcription in liver fibrosis

Since HCC predominantly develops in damaged fibrotic liver tissue, we decided to implant tumor cells into pre-damaged fibrotic livers, in order to study the effect of pre-existing fibrosis on tumor growth and on tumor progression markers.

Usually, experimental anti tumor strategies are tested in subcutaneous, but rarely in orthotopic hepatoma models (Schmitz, Wang et al. 2004; Lee, Yun et al. 2006; Schmitz, Raskopf et al. 2006; Son, Hirano et al. 2006; Torimura, Ueno et al. 2006; Zhao, Zhang et al. 2006). Previously, the Hepa129 hepatoma cell line has been

demonstrated to be suitable for orthotopic tumor growth and also for therapeutic intervention studies on tumor growth inhibition and anti-angiostatic effects (Schmitz, Tirado-Ledo et al. 2004; Raskopf, Dzienisowicz et al. 2005). The present thesis showed that orthotopic tumor growth was significantly accelerated in fibrotic compared to non-fibrotic livers, as evidenced by 3.6 fold increased tumor size and numerous intrahepatic HCC satellites, if pre-fibrotic mice were treated with the combination of TAA i.p. and EtOH in the drinking water for at least 19 wks.

In 1999, Kuriyama et al. showed an early occurrence of intrahepatic metastasis in their model, in which fibrosis was induced only by TAA monotherapy for ten weeks. These observation were obtained using a syngenic HCC labeled tumor cell line (BNL1ME A.7R.1) injected into fibrotic BALB/c mice livers (Kuriyama, Yamazaki et al. 1999). However, this publication did not demonstrate tumor growth acceleration and did not investigate the VEGF signal transduction.

Interestingly, a further effect of fibrosis on implanted syngenic Hepa129 HCC tumor cells was observed if tumor cells were implanted in pre-fibrotic C3H/He mice, which were treated with a TAA i.p. and EtOH combination for 24 weeks. In this setting, no solid tumor were detectable on the fibrotic liver surface, but almost the whole injected fibrotic liver lobe was infiltrated with HCC satellites with a larger diameter when the satellites were closer to the injection site (data not shown). Since Kuriyama et al. did not grade the fibrosis in their model with an accepted grading system, such as those proposed by Desmet et al or by Ishak et al. (Desmet, Gerber et al. 1994; Ishak, Baptista et al. 1995), these two models are not comparable, also due to the different fibrosis induction technique. It has been discussed above that the combination of TAA i.p. and EtOH led to an acceleration of fibrosis in C3H/He mice, and therefore raised the fibrosis grade (Kornek, Raskopf et al. 2005; Kornek, Raskopf et al. 2006). But the presence of fibrosis and the fibrosis grade seem to have an effect on the behavior of implanted tumor cells. Furthermore Kuriyama et al. injected the syngenic tumor cells subcapsularly, whereas in this PhD thesis the tumor cells were directly injected into the pre-fibrotic mice liver. An artificial distribution of injected tumor cells due to the direct injection into the fibrotic liver itself appears unlikely, because non hepatoma derived tumor cells (MC38, colon carcinoma, syngenic to C57/B6 mice, 24th week of fibrosis induction) did not form any surface satellites (data

not shown) when injected into fibrotic livers in C57/B6 mice. Therefore a random diffuse distribution of implanted tumor cells due to the direct injection can be excluded, but Kuriyama et al. did not provide evidence that can exclude a random distribution in fibrotic BALB/c mice.

Additionally, in the C3H/He fibrosis-HCC model, systemic and extra hepatic tumor promoting effects due to immune-suppressive effects of the weekly TAA i.p. and EtOH in the drinking water administration seems to be irrelevant, since intrasplenic tumor sizes did not differ between fibrotic and non-fibrotic mice, when Hepa129 hepatoma cell were injected into the spleen and not into the liver (data not shown).

Nevertheless, these data clearly show that tumor development is accelerated in pre-damaged fibrotic murine livers. Advanced tumor growth was associated with elevated transcription levels the two main VEGF receptors Flt-1, Flk-1, MMP-2, and MMP-9. This HCC implantation studies was not designed as intervention study, but considering published data it is plausible to conclude that these factors partly contribute to accelerated tumor growth in this model (Qin and Tang 2002; Qin and Tang 2004).

TAA i.p. and EtOH induced liver damage resulted in fibrosis F4 (max. score F6) as demonstrated by van Gieson collagen staining. Although the porto-portal fibrotic bridging was thin, fibrosis induction was functionally relevant when considering the hepatic microcirculation, which was significantly reduced (by about 60%) in fibrotic mice. This observation, obtained for the first time in a murine model, is consistent with published data on HM in fibrotic rabbits, showing a similar decline (by about 60%) also using a non-invasive laser Doppler flowmeter (Jiao, Seifalian et al. 1999). Reduced HM is generally considered to be a surrogate marker for portal hypertension in liver fibrosis (Newby and Hayes 2002). Thus, although porto-portal bridging was gaunt, fibrosis induction was associated with expected changes in HM in this liver fibrosis model. Reduced intratumoral HM might partly be compensated by increased intratumoral HIF-1 alpha transcription and may have attributed to increased VEGF-A, Flt-1, and KDR levels in this model

Supplementary tumor growth and formation of tumor satellites were significantly accelerated in fibrotic livers in this model. To further explain this observation, additional pathologically relevant HCC biomarkers were analyzed. Consistent with data in humans, soluble VEGF, intratumoral Flt-1 (VEGFR-1), intratumoral Flk-1 (KDR/VEGFR-2) were significantly increased in tumor-bearing fibrotic compared to non-fibrotic mice (Ng, Poon et al. 2001; el-Houseini, Mohammed et al. 2005). VEGFR-1/-2 are supposed to be important pathophysiological factors that promote HCC development in early and advanced HCC disease (Yoshiji, Kuriyama et al. 2004). The importance of the VEGF signal pathways was consistent with intervention studies that successfully blocked the VEGF to control tumor growth including also experimental HCC and CRC (Yoshiji, Kuriyama et al. 2004; Yoshiji, Kuriyama et al. 2004; Raskopf, Dzienisowicz et al. 2005; Schmitz, Kornek et al. 2005). This data imply that intratumoral VEGF receptor expression might gain additional pathophysiological relevance in advanced HCC development in the case of liver fibrosis. Although intratumoral VEGFR-1/-2 up-regulation helps to understand advanced tumor sizes, it does not satisfactorily explain the appearance of numerous HCC satellites in the pre-damaged liver in this model.

It was hypothesized by others that tumor can spread directly into the local tissue or *via* blood vessels and lymphatics. In case of tumor cell invasion through blood vessels, penetration of the basement membrane and migration through the cellular layers and vessel is required (Ruoslahti 1996). The entry into the lymphatic circulation system is thought to be easier due to the structure of lymphatic vessels (Swartz and Skobe 2001). In line with clinical and pathological data, the spread of solid tumors via lymphatics is considered to be an important early event in metastasis (Greenlee, Hill-Harmon et al. 2001). Although, it was already discussed that the observed satellites have been established probably not due to injection or diffuse distribution, but more evidently by later tumor spread from a primary tumor grown at the injection site associated with tumor cell migration through lymphatic vessels or blood vessels. But no evidences were provided that could exclude preferential tumor cell spread *via* the lymphatic system or exclusively *via* blood vessels. Both ways were described as possible tumor spreading mechanisms. One supportive explanation for HCC satellite-spread trough blood or lymphatic vessels could be the finding that VEGF-C was able to induce vascular permeability. Therefore it could promote

metastasis by increasing the interstitial pressure inside the tumor, which might be important factor driving tumor cell seeding both into blood and lymphatic vessels (Padera, Kadambi et al. 2002; Isaka, Padera et al. 2004). Increased VEGF-C and VEGFR-3 (Flt-4) expression may help to understand the latter observation, as these were strongly associated with high risk of metastasis in other studies (Stacker, Baldwin et al. 2002; Dadras, Lange-Asschenfeldt et al. 2005; Hirakawa, Brown et al. 2007) or as observed in the present study, connected with metastatic spread itself in various cancer types (table3, page 26). There is only one human study providing data that linked VEGF-C and advanced metastasis in case of HCC beside this work (Yamaguchi, Yano et al. 2006). Another interesting finding was published by Mattila et al., who showed that VEGF-C over expression in tumor cells, which had been previously described as poorly metastic, turned the same tumor cells into metastatic tumor cells after VEGF-C over expression *in vivo* (Mattila, Ruohola et al. 2002). According to these published results, this PhD thesis show a similar over expression of VEGF-C situation in tumor samples derived from fibrotic mice. Both, VEGF-C and its main receptor VEGFR-3, were significantly increased in tumor bearing fibrotic mice. A possible link that could promote VEGF-C over expression in this study could be TGF-beta. VEGF-C expression is regulated not by hypoxia as VEGF-A, but instead by cytokines and some growth factors including EGF (epidermal growth factor) and TGF-β (tumor transforming growth factor β) (Ristimaki, Honkanen et al. 1997; Ristimaki, Jaatinen et al. 1997). Moreover it is well known that TGF-β is up regulated in fibrosis and induces apoptosis in hepatic cells during ongoing liver inflammation (Mauviel 2005; Peterson 2005).

Acknowledging the function of the proteinases MMP-2 and MMP-9 to degrade ECM and vascular basal membrane, their elevated expression strongly argues in favor of a relevant pathophysiological role for intrahepatic metastases in this novel fibrotic HCC model. Elevated MMP-2 and MMP-9 transcription strongly argues for a complementary role of invasion factors at promoting tumor growth. Specifically, MMP-2 and MMP-9 have been described to possess prognostic relevance in HCC, so that they can be applied to evaluate HCC invasion and metastasis (Bu, Huang et al. 1997; Wei, Wu et al. 2003). Consequently, (over) expression of MMP-2 or MMP-9 in mouse cancer cells favored tumor growth and metastasis (Kawamata, Kameyama et al. 1995; Cockett, Murphy et al. 1998; Aoudjit, Masure et al. 1999). Analogously,

tumor volumes were decreased by 39% for B16-BL6 melanomas and by 24% for Lewis lung carcinomas in MMP-2 deficient mice (Bu, Huang et al. 1997; Wei, Wu et al. 2003).

Taken together, the data from the present PhD thesis in fibrotic HCC bearing C3H/He mice suggest that the intratumoral VEGF receptor status contributes to accelerated HCC development in fibrotic mice and that elevated VEGF-C, their receptor VEGFR-3, MMP-2 and MMP-9 levels drive satellite formation. Thus, this model provides an interesting tool for further assessing intervention strategies to control orthotopic hepatoma growth in liver fibrosis in a murine animal model, in order to answer the question which factors force the HCC tumor cell to switch from a non-metastatic growth toward metastasis.

6 Summary

Treatment of HCC is challenging and improved animal models are needed for testing innovative therapies. In particular, a well characterized fibrosis tumor model is urgently needed. Here, a novel HCC tumor model was established based on the use of pre-fibrotic mice. Common methods such as CCL_4 failed to induce fibrosis with a tolerable mortality rate in C3H/He mice. Instead, a combination of TAA (thioacetamide) i.p. and EtOH (ethanol) effectively induced liver fibrosis at lower mortality rate then CCL_4. Fibrogenesis was characterized by typical histological changes besides protein level and steady state mRNA transcription measurement of alpha 1 procollagen (I), and quantification of hepatic MMP-2, sVEGF and sICAM-1 protein. All these biomarkers have been shown to be up regulated during fibrosis induction in rodents and human. This fibrosis model resembles critical aspects of human liver fibrosis, including haemodynamic microcirculation (HM) change manifesting in marked HM reduction in the fibrotic mouse liver.

For first time a marked intrahepatic HM was observed in mice as a result of induced fibrogenesis. Of great interest also was the second finding in this model: Pre-existing liver fibrosis was associated with advanced orthotopic hepatoma (Hepa129 tumor cells) and metastasis growth. In particular, intratumoral VEGF-A and VEGF-C and their VEGFR expression was increased, which might account for the observed rapid tumor development at the tumor cell implantation site and satellite formation. Thus, VEGF-C and its receptor could serve as a predictable marker for metastasis in HCC. MMP expression was increased as well, consistent with the fact that MMP-2 and MMP-9 are important HCC invasion factors.

In summary, this novel tumor model might serve as a valuable tool for future studies on HCC tumor development and formation of tumor and tumor satellites in liver fibrosis. It appears suitable for future tumor cell implantation experiments and further fibrosis studies. In addition, it will permit investigating the effect of fibrosis on HCC orthotopic tumor growth *in vivo* and testing innovative intervention studies aimed at treatment of HCC. Hopefully, these experimental studies can be helpful to improve treatment of human HCC patients with cirrhosis.

7 References

(1999). "Global surveillance and control of hepatitis C. Report of a WHO Consultation organized in collaboration with the Viral Hepatitis Prevention Board, Antwerp, Belgium." J Viral Hepat **6**(1): 35-47.

Akagi, K., Y. Ikeda, et al. (2000). "Vascular endothelial growth factor-C (VEGF-C) expression in human colorectal cancer tissues." Br J Cancer **83**(7): 887-91.

Albano, E. (2006). "Alcohol, oxidative stress and free radical damage." Proc Nutr Soc **65**(3): 278-90.

Anthony, P. P., K. G. Ishak, et al. (1978). "The morphology of cirrhosis. Recommendations on definition, nomenclature, and classification by a working group sponsored by the World Health Organization." J Clin Pathol **31**(5): 395-414.

Aoudjit, F., S. Masure, et al. (1999). "Gelatinase B (MMP-9), but not its inhibitor (TIMP-1), dictates the growth rate of experimental thymic lymphoma." Int J Cancer **82**(5): 743-7.

Basset, P., A. Okada, et al. (1997). "Matrix metalloproteinases as stromal effectors of human carcinoma progression: therapeutic implications." Matrix Biol **15**(8-9): 535-41.

Bataller, R. and D. A. Brenner (2005). "Liver fibrosis." J Clin Invest **115**(2): 209-18.

Beasley, R. P. and L. Y. Hwang (1984). "Hepatocellular carcinoma and hepatitis B virus." Semin Liver Dis **4**(2): 113-21.

Benyon, R. C. and M. J. Arthur (2001). "Extracellular matrix degradation and the role of hepatic stellate cells." Semin Liver Dis **21**(3): 373-84.

Benyon, R. C., J. P. Iredale, et al. (1996). "Expression of tissue inhibitor of metalloproteinases 1 and 2 is increased in fibrotic human liver." Gastroenterology **110**(3): 821-31.

Bhushan, M., H. S. Young, et al. (2002). "Recent advances in cutaneous angiogenesis." Br J Dermatol **147**(3): 418-25.

Bluteau, O., E. Jeannot, et al. (2002). "Bi-allelic inactivation of TCF1 in hepatic adenomas." Nat Genet **32**(2): 312-5.

Bohle, A. S. and H. Kalthoff (1999). "Molecular mechanisms of tumor metastasis and angiogenesis." Langenbecks Arch Surg **384**(2): 133-40.

Bosch, F. X., J. Ribes, et al. (1999). "Epidemiology of primary liver cancer." Semin Liver Dis **19**(3): 271-85.

Bosma, A., A. Brouwer, et al. (1988). "Synergism between ethanol and carbon tetrachloride in the generation of liver fibrosis." J Pathol **156**(1): 15-21.

Brandao, D. F., L. N. Ramalho, et al. (2006). "Liver cirrhosis and hepatic stellate cells." Acta Cir Bras **21 Suppl 1**: 54-7.

Brechot, C., D. Gozuacik, et al. (2000). "Molecular bases for the development of hepatitis B virus (HBV)-related hepatocellular carcinoma (HCC)." Semin Cancer Biol **10**(3): 211-31.

Breier, G., U. Albrecht, et al. (1992). "Expression of vascular endothelial growth factor during embryonic angiogenesis and endothelial cell differentiation." Development **114**(2): 521-32.

Bruix, J. and M. Sherman (2005). "Management of hepatocellular carcinoma." Hepatology **42**(5): 1208-36.

Bu, W., X. Huang, et al. (1997). "[The role of MMP-2 in the invasion and metastasis of hepatocellular carcinoma (HCC)]." Zhonghua Yi Xue Za Zhi **77**(9): 661-4.

Buendia, M. A. (2000). "Genetics of hepatocellular carcinoma." Semin Cancer Biol **10**(3): 185-200.

Carter, E. A., M. J. McCarron, et al. (1982). "Lysyl oxidase and collagenase in experimental acute and chronic liver injury." Gastroenterology **82**(3): 526-34.

Caselmann, W. H. (1998). "Pathogenesis of hepatocellular carcinoma." Digestion **59 Suppl 2**: 60-3.

Caselmann, W. H., H. E. Blum, et al. (1999). "[Guidelines of the German Society of Digestive and Metabolic Diseases for diagnosis and therapy of hepatocellular carcinoma. German Society of Digestive and Metabolic Diseases]." Z Gastroenterol **37**(5): 353-65.

Cerny, A. and F. V. Chisari (1999). "Pathogenesis of chronic hepatitis C: immunological features of hepatic injury and viral persistence." Hepatology **30**(3): 595-601.

Chen, C. J., H. I. Yang, et al. (2006). "Risk of hepatocellular carcinoma across a biological gradient of serum hepatitis B virus DNA level." Jama **295**(1): 65-73.

Chen, Z., M. L. Varney, et al. (2005). "Down-regulation of vascular endothelial cell growth factor-C expression using small interfering RNA vectors in mammary tumors inhibits tumor lymphangiogenesis and spontaneous metastasis and enhances survival." Cancer Res **65**(19): 9004-11.

Cockett, M. I., G. Murphy, et al. (1998). "Matrix metalloproteinases and metastatic cancer." Biochem Soc Symp **63**: 295-313.

Coleman, W. B. (2003). "Mechanisms of human hepatocarcinogenesis." Curr Mol Med **3**(6): 573-88.

Constandinou, C., N. Henderson, et al. (2005). "Modeling liver fibrosis in rodents." Methods Mol Med **117**: 237-50.

Corpechot, C., V. Barbu, et al. (2002). "Hypoxia-induced VEGF and collagen I expressions are associated with angiogenesis and fibrogenesis in experimental cirrhosis." Hepatology **35**(5): 1010-21.

Couto, O. F., I. Dvorchik, et al. (2007). "Causes of Death in Patients with Unresectable Hepatocellular Carcinoma." Dig Dis Sci.

Cremonese, R. V., A. A. Pereira-Filho, et al. (2001). "[Experimental cirrhosis induced by carbon tetrachloride inhalation: adaptation of the technique and evaluation of lipid peroxidation]." Arq Gastroenterol **38**(1): 40-7.

Dadras, S. S., B. Lange-Asschenfeldt, et al. (2005). "Tumor lymphangiogenesis predicts melanoma metastasis to sentinel lymph nodes." Mod Pathol **18**(9): 1232-42.

Desmet, V. J., M. Gerber, et al. (1994). "Classification of chronic hepatitis: diagnosis, grading and staging." Hepatology **19**(6): 1513-20.

Desmet, V. J. and T. Roskams (2004). "Cirrhosis reversal: a duel between dogma and myth." J Hepatol **40**(5): 860-7.

Distler, O., M. Neidhart, et al. (2002). "The molecular control of angiogenesis." Int Rev Immunol **21**(1): 33-49.

Dragan, Y. P. and H. C. Pitot (1992). "The role of the stages of initiation and promotion in phenotypic diversity during hepatocarcinogenesis in the rat." Carcinogenesis **13**(5): 739-50.

Du, W., Y. Zhang, et al. (1997). "[A study on type I, III and IV collagen production in CCl4 induced rat liver fibrosis]." Zhonghua Bing Li Xue Za Zhi **26**(2): 74-7.

Duffield, J. S. (2003). "The inflammatory macrophage: a story of Jekyll and Hyde." Clin Sci (Lond) **104**(1): 27-38.
Duffield, J. S., S. J. Forbes, et al. (2005). "Selective depletion of macrophages reveals distinct, opposing roles during liver injury and repair." J Clin Invest **115**(1): 56-65.
Durr, R. and W. H. Caselmann (2000). "Carcinogenesis of primary liver malignancies." Langenbecks Arch Surg **385**(3): 154-61.
Dvorak, H. F., M. Detmar, et al. (1995). "Vascular permeability factor/vascular endothelial growth factor: an important mediator of angiogenesis in malignancy and inflammation." Int Arch Allergy Immunol **107**(1-3): 233-5.
el-Houseini, M. E., M. S. Mohammed, et al. (2005). "Enhanced detection of hepatocellular carcinoma." Cancer Control **12**(4): 248-53.
Eliceiri, B. P. (2001). "Integrin and growth factor receptor crosstalk." Circ Res **89**(12): 1104-10.
Eliceiri, B. P. and D. A. Cheresh (2001). "Adhesion events in angiogenesis." Curr Opin Cell Biol **13**(5): 563-8.
El-Serag, H. B. and A. C. Mason (2000). "Risk factors for the rising rates of primary liver cancer in the United States." Arch Intern Med **160**(21): 3227-30.
Fan, F., J. S. Wey, et al. (2005). "Expression and function of vascular endothelial growth factor receptor-1 on human colorectal cancer cells." Oncogene **24**(16): 2647-53.
Farinati, F., D. Marino, et al. (2006). "Diagnostic and prognostic role of alpha-fetoprotein in hepatocellular carcinoma: both or neither?" Am J Gastroenterol **101**(3): 524-32.
Fattovich, G., T. Stroffolini, et al. (2004). "Hepatocellular carcinoma in cirrhosis: incidence and risk factors." Gastroenterology **127**(5 Suppl 1): S35-50.
Ferber, M. J., D. P. Montoya, et al. (2003). "Integrations of the hepatitis B virus (HBV) and human papillomavirus (HPV) into the human telomerase reverse transcriptase (hTERT) gene in liver and cervical cancers." Oncogene **22**(24): 3813-20.
Ferrara, N. (1999). "Molecular and biological properties of vascular endothelial growth factor." J Mol Med **77**(7): 527-43.
Ferrara, N. and K. Alitalo (1999). "Clinical applications of angiogenic growth factors and their inhibitors." Nat Med **5**(12): 1359-64.
Fidler, I. J. (1990). "Critical factors in the biology of human cancer metastasis: twenty-eighth G.H.A. Clowes memorial award lecture." Cancer Res **50**(19): 6130-8.
Fingleton, B. (2006). "Matrix metalloproteinases: roles in cancer and metastasis." Front Biosci **11**: 479-91.
Friedman, S. L. (2000). "Molecular regulation of hepatic fibrosis, an integrated cellular response to tissue injury." J Biol Chem **275**(4): 2247-50.
Friedman, S. L. (2005). "Mac the knife? Macrophages- the double-edged sword of hepatic fibrosis." J Clin Invest **115**(1): 29-32.
Gimbrone, M. A., Jr. (1995). "Vascular endothelium: an integrator of pathophysiologic stimuli in atherosclerosis." Am J Cardiol **75**(6): 67B-70B.
Gimbrone, M. A., Jr., T. Nagel, et al. (1997). "Biomechanical activation: an emerging paradigm in endothelial adhesion biology." J Clin Invest **99**(8): 1809-13.
Gnant, M. F., M. Puhlmann, et al. (1999). "Systemic administration of a recombinant vaccinia virus expressing the cytosine deaminase gene and subsequent

treatment with 5-fluorocytosine leads to tumor-specific gene expression and prolongation of survival in mice." Cancer Res **59**(14): 3396-403.
Gombos, Z., X. Xu, et al. (2005). "Peritumoral lymphatic vessel density and vascular endothelial growth factor C expression in early-stage squamous cell carcinoma of the uterine cervix." Clin Cancer Res **11**(23): 8364-71.
Greenlee, R. T., M. B. Hill-Harmon, et al. (2001). "Cancer statistics, 2001." CA Cancer J Clin **51**(1): 15-36.
Groszmann, R. J. and J. G. Abraldes (2005). "Portal hypertension: from bedside to bench." J Clin Gastroenterol **39**(4 Suppl 2): S125-30.
Guo, J. T., H. Zhou, et al. (2000). "Apoptosis and regeneration of hepatocytes during recovery from transient hepadnavirus infections." J Virol **74**(3): 1495-505.
Hanahan, D. (1997). "Signaling vascular morphogenesis and maintenance." Science **277**(5322): 48-50.
Hanahan, D. and J. Folkman (1996). "Patterns and emerging mechanisms of the angiogenic switch during tumorigenesis." Cell **86**(3): 353-64.
Hashimoto, I., J. Kodama, et al. (2001). "Vascular endothelial growth factor-C expression and its relationship to pelvic lymph node status in invasive cervical cancer." Br J Cancer **85**(1): 93-7.
He, Y., T. Karpanen, et al. (2004). "Role of lymphangiogenic factors in tumor metastasis." Biochim Biophys Acta **1654**(1): 3-12.
Heppner, K. J., L. M. Matrisian, et al. (1996). "Expression of most matrix metalloproteinase family members in breast cancer represents a tumor-induced host response." Am J Pathol **149**(1): 273-82.
Hessein, M., G. Saad el, et al. (2005). "Hit-and-run mechanism of HBV-mediated progression to hepatocellular carcinoma." Tumori **91**(3): 241-7.
Higuchi, H., I. Kurose, et al. (1996). "Ethanol-induced apoptosis and oxidative stress in hepatocytes." Alcohol Clin Exp Res **20**(9 Suppl): 340A-346A.
Hillebrandt, S., C. Goos, et al. (2002). "Genome-wide analysis of hepatic fibrosis in inbred mice identifies the susceptibility locus Hfib1 on chromosome 15." Gastroenterology **123**(6): 2041-51.
Hirai, M., A. Nakagawara, et al. (2001). "Expression of vascular endothelial growth factors (VEGF-A/VEGF-1 and VEGF-C/VEGF-2) in postmenopausal uterine endometrial carcinoma." Gynecol Oncol **80**(2): 181-8.
Hirakawa, S., L. F. Brown, et al. (2007). "VEGF-C-induced lymphangiogenesis in sentinel lymph nodes promotes tumor metastasis to distant sites." Blood **109**(3): 1010-7.
Holstege, A., P. Bedossa, et al. (1994). "Acetaldehyde-modified epitopes in liver biopsy specimens of alcoholic and nonalcoholic patients: localization and association with progression of liver fibrosis." Hepatology **19**(2): 367-74.
Horikawa, I. and J. C. Barrett (2001). "cis-Activation of the human telomerase gene (hTERT) by the hepatitis B virus genome." J Natl Cancer Inst **93**(15): 1171-3.
Ijichi, M., T. Takayama, et al. (2002). "alpha-Fetoprotein mRNA in the circulation as a predictor of postsurgical recurrence of hepatocellular carcinoma: a prospective study." Hepatology **35**(4): 853-60.
Inoue, H. and H. K. Seitz (2001). "Viruses and alcohol in the pathogenesis of primary hepatic carcinoma." Eur J Cancer Prev **10**(1): 107-10.
Iredale, J. P., R. C. Benyon, et al. (1996). "Tissue inhibitor of metalloproteinase-1 messenger RNA expression is enhanced relative to interstitial collagenase messenger RNA in experimental liver injury and fibrosis." Hepatology **24**(1): 176-84.

Iredale, J. P., S. Goddard, et al. (1995). "Tissue inhibitor of metalloproteinase-I and interstitial collagenase expression in autoimmune chronic active hepatitis and activated human hepatic lipocytes." Clin Sci (Lond) **89**(1): 75-81.

Isaka, N., T. P. Padera, et al. (2004). "Peritumor lymphatics induced by vascular endothelial growth factor-C exhibit abnormal function." Cancer Res **64**(13): 4400-4.

Ishak, K., A. Baptista, et al. (1995). "Histological grading and staging of chronic hepatitis." J Hepatol **22**(6): 696-9.

Ishak, K. G. (1994). "Chronic hepatitis: morphology and nomenclature." Mod Pathol **7**(6): 690-713.

Ishida, A., J. Murray, et al. (2001). "Expression of vascular endothelial growth factor receptors in smooth muscle cells." J Cell Physiol **188**(3): 359-68.

Itoh, T., M. Tanioka, et al. (1999). "Experimental metastasis is suppressed in MMP-9-deficient mice." Clin Exp Metastasis **17**(2): 177-81.

Itoh, T., M. Tanioka, et al. (1998). "Reduced angiogenesis and tumor progression in gelatinase A-deficient mice." Cancer Res **58**(5): 1048-51.

Janeway, C. A., P. Travers, et al. (2005). IMMUNOBIOLOGY 6th EDITION. New York, Garland Science Publishing.

Jiao, L. R., A. M. Seifalian, et al. (1999). "The effect of mechanically enhancing portal venous inflow on hepatic oxygenation, microcirculation, and function in a rabbit model with extensive hepatic fibrosis." Hepatology **30**(1): 46-52.

Johnsen, M., L. R. Lund, et al. (1998). "Cancer invasion and tissue remodeling: common themes in proteolytic matrix degradation." Curr Opin Cell Biol **10**(5): 667-71.

Johnson, R. C. (1997). "Hepatocellular carcinoma." Hepatogastroenterology **44**(13): 307-12.

Kaio, E., S. Tanaka, et al. (2003). "Clinical significance of angiogenic factor expression at the deepest invasive site of advanced colorectal carcinoma." Oncology **64**(1): 61-73.

Karpanen, T. and K. Alitalo (2001). "Lymphatic vessels as targets of tumor therapy?" J Exp Med **194**(6): F37-42.

Kawakami, M., T. Furuhata, et al. (2003). "Expression analysis of vascular endothelial growth factors and their relationships to lymph node metastasis in human colorectal cancer." J Exp Clin Cancer Res **22**(2): 229-37.

Kawakami, M., Y. Yanai, et al. (2005). "Vascular endothelial growth factor C promotes lymph node metastasis in a rectal cancer orthotopic model." Surg Today **35**(2): 131-8.

Kawamata, H., S. Kameyama, et al. (1995). "Marked acceleration of the metastatic phenotype of a rat bladder carcinoma cell line by the expression of human gelatinase A." Int J Cancer **63**(4): 568-75.

Keck, P. J., S. D. Hauser, et al. (1989). "Vascular permeability factor, an endothelial cell mitogen related to PDGF." Science **246**(4935): 1309-12.

Kim, I., S. O. Moon, et al. (2001). "Vascular endothelial growth factor expression of intercellular adhesion molecule 1 (ICAM-1), vascular cell adhesion molecule 1 (VCAM-1), and E-selectin through nuclear factor-kappa B activation in endothelial cells." J Biol Chem **276**(10): 7614-20.

Kisseleva, T. and D. A. Brenner (2006). "Hepatic stellate cells and the reversal of fibrosis." J Gastroenterol Hepatol **21 Suppl 3**: S84-7.

Kitadai, Y., T. Amioka, et al. (2001). "Clinicopathological significance of vascular endothelial growth factor (VEGF)-C in human esophageal squamous cell carcinomas." Int J Cancer **93**(5): 662-6.

Komuro, H., S. Kaneko, et al. (2001). "Expression of angiogenic factors and tumor progression in human neuroblastoma." J Cancer Res Clin Oncol **127**(12): 739-43.

Korn, W. M. (2001). "Moving toward an understanding of the metastatic process in hepatocellular carcinoma." World J Gastroenterol **7**(6): 777-8.

Kornek, M., E. Raskopf, et al. (2005). "Systemic thioacetamide (TAA) and ethanol injections accelerate hepatic fibrosis in C3H/He mice (Abstract 291)." Hepatology **42**(S1): 299A-401A.

Kornek, M., E. Raskopf, et al. (2006). "Combination of systemic thioacetamide (TAA) injections and ethanol feeding accelerates hepatic fibrosis in C3H/He mice and is associated with intrahepatic up regulation of MMP-2, VEGF and ICAM-1." J Hepatol **45**(3): 370-6.

Kountouras, J. and N. J. Lygidakis (2000). "New epidemiological data on liver oncogenesis." Hepatogastroenterology **47**(33): 855-61.

Kurebayashi, J., T. Otsuki, et al. (1999). "Expression of vascular endothelial growth factor (VEGF) family members in breast cancer." Jpn J Cancer Res **90**(9): 977-81.

Kuriyama, S., M. Yamazaki, et al. (1999). "Hepatocellular carcinoma in an orthotopic mouse model metastasizes intrahepatically in cirrhotic but not in normal liver." Int J Cancer **80**(3): 471-6.

Laakkonen, P., M. Waltari, et al. (2007). "Vascular endothelial growth factor receptor 3 is involved in tumor angiogenesis and growth." Cancer Res **67**(2): 593-9.

Lai, C. L., P. B. Gregory, et al. (1987). "Hepatocellular carcinoma in Chinese males and females. Possible causes for the male predominance." Cancer **60**(5): 1107-10.

Laleman, W., L. Landeghem, et al. (2005). "Portal hypertension: from pathophysiology to clinical practice." Liver Int **25**(6): 1079-90.

Lee, K., S. T. Yun, et al. (2006). "Adeno-associated virus-mediated expression of apolipoprotein (a) kringles suppresses hepatocellular carcinoma growth in mice." Hepatology **43**(5): 1063-73.

Lee, S. W., Y. M. Lee, et al. (2000). "Human hepatitis B virus X protein is a possible mediator of hypoxia-induced angiogenesis in hepatocarcinogenesis." Biochem Biophys Res Commun **268**(2): 456-61.

Leung, D. W., G. Cachianes, et al. (1989). "Vascular endothelial growth factor is a secreted angiogenic mitogen." Science **246**(4935): 1306-9.

Levrero, M. (2006). "Viral hepatitis and liver cancer: the case of hepatitis C." Oncogene **25**(27): 3834-47.

Li, D. and S. L. Friedman (1999). "Liver fibrogenesis and the role of hepatic stellate cells: new insights and prospects for therapy." J Gastroenterol Hepatol **14**(7): 618-33.

Li, J., C. I. Kim, et al. (1992). "Polyunsaturated lecithin prevents acetaldehyde-mediated hepatic collagen accumulation by stimulating collagenase activity in cultured lipocytes." Hepatology **15**(3): 373-81.

Liabakk, N. B., I. Talbot, et al. (1996). "Matrix metalloprotease 2 (MMP-2) and matrix metalloprotease 9 (MMP-9) type IV collagenases in colorectal cancer." Cancer Res **56**(1): 190-6.

Liang, T. J. and T. Heller (2004). "Pathogenesis of hepatitis C-associated hepatocellular carcinoma." Gastroenterology **127**(5 Suppl 1): S62-71.
Lieber, C. S. (1993). "Biochemical factors in alcoholic liver disease." Semin Liver Dis **13**(2): 136-53.
Lieber, C. S., M. A. Leo, et al. (2003). "Silymarin retards the progression of alcohol-induced hepatic fibrosis in baboons." J Clin Gastroenterol **37**(4): 336-9.
Llovet, J. M., A. Burroughs, et al. (2003). "Hepatocellular carcinoma." Lancet **362**(9399): 1907-17.
Lu, L., M. Zeng, et al. (1999). "[Intercellular adhesion molecule-1 expression in experimental liver fibrosis]." Zhonghua Nei Ke Za Zhi **38**(1): 37-9.
Lynch, C. C. and L. M. Matrisian (2002). "Matrix metalloproteinases in tumor-host cell communication." Differentiation **70**(9-10): 561-73.
Mandriota, S. J., L. Jussila, et al. (2001). "Vascular endothelial growth factor-C-mediated lymphangiogenesis promotes tumour metastasis." Embo J **20**(4): 672-82.
Maruyama, K., L. Feinman, et al. (1982). "Mammalian collagenase increases in early alcoholic liver disease and decreases with cirrhosis." Life Sci **30**(16): 1379-84.
Masson, R., O. Lefebvre, et al. (1998). "In vivo evidence that the stromelysin-3 metalloproteinase contributes in a paracrine manner to epithelial cell malignancy." J Cell Biol **140**(6): 1535-41.
Mattila, M. M., J. K. Ruohola, et al. (2002). "VEGF-C induced lymphangiogenesis is associated with lymph node metastasis in orthotopic MCF-7 tumors." Int J Cancer **98**(6): 946-51.
Mauviel, A. (2005). "Transforming growth factor-beta: a key mediator of fibrosis." Methods Mol Med **117**: 69-80.
Meister, B., F. Grunebach, et al. (1999). "Expression of vascular endothelial growth factor (VEGF) and its receptors in human neuroblastoma." Eur J Cancer **35**(3): 445-9.
Melero, I., I. Gabari, et al. (2003). "Anti-ICAM-2 monoclonal antibody synergizes with intratumor gene transfer of interleukin-12 inhibiting activation-induced T-cell death." Clin Cancer Res **9**(10 Pt 1): 3546-54.
Menon, C., M. Iyer, et al. (2003). "TNF-alpha downregulates vascular endothelial Flk-1 expression in human melanoma xenograft model." Am J Physiol Heart Circ Physiol **284**(1): H317-29.
Minami, M., Y. Daimon, et al. (2005). "Hepatitis B virus-related insertional mutagenesis in chronic hepatitis B patients as an early drastic genetic change leading to hepatocarcinogenesis." Oncogene **24**(27): 4340-8.
Montfort, I., R. Perez-Tamayo, et al. (1990). "Collagenase of hepatocytes and sinusoidal liver cells in the reversibility of experimental cirrhosis of the liver." Virchows Arch B Cell Pathol Incl Mol Pathol **59**(5): 281-9.
Moradpour, D., A. Cerny, et al. (2001). "Hepatitis C: an update." Swiss Med Wkly **131**(21-22): 291-8.
Murawaki, Y., S. Yamada, et al. (1990). "Collagenase and collagenolytic cathepsin in normal and fibrotic rat liver." J Biochem (Tokyo) **108**(2): 241-4.
Nakashima, T., S. Kondoh, et al. (2003). "Vascular endothelial growth factor-C expression in human gallbladder cancer and its relationship to lymph node metastasis." Int J Mol Med **11**(1): 33-9.
Nakau, M., H. Miyoshi, et al. (2002). "Hepatocellular carcinoma caused by loss of heterozygosity in Lkb1 gene knockout mice." Cancer Res **62**(16): 4549-53.

Neufeld, G., T. Cohen, et al. (1999). "Vascular endothelial growth factor (VEGF) and its receptors." Faseb J **13**(1): 9-22.

Newby, D. E. and P. C. Hayes (2002). "Hyperdynamic circulation in liver cirrhosis: not peripheral vasodilatation but 'splanchnic steal'." Qjm **95**(12): 827-30.

Ng, I. O., R. T. Poon, et al. (2001). "Microvessel density, vascular endothelial growth factor and its receptors Flt-1 and Flk-1/KDR in hepatocellular carcinoma." Am J Clin Pathol **116**(6): 838-45.

Ogawa, S., A. Oku, et al. (1998). "A novel type of vascular endothelial growth factor, VEGF-E (NZ-7 VEGF), preferentially utilizes KDR/Flk-1 receptor and carries a potent mitotic activity without heparin-binding domain." J Biol Chem **273**(47): 31273-82.

Okuda, K. (2000). "Hepatocellular carcinoma." J Hepatol **32**(1 Suppl): 225-37.

Padera, T. P., A. Kadambi, et al. (2002). "Lymphatic metastasis in the absence of functional intratumor lymphatics." Science **296**(5574): 1883-6.

Padera, T. P., B. R. Stoll, et al. (2002). "Conventional and high-speed intravital multiphoton laser scanning microscopy of microvasculature, lymphatics, and leukocyte-endothelial interactions." Mol Imaging **1**(1): 9-15.

Paradis, V., D. Dargere, et al. (1999). "Expression of connective tissue growth factor in experimental rat and human liver fibrosis." Hepatology **30**(4): 968-76.

Park, J. E., G. A. Keller, et al. (1993). "The vascular endothelial growth factor (VEGF) isoforms: differential deposition into the subepithelial extracellular matrix and bioactivity of extracellular matrix-bound VEGF." Mol Biol Cell **4**(12): 1317-26.

Parkin, D. M. (2001). "Global cancer statistics in the year 2000." Lancet Oncol **2**(9): 533-43.

Paterlini-Brechot, P., K. Saigo, et al. (2003). "Hepatitis B virus-related insertional mutagenesis occurs frequently in human liver cancers and recurrently targets human telomerase gene." Oncogene **22**(25): 3911-6.

Pepper, M. S. (2001). "Extracellular proteolysis and angiogenesis." Thromb Haemost **86**(1): 346-55.

Pepper, M. S., J. C. Tille, et al. (2003). "Lymphangiogenesis and tumor metastasis." Cell Tissue Res **314**(1): 167-77.

Perez-Tamayo, R., I. Montfort, et al. (1987). "Collagenolytic activity in experimental cirrhosis of the liver." Exp Mol Pathol **47**(3): 300-8.

Peterson, M. C. (2005). "Circulating transforming growth factor beta-1: a partial molecular explanation for associations between hypertension, diabetes, obesity, smoking and human disease involving fibrosis." Med Sci Monit **11**(7): RA229-32.

Poole, T. J., E. B. Finkelstein, et al. (2001). "The role of FGF and VEGF in angioblast induction and migration during vascular development." Dev Dyn **220**(1): 1-17.

Price, D. J., T. Miralem, et al. (2001). "Role of vascular endothelial growth factor in the stimulation of cellular invasion and signaling of breast cancer cells." Cell Growth Differ **12**(3): 129-35.

Qin, L. X. and Z. Y. Tang (2002). "The prognostic molecular markers in hepatocellular carcinoma." World J Gastroenterol **8**(3): 385-92.

Qin, L. X. and Z. Y. Tang (2004). "Recent progress in predictive biomarkers for metastatic recurrence of human hepatocellular carcinoma: a review of the literature." J Cancer Res Clin Oncol **130**(9): 497-513.

Rabe, C. and W. H. Caselmann (2000). "Interaction of Hepatitis B virus with cellular processes in liver carcinogenesis." Crit Rev Clin Lab Sci **37**(5): 407-29.

Raskopf, E., C. Dzienisowicz, et al. (2005). "Effective angiostatic treatment in a murine metastatic and orthotopic hepatoma model." Hepatology **41**(6): 1233-40.
Risau, W. and I. Flamme (1995). "Vasculogenesis." Annu Rev Cell Dev Biol **11**: 73-91.
Ristimaki, A., N. Honkanen, et al. (1997). "Expression of cyclooxygenase-2 in human gastric carcinoma." Cancer Res **57**(7): 1276-80.
Ristimaki, A., R. Jaatinen, et al. (1997). "Regulation of prostaglandin F2 alpha receptor expression in cultured human granulosa-luteal cells." Endocrinology **138**(1): 191-5.
Roberts, N., B. Kloos, et al. (2006). "Inhibition of VEGFR-3 activation with the antagonistic antibody more potently suppresses lymph node and distant metastases than inactivation of VEGFR-2." Cancer Res **66**(5): 2650-7.
Roskams, T., A. Baptista, et al. (2003). "Histopathology of portal hypertension: a practical guideline." Histopathology **42**(1): 2-13.
Rosmorduc, O., D. Wendum, et al. (1999). "Hepatocellular hypoxia-induced vascular endothelial growth factor expression and angiogenesis in experimental biliary cirrhosis." Am J Pathol **155**(4): 1065-73.
Ruoslahti, E. (1996). "How cancer spreads." Sci Am **275**(3): 72-7.
Saaristo, A., T. Karpanen, et al. (2000). "Mechanisms of angiogenesis and their use in the inhibition of tumor growth and metastasis." Oncogene **19**(53): 6122-9.
Sacanella, E. and R. Estruch (2003). "The effect of alcohol consumption on endothelial adhesion molecule expression." Addict Biol **8**(4): 371-8.
Schmitz, V., M. Barajas, et al. (2001). "Adenovirus-mediated CD40 ligand gene therapy in a rat model of orthotopic hepatocellular carcinoma." Hepatology **34**(1): 72-81.
Schmitz, V., M. Kornek, et al. (2005). "Treatment of metastatic colorectal carcinomas by systemic inhibition of vascular endothelial growth factor signaling in mice." World J Gastroenterol **11**(28): 4332-6.
Schmitz, V., E. Raskopf, et al. (2006). "Plasminogen fragment K1-5 improves survival in a murine HCC model." Gut.
Schmitz, V., L. Tirado-Ledo, et al. (2004). "Establishment of an orthotopic tumour model for hepatocellular carcinoma and non-invasive in vivo tumour imaging by high resolution ultrasound in mice." J Hepatol **40**(5): 787-91.
Schmitz, V., H. Vilanueva, et al. (2006). "Increased VEGF levels induced by anti-VEGF treatment are independent of tumor burden in colorectal carcinomas in mice." Gene Ther **13**(16): 1198-205.
Schmitz, V., L. Wang, et al. (2004). "Treatment of colorectal and hepatocellular carcinomas by adenoviral mediated gene transfer of endostatin and angiostatin-like molecule in mice." Gut **53**(4): 561-7.
Seifalian, A. M., V. Chidambaram, et al. (1998). "In vivo demonstration of impaired microcirculation in steatotic human liver grafts." Liver Transpl Surg **4**(1): 71-7.
Senger, D. R., S. J. Galli, et al. (1983). "Tumor cells secrete a vascular permeability factor that promotes accumulation of ascites fluid." Science **219**(4587): 983-5.
Shachaf, C. M., A. M. Kopelman, et al. (2004). "MYC inactivation uncovers pluripotent differentiation and tumour dormancy in hepatocellular cancer." Nature **431**(7012): 1112-7.

Shibuya, M. (2006). "Vascular endothelial growth factor (VEGF)-Receptor2: its biological functions, major signaling pathway, and specific ligand VEGF-E." Endothelium **13**(2): 63-9.

Shibuya, M., S. Yamaguchi, et al. (1990). "Nucleotide sequence and expression of a novel human receptor-type tyrosine kinase gene (flt) closely related to the fms family." Oncogene **5**(4): 519-24.

Shimizu, K., H. Kubo, et al. (2004). "Suppression of VEGFR-3 signaling inhibits lymph node metastasis in gastric cancer." Cancer Sci **95**(4): 328-33.

Shiota, G. and H. Kawasaki (1998). "Hepatocyte growth factor in transgenic mice." Int J Exp Pathol **79**(5): 267-77.

Siegers, C. P., V. Pauli, et al. (1986). "Hepatoprotection by malotilate against carbon tetrachloride-alcohol-induced liver fibrosis." Agents Actions **18**(5-6): 600-3.

Simmonds, P., A. Alberti, et al. (1994). "A proposed system for the nomenclature of hepatitis C viral genotypes." Hepatology **19**(5): 1321-4.

Simpson, K. J., N. W. Lukacs, et al. (1997). "Cytokines and the liver." J Hepatol **27**(6): 1120-32.

Skobe, M., T. Hawighorst, et al. (2001). "Induction of tumor lymphangiogenesis by VEGF-C promotes breast cancer metastasis." Nat Med **7**(2): 192-8.

Son, G., T. Hirano, et al. (2006). "Blockage of HGF/c-Met system by gene therapy (adenovirus-mediated NK4 gene) suppresses hepatocellular carcinoma in mice." J Hepatol.

Stacker, S. A., M. E. Baldwin, et al. (2002). "The role of tumor lymphangiogenesis in metastatic spread." Faseb J **16**(9): 922-34.

Stacker, S. A., C. Caesar, et al. (2001). "VEGF-D promotes the metastatic spread of tumor cells via the lymphatics." Nat Med **7**(2): 186-91.

Straume, O. and L. A. Akslen (2003). "Increased expression of VEGF-receptors (FLT-1, KDR, NRP-1) and thrombospondin-1 is associated with glomeruloid microvascular proliferation, an aggressive angiogenic phenotype, in malignant melanoma." Angiogenesis **6**(4): 295-301.

Su, J. L., P. C. Yang, et al. (2006). "The VEGF-C/Flt-4 axis promotes invasion and metastasis of cancer cells." Cancer Cell **9**(3): 209-23.

Su, J. L., C. J. Yen, et al. (2007). "The role of the VEGF-C/VEGFR-3 axis in cancer progression." Br J Cancer **96**(4): 541-545.

Sun, J. J., X. D. Zhou, et al. (1999). "Invasion and metastasis of liver cancer: expression of intercellular adhesion molecule 1." J Cancer Res Clin Oncol **125**(1): 28-34.

Suruki, R., K. Hayashi, et al. (2006). "Alanine aminotransferase level as a predictor of hepatitis C virus-associated hepatocellular carcinoma incidence in a community-based population in Japan." Int J Cancer **119**(1): 192-5.

Swartz, M. A. and M. Skobe (2001). "Lymphatic function, lymphangiogenesis, and cancer metastasis." Microsc Res Tech **55**(2): 92-9.

Takahara, T., K. Furui, et al. (1995). "Increased expression of matrix metalloproteinase-II in experimental liver fibrosis in rats." Hepatology **21**(3): 787-95.

Tanaka, K., J. Kurebayashi, et al. (2002). "Expression of vascular endothelial growth factor family messenger RNA in diseased thyroid tissues." Surg Today **32**(9): 761-8.

Tang, R. F., J. Itakura, et al. (2001). "Overexpression of lymphangiogenic growth factor VEGF-C in human pancreatic cancer." Pancreas **22**(3): 285-92.

Tangkijvanich, P., N. Anukulkarnkusol, et al. (2000). "Clinical characteristics and prognosis of hepatocellular carcinoma: analysis based on serum alpha-fetoprotein levels." J Clin Gastroenterol **31**(4): 302-8.

Terman, B. I., M. E. Carrion, et al. (1991). "Identification of a new endothelial cell growth factor receptor tyrosine kinase." Oncogene **6**(9): 1677-83.

Tian, X., S. Song, et al. (2001). "Vascular endothelial growth factor: acting as an autocrine growth factor for human gastric adenocarcinoma cell MGC803." Biochem Biophys Res Commun **286**(3): 505-12.

Tonini, T., F. Rossi, et al. (2003). "Molecular basis of angiogenesis and cancer." Oncogene **22**(42): 6549-56.

Torimura, T., T. Ueno, et al. (2006). "Gene transfer of kringle 1-5 suppresses tumor development and improves prognosis of mice with hepatocellular carcinoma." Gastroenterology **130**(4): 1301-10.

Tsukuma, H., T. Hiyama, et al. (1993). "Risk factors for hepatocellular carcinoma among patients with chronic liver disease." N Engl J Med **328**(25): 1797-801.

Tsurusaki, T., S. Kanda, et al. (1999). "Vascular endothelial growth factor-C expression in human prostatic carcinoma and its relationship to lymph node metastasis." Br J Cancer **80**(1-2): 309-13.

Ueda, M., Y. Terai, et al. (2001). "Vascular endothelial growth factor C gene expression is closely related to invasion phenotype in gynecological tumor cells." Gynecol Oncol **82**(1): 162-6.

Van Trappen, P. O., A. Ryan, et al. (2002). "A model for co-expression pattern analysis of genes implicated in angiogenesis and tumour cell invasion in cervical cancer." Br J Cancer **87**(5): 537-44.

Wang, J. H., R. G. Batey, et al. (2006). "Role of ethanol in the regulation of hepatic stellate cell function." World J Gastroenterol **12**(43): 6926-32.

Wang, Y., S. H. Lau, et al. (2004). "Characterization of HBV integrants in 14 hepatocellular carcinomas: association of truncated X gene and hepatocellular carcinogenesis." Oncogene **23**(1): 142-8.

Wei, Q. Y., Y. Q. Wu, et al. (2003). "[Expression of matrix metalloproteinases and tissue inhibitors of matrix metalloproteinases in the hepatocellular carcinomas]." Hunan Yi Ke Da Xue Xue Bao **28**(3): 212-6.

Weiler-Normann, C., J. Herkel, et al. (2007). "Mouse models of liver fibrosis." Z Gastroenterol **45**(1): 43-50.

Wen, Y., D. Yu, et al. (2001). "[Expression of VEGF-C and its correlation with cervical lymph nodes metastasis of oral cancers]." Hua Xi Kou Qiang Yi Xue Za Zhi **19**(1): 5-8.

Westermarck, J. and V. M. Kahari (1999). "Regulation of matrix metalloproteinase expression in tumor invasion." Faseb J **13**(8): 781-92.

Wey, J. S., F. Fan, et al. (2005). "Vascular endothelial growth factor receptor-1 promotes migration and invasion in pancreatic carcinoma cell lines." Cancer **104**(2): 427-38.

Wheatley, A. M., N. E. Almond, et al. (1993). "Interpretation of the laser Doppler flow signal from the liver of the rat." Microvasc Res **45**(3): 290-301.

Wheatley, A. M. and D. Zhao (1993). "Intraoperative assessment by laser Doppler flowmetry of hepatic perfusion during orthotopic liver transplantation in the rat." Transplantation **56**(6): 1315-8.

Wong, I. H., W. Y. Lau, et al. (2000). "Quantitative comparison of alpha-fetoprotein and albumin mRNA levels in hepatocellular carcinoma/adenoma, non-tumor

liver and blood: implications in cancer detection and monitoring." Cancer Lett **156**(2): 141-9.

Wong, I. H., W. Y. Lau, et al. (1999). "Hematogenous dissemination of hepatocytes and tumor cells after surgical resection of hepatocellular carcinoma: a quantitative analysis." Clin Cancer Res **5**(12): 4021-7.

Wongcharatrawee, S. and R. J. Groszmann (2000). "Diagnosing portal hypertension." Baillieres Best Pract Res Clin Gastroenterol **14**(6): 881-94.

Yamaguchi, R., H. Yano, et al. (2006). "Expression of vascular endothelial growth factor-C in human hepatocellular carcinoma." J Gastroenterol Hepatol **21**(1 Pt 1): 152-60.

Yancopoulos, G. D., S. Davis, et al. (2000). "Vascular-specific growth factors and blood vessel formation." Nature **407**(6801): 242-8.

Yokoyama, Y., A. Sakamoto, et al. (2003). "A case of adenocarcinoma of the endometrial type mixed with a clear cell component that metastasized to the vagina." Eur J Gynaecol Oncol **24**(5): 435-7.

Yoo, Y. G. and M. O. Lee (2004). "Hepatitis B virus X protein induces expression of Fas ligand gene through enhancing transcriptional activity of early growth response factor." J Biol Chem **279**(35): 36242-9.

Yoo, Y. G., S. H. Oh, et al. (2003). "Hepatitis B virus X protein enhances transcriptional activity of hypoxia-inducible factor-1alpha through activation of mitogen-activated protein kinase pathway." J Biol Chem **278**(40): 39076-84.

Yoon, S. O., S. J. Park, et al. (2002). "Sustained production of H(2)O(2) activates pro-matrix metalloproteinase-2 through receptor tyrosine kinases/phosphatidylinositol 3-kinase/NF-kappa B pathway." J Biol Chem **277**(33): 30271-82.

Yoshiji, H., S. Kuriyama, et al. (2004). "Halting the interaction between vascular endothelial growth factor and its receptors attenuates liver carcinogenesis in mice." Hepatology **39**(6): 1517-24.

Yoshiji, H., S. Kuriyama, et al. (2003). "Vascular endothelial growth factor and receptor interaction is a prerequisite for murine hepatic fibrogenesis." Gut **52**(9): 1347-54.

Yoshiji, H., S. Kuriyama, et al. (2004). "Involvement of the vascular endothelial growth factor receptor-1 in murine hepatocellular carcinoma development." J Hepatol **41**(1): 97-103.

Zhao, J., X. Zhang, et al. (2006). "TIP30 inhibits growth of HCC cell lines and inhibits HCC xenografts in mice in combination with 5-FU." Hepatology **44**(1): 205-15.

Zheng, W. D., L. J. Zhang, et al. (2005). "Expression of matrix metalloproteinase-2 and tissue inhibitor of metalloproteinase-1 in hepatic stellate cells during rat hepatic fibrosis and its intervention by IL-10." World J Gastroenterol **11**(12): 1753-8.

8 Appendix

8.1 Abbreviations

AASLD	American Association for the Study of Liver Diseases
APCs	antigene presenting cells
aFGF	acidic fibroblast growth factor
AFP	alpha-fetoprotein
ALT	alanine transaminase
AU	absorption units
CCL_4	carbon tetrachloride
CRC	colorectal carcinoma
DNA	deoxyribonucleic acid
EASL	European Association for the Study of the Liver
ECM	extra cellular matrix
EGF	epidermal growth factor
EtOH	ethanol
Flk-1	VEGFR-2
Flt-1	VEGFR-1
Flt-4	VEGFR-3
GPT	Glutamat-Pyruvat-Transaminases
HBV	hepatitis B virus
HBx	hepatitis B protein x
HCC	hepatocellular carcinoma
HCS	hepatic stellate cells
HCV	hepatitis C virus
H.E	hematoxylin-eosin
HGF	hepatocytes growth factor
HIF-1	hypoxia inducible factor-1
HM	hepatic microcirculation
HPF	high power field

ICAM-1	intracellular adhesion molecule-1
IGF-2	insulin-like growth factor-2
IHVR	intrahepatic vascular resistence
ILCA	International Liver Cancer Accsosiation
KDR	VEGFR2
MMP	metalloproteinase
MMP-2	metalloproteinase-2
MMP-9	metalloproteinase-9
MMP-7	metalloproteinase-7
MMP-26	metalloproteinase-26
MT1-MMP	membrane-type metalloprotease1
MT-MMP	membrane-type metalloprotease
NIH	National Institutes of Health
ORF	open reading frame
PCR	polymerase chain reaction
PHT	portal hypertension
RNA	ribonucleic acid
SD	standard division
SEM	standard error of mean
s.c.	subcutaneous
TAA	thioacetamide
TGF-β	transforming growth factor-β
TNF	tumor necrosis factor
TNF-α	tumor necrosis factor-α
TIMP	tissue inhibitor of metalloproteinases
TIMP-2	tissue inhibitor of metalloproteinases-2
TRAIL	TNF-related apoptosis-induced ligand
VEGF	vascular endothelial growth factor

VEGF-A	vascular endothelial growth factor-A
VEGF-B	vascular endothelial growth factor-B
VEGF-C	vascular endothelial growth factor-C
VEGF-D	vascular endothelial growth factor-D
VEGF-E	vascular endothelial growth factor-E
VEGFR	vascular endothelial growth factor receptor
VEGFR-1	vascular endothelial growth factor receptor-1
VEGFR-2	vascular endothelial growth factor receptor-2
VEGFR-3	vascular endothelial growth factor receptor-3
VPF	vascular permeability factor
WHO	World Health Organization

8.2 Curriculum vitae

<u>Miroslaw</u> Theodor Kornek

Personal Data

Date of birth:	[redacted]
Place of birth:	[redacted]
Nationality:	German
Marital status:	married
Address:	[redacted]
E-mail:	[redacted]

Education

1982-1986	Staat. Kat. Grundschule Köln Seeberg (Primary School)
1986-1992	Realschule Karl-Marx-Allee Köln Seeberg (Secondary School)
1992-1996	Norbert-Gymnasium Knechtsteden
1997-2003	Biology study at the University of Cologne
2002-2003	Institute of Biochemistry II, University of Cologne Medical Faculty Thesis: "Klonierung und Charakterisierung der RICH1/NADRIN-PACSIN" (The cloning and characterization of the RICH1/NADRIN-PACSIN interaction) Supervisor: Dr. rer. nat. M. Plomann
Since 2004	Department of Internal Medicine I, University Hospital Bonn Supervisor: PD Dr. med. V. Schmitz

Additional non-educational activities

1996-1997	10 month army duty plus 2 month voluntarily extension (Wehrübung),
StKp	Fm/EloAufklBrig 94, Daun
Since 2007	EASL (European Association for the Study of the Liver) trainee member
Since 2007	ILCA (International Liver Cancer Association) trainee member

8.3 Publications which are a part of this thesis

Kornek M, Raskopf E, Guetgemann I, Ocker M, Gerceker S, Gonzalez-Carmona MA, Rabe C, Sauerbruch T, Schmitz V. Combination of systemic thioacetamide (TAA) injections and ethanol feeding accelerates hepatic fibrosis in C3H/He mice and is associated with intrahepatic up regulation of MMP-2, VEGF and ICAM-1. J Hepatol 2006;45:370-6.

Kornek M, Raskopf E, Tolba R, Becker U, Berger D, Klöckner M, Sauerbruch T, Schmitz V. Accelerated orthotopic HCC growth is linked with increased transcription of pro-angiogenic and pro-metastatic factors in murine liver fibrosis (in Review, Liver International 2007).

8.4 First Author posters which are connected to this thesis

Kornek M, Raskopf E, Tolba R, Sauerbruch T, Schmitz V. Accelerated orthotopic HCC growth is linked with increased pro-angiogeneic and pro-metastatic factors in murine liver fibrosis (P 1070, AASLD2007).

Kornek M, Raskopf E, Tolba R, Sauerbruch T, Schmitz V. Experimental orthotopic HCC growth is accelerated in hepatic fibrosis. (P003, ILCA 2007) ***This poster has been selected as a TOP SCORED POSTER.***

Kornek M, Raskopf E, Tolba R, Sauerbruch T, Schmitz V. Experimental orthotopic HCC growth is accelerated in hepatic fibrosis (P1310, EASL2007). ***This poster has been granted with a full bursary in order to attend the annual meeting.***

Kornek M, Raskopf E, Tolba R, Gonzalez-Carmona MA, Rabe C, Sauerbruch T, Schmitz V. Hämodynamische Auswirkung im TAA/EtOH induziertem

murinem Fibrosemodell (P241, DGVS 2006). Zeitschrift für Gastroenterologie; 2006; 08.

Kornek M, Raskopf E, Guetgemann I, Gonzalez-Carmona MA, Rabe C, Knolle PA, Sauerbruch T, Schmitz V. Systemic thioacetamide (TAA) and ethanol injections accelerate hepatic fibrosis in C3H/He mice (P291, AASLD 2005). Hepatology 2005;42:299A-401A.

Kornek M, Raskopf E., Gonzalez-Carmona M., Gütgemann I., Rabe C., Sauerbruch T., Schmitz V. Thioacetamid und Alkohol zur Fibroseinduktion in der C3H Maus (P228, DGVS 2005). Zeitschrift für Gastroenterologie; 2005; 05.

ELSEVIER

Journal of Hepatology 45 (2006) 370–376

Journal of Hepatology

www.elsevier.com/locate/jhep

Combination of systemic thioacetamide (TAA) injections and ethanol feeding accelerates hepatic fibrosis in C3H/He mice and is associated with intrahepatic up regulation of MMP-2, VEGF and ICAM-1

Miroslaw Kornek[1], Esther Raskopf[1], Ines Guetgemann[3], Matthias Ocker[2], Sevil Gerceker[1], Maria A. Gonzalez-Carmona[1], Christian Rabe[1], Tilman Sauerbruch[1], Volker Schmitz[1,*]

[1]*Department of Internal Medicine I, University Hospital Bonn, Germany*
[2]*Department of Medicine I, Friedrich-Alexander-University Erlangen-Nuernberg, Germany*
[3]*Institute of Pathology, University of Bonn, Germany*

***Background/Aims*: The induction of liver fibrosis is difficult in mice. Here, we intended to improve fibrosis induction by combination of thioacetamide (TAA) injections and ethanol (EtOH) feeding and to characterize features of liver damage in this model. Most experimental therapeutic studies are performed in mice without pre-damaged livers.**

***Methods*: C3H mice were injected three times/week (0.15 mg/g body weight) and fed with EtOH. Tissue and serum samples were collected and analysed.**

***Results*: Portal fibrosis was verified by van Gieson staining showing a mild fibrosis (score F2) in TAA-treated mice and liver fibrosis (score F4) in the combination group using TAA/EtOH. Consonant with the histological results, the fibrosis marker MMP-2 and alpha 1 procollagen (I) were elevated at week 10 and 15 after treatment initiation in the combination group, whereas tissue protective proteinase, TIMP-1, was 18.5-fold increased only at week 10 but normalized until week 15. Fibrosis development was associated with elevated ICAM-1 expression.**

***Conclusions*: Taken together, TAA/EtOH application was suitable to induce liver fibrosis characterized by typical biomarkers in C3H/He.**

***Keywords*: Fibrosis; MMP-2; VEGF; Thioacetamide; ICAM-1**

1. Introduction

Liver cirrhosis is considered to be a pre-malignant condition and is mostly caused by chronic viral, toxic, autoimmune or cholestatic liver injury. Alcohol abuse and HCV infection are the most prominent causes of liver cirrhosis in Europe and North America [1,2]. The vast majority of hepatocellular carcinomas (HCC) develop in patients suffering from liver fibrosis. Experimental therapy studies are regularly performed in mice that bear subcutaneous or orthotopic hepatomas but are non-cirrhotic [3–6]. Therefore we intended to establish a fibrotic C3H/He mouse model for future application to antitumor studies in an orthotopic syngenic hepatoma implantation model. Carbon tetrachloride (CCl_4) is the most common agent to cause liver damage and induce liver fibrosis, however, application to C3H mice was associated with an intolerable high mortality rate of 60% [7]. We intended to induce fibrosis by thioacetamide (TAA) injections or combination with EtOH feeding. Liver fibrosis can be

Received 13 September 2005; received in revised form 21 February 2006; accepted 17 March 2006; available online 3 May 2006

* Corresponding author. Tel.: +49 228 2876469; fax: +49 228 2874698.

E-mail address: volker.schmitz@ukb.uni-bonn.de (V. Schmitz).

Abbreviations: TAA, thioacetamide; EtOH, ethanol; HPF, high power fields; wk, week; i.p., intraperitoneal; vWF, von-Willebrand factor; CCL_4, carbon tetrachloride.

0168-8278/$32.00
doi:10.1016/j.jhep.2006.03.017

characterized by several bio-markers which are – among others – MMP-2, alpha 1 procollagen (I), TIMP-1 and ICAM. MMP-2 had been demonstrated to be increased in experimental fibrotic livers in rats and can functionally be inhibited by TIMP-1 (tissue inhibitor of matrix metalloproteinases-1) [8,9]. Furtherly, it has been shown that fibrosis is correlated with elevated VEGF levels in experimental studies. VEGF also has a prominent role in the sinusoidal capillarisation of the liver [10,11] and induces up regulation of ICAM [12].

Here, we show that induction of hepatic fibrosis can be accelerated by combination of TAA together with EtOH feeding in C3H mice. Liver fibrosis was characterized by typical bio-markers indicating suitability of this novel fibrosis model for potential use as fibrotic tumor implantation model in future studies.

2. Materials and methods

2.1. Animals

C3H/He mice were obtained from Charles River and housed under standard conditions in the animal facility of the Institute of Molecular Medicine and Experimental Immunology (IMMEI) at the University Hospital of Bonn. Animal procedures were performed in accordance with approved protocols and followed recommendations for proper care and use of laboratory animals.

2.2. Administration of TAA (thioacetamide) and ethanol (EtOH)

Induction of fibrosis was studied in C3H/He mice using either i.p. injections of TAA (Sigma–Aldrich; 0.15 mg/g body weight) three times per week for 15 weeks alone ($n = 12$) or combination of TAA with alcohol feeding in sweetened drinking water, always freshly prepared (10% v/v, $n = 21$).

2.3. Alanine transaminase (aminotransferase) (ALT) assay

Blood serum levels of ALT activity were measured using the GPTransaminase kit (Roche Diagnostics, Germany) according to the manufacturer's instructions.

2.4. Histology

Paraffin liver sections were treated with proteinase K (DAKO, Glostrup, Denmark) for 10 min at room temperature. Samples were then blocked with 5% pig serum in PBS, followed by incubation with rabbit anti-von Willebrand factor (factor VIII-related antigen, 1:1500, DAKO) for 60 min at RT. Endogenous peroxidase activity was quenched by H_2O_2-treatment (DAKO) for 10 min. After washing with PBS, sections were incubated with a secondary antibody dilution of biotinylated pig anti-rabbit immunoglobin G (1:300) and streptavidin conjugated to horseradish peroxidase (DAKO). Sections were visualized by using the Dako ChemMate™ detection kit and counter-stained with hematoxylin (DAKO). Areas presenting highest vascularization were identified and blood vessels were counted in high power fields (HPF, 40× magnification), 5 HPF were evaluated in each section.

To determine ICAM-1 expression, cryopreserved liver sample sections were immune-stained with rat anti-mouse ICAM-1 (CD54) (1:50, BD Pharmingen, Germany) and incubated with a biotinylated anti-Armenian and Syrian hamster IgG antibody cocktail (BD Pharmingen, Germany, Germany) and streptavidin peroxidase. Enzymatic activity was developed using AEC (Dako, Hamburg, Germany) as substrate and sections were counter-stained with Mayer's hematoxylin.

For hematoxylin–eosin (HE) and van Gieson staining, 4% formaldehyde-fixed liver samples were paraffin embedded and sections of 5 μm thickness were stained according to standard procedures. Fibrosis was assessed according to the fibrosis proposed by Ishak et al. [13].

2.5. ELISA tests for MMP-2, TIMP-1, ICAM-1 and VEGF

Liver damage and fibrosis induction were characterized in the TAA/EtOH group by determination of ALT, VEGF-, ICAM-, TIMP-1 and MMP-2 concentrations, respectively, in liver samples at week 5, 10 and 15. To extract protein, liver tissue samples were homogenized in 500 μl PBS with proteinase inhibitor (Complete Mini, Roche Applied Sciences, Mannheim). Separated cells were broken up by repeated freeze–thaw cycles and debris was pelleted by centrifugation. Protein concentrations were determined using the Bio-Rad DC Protein Assay kit (Bio-Rad, Munich, Germany) according to the manufacturer's protocol. Ten microgram of protein was used in each test (VEGF-, MMP-2-, ICAM-ELISA Quantikine murine VEGF ELISA, Quantikine murine sICAM ELISA, Quantikine human/murine MMP-2 ELISA, R&D Systems, Wiesbaden-Nordenstadt).

2.6. Preparation of RNA, cDNA and quantitative real-time PCR

RNA from liver tissue samples of TAA/EtOH treated or control mice was isolated by using the GenElute Total Mammalian RNA Kit (Sigma, Taufkirchen, Germany) according to the manufacturer's protocol. RNA was then digested with RQ1 DNase (Promega, Mannheim, Germany). RNA concentrations were determined and 1 μg RNA was used in the RT-Reaction with random primers (Promega, Mannheim, Germany) and MMLV-Reverse Transcriptase (Promega, Mannheim, Germany). Transcript levels of the α_1-helix of procollagen I were determined in relation to GAPDH mRNA levels by quantitative real-time PCR (LightCycler, Roche Diagnostics, Mannheim) as described previously [14]. Primers (0.5 μM each) and probes (0.125 μM) were obtained from MWG Biotech (Ebersberg, Germany). Sequences are given in Table 1. PCR was performed with 1.5 μl of template cDNA in a total volume of 15 μl including *Taq* DNA polymerase, dNTP-mix, reaction buffer, and 3 mM $MgCl_2$ (Roche Molecular Biochemicals, Mannheim, Germany) according to the manufacturer's instructions. A precycling step at 95 °C for 10 min for activation of *Taq* DNA polymerase was followed by 45 cycles with a denaturation step at 95 °C for less than 1 s, 15 s annealing at 55 °C, and 15 s extension at 65 °C. A 1:2 to 1:32 dilution series of one sample was used as standard. Data were analysed with the LightCycler software using the proportional second derivative maximum option and normalized to GAPDH levels. Probes were labeled with the reporter dye FAM (carboxy-fluorescein) at the 5′-end and with the quencher molecule TAMRA (carboxy-tetramethylrhodamine) at the 3′-end.

2.7. Statistical analysis

All data are given as means with SEM. Differences between values of independent experimental groups were analysed for statistical significance by unpaired Student's *t*-test. An error level (p) < 0.05 was supposed to indicate significance.

3. Results

3.1. Fibrosis induction

Induction of fibrosis was low in mice that were only exposed to TAA, fibrosis score F2 was reached

Table 1
Primers and probes for quantitative RT-PCR, sequences are given in 5′ → 3′ direction

Target gene	5′-primer	Probe	3′-primer
GAPDH	CCTGCCAAGTATGATGACATCAAGA	TGGTGAAGCAGGCGGCCGAG	GTAGCCCAGGATGCCCTTTAGT
Alpha1 procollagen (I)	TCCGGCTCCTGCTCCTCTTA	TTCTTGGCCATGCGTCAGGAGGG	GTATGCAGCTGACTTCAGGGATGT

15 weeks after initiation. Combination of TAA with EtOH considerably accelerated the development of fibrosis resulting in score F4 (out of max. F6) at week 15, respectively (Fig. 1). Fibrosis induction by TAA alone was associated with a 17% mortality rate but in the combination group receiving TAA and EtOH mortality was increased (38%, Fig. 2). Mortality was almost completely restricted to the first treatment week, whereas all animals that survived the first two weeks had long-term survival. Macroscopically, livers of the TAA and EtOH treated animals were slightly enlarged with an irregular, nodular liver surface (Fig. 2). In cross sections of both treatment groups, the normal radial liver-cell alignment disintegrated. In the combination group a dense mixed infiltrate lymphocytes could be observed around the developing fibrotic septal areas (Fig. 3). van Gieson staining demonstrated continues gain of fibrotic fibers, resulting in portal fibrosis (score F2) in the TAA group and in fibrosis (score F4) in the TAA/EtOH group. Fibrosis was characterized by fibrotic septa, traversing the lobular liver parenchyma by porto–porto bridging resulting in pseudolobuli (Fig. 1). The above-described inflammatory reactions around fibrotic septa (Fig. 3) at week 10 (TAA/EtOH group) were resembled by increased ALT levels of up to 2290 U/L (Fig. 3). After 15 weeks, the ALT values fell back to almost normal levels of control mice (10th week TAA/EtOH: 2290 U/L, 15th week TAA/EtOH: 89 U/L, $p = 0.0136$].

3.2. Blood vessels distribution and VEGF up regulation in the fibrotic liver

To investigate effects on liver angiogenesis, the blood vessel density was quantified using vWF staining. Although the overall number of major blood vessels was not significantly influenced (control 18.6/HPF vs. TAA/EtOH 21.5/HPF at week 15, $p = 0.1338$ Fig. 4), vWF-labeled capillary vessels were increased within fibrotic bridges (Fig. 5). This observation was confirmed by CD31 staining (data not shown).

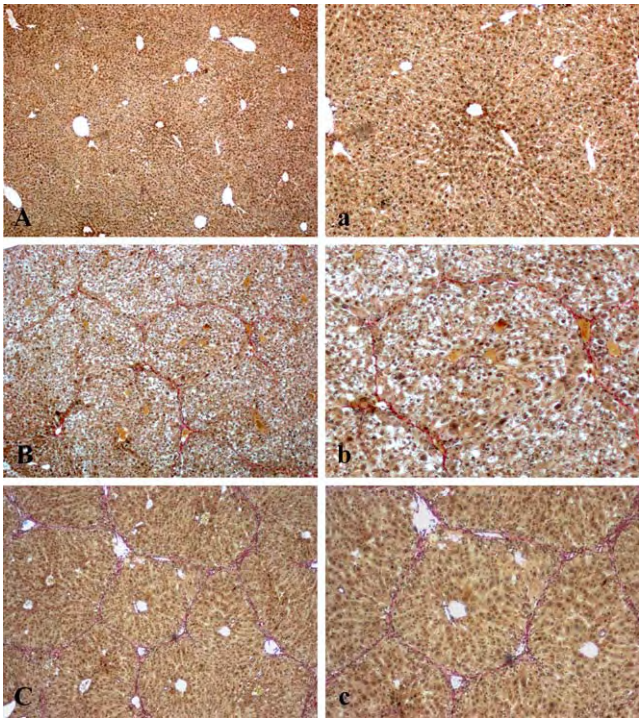

Fig. 1. Progression of liver fibrosis in C3H/He mice. Liver fibrosis was assessed by van Gieson staining at different time points of treatment. Scoring of fibrosis was performed by using the score systems proposed by Ishak et al. [13]: (A/a) Untreated liver, liver-cell alignment (score F0); (B/b) 15th week of TAA i.p. monotreatment, fibrous septa areas were less defined and discontinuous (score F2); (C/c) 15th week of TAA i.p. and EtOH feeding, obvious pseudolobuli appearance and liver parenchyma regeneration (score F4). Original magnification 40× (A–C) or 64× (a–c).

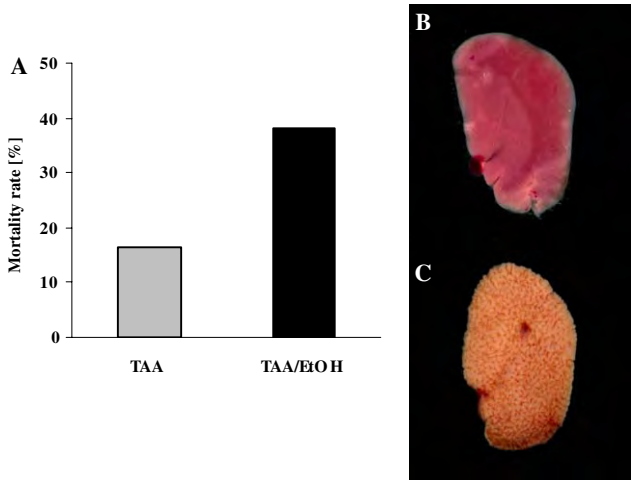

Fig. 2. Mortality rate in C3H/He mice. Mice received TAA i.p. alone or TAA/EtOH combination to induce fibrosis (A) and live morphology comparing livers of TAA/EtOH or control mice (B and C): (A) 17% vs. 38% animals died in the TAA i.p. vs. TAA/EtOH treatment group, within 2 weeks; (B) liver lobe of a control mouse; (C) liver lobe of TAA/EtOH mouse after 15 weeks showed a micronodular organ surface.

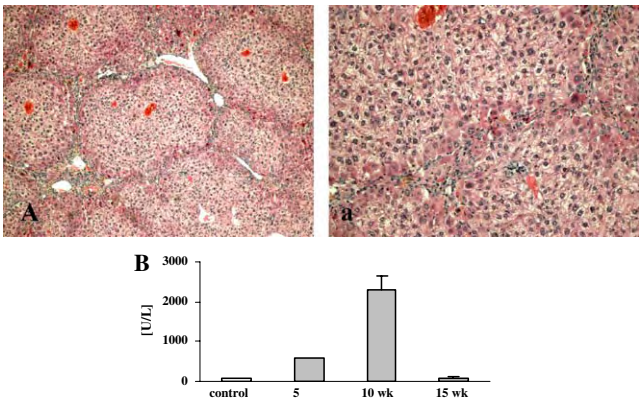

Fig. 3. Hematoxylin–eosin staining confirmed the morphological liver structure changes (A/a). ALT values evaluation during fibrosis development in TAA/EtOH treated C3H/He mice (B): (A/a) 10th week: normal radial liver-cell alignment disappeared and a strong inflammation was observed around the developing fibrotic septa areas; (B) ALT levels were up to 2290 U/L during the 10th week (week), which fell back to almost normal levels in control mice after 15 week. Original magnification 40× (A) and 64×(a).

Interestingly, fibrosis induction was associated with hepatic VEGF up regulation on protein level in TAA + EtOH treated mice (261 pg/mL, 10th week TAA/EtOH: 483 pg/mL, $p = 0.0015$, Fig. 4).

3.3. ICAM, MMP-2, TIMP-1 and procollagen I expression in cirrhotic livers

Elevated hepatic ICAM-1 values were detected on protein level (ICAM-1 ELISA) in homogenized fibrotic liver samples at different time points compared to control mice. Being up to 3.5-fold higher in cirrhotic mice after 15th week of treatment (score F4) as compared to control mice (score F0). We also monitored increased liver ICAM-1 levels that correlated to fibrosis induction (control 12.24 ng/mL, 15th week TAA/EtOH 43.28 ng/mL, $p = 0.0044$; Fig. 6A). To verify the ICAM-1 result anti-ICAM-1 immuno-histochemistry was done in paraffin sections. We observed a denser liver ICAM-1 staining in fibrotic liver samples (Fig. 5C).

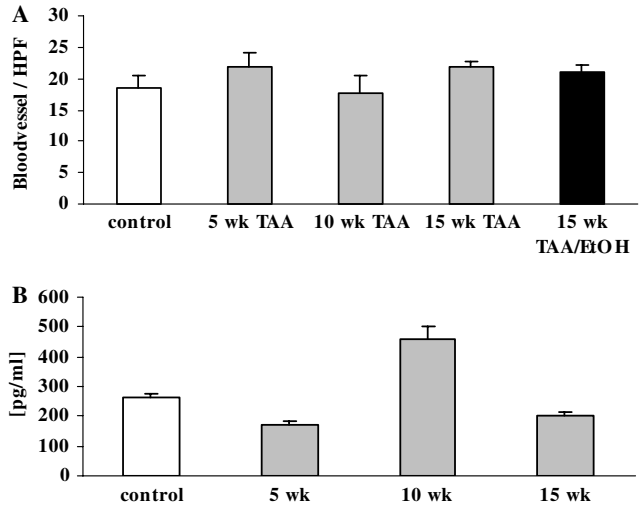

Fig. 4. Hepatic blood vessel density (A) and hepatic VEGF protein levels (B) in untreated C3H/He mice and after TAA/EtOH treatment at week 5, 10 and 15: (A) vWF stained liver sections were divided in high power fields and major blood vessels numbers were analysed (control 18.6/HPF vs. TAA i.p. 21.5/HPF at week 15, $p = 0.1338$); (B) VEGF upregulation on protein level has been monitored during liver fibrosis development at week 10.

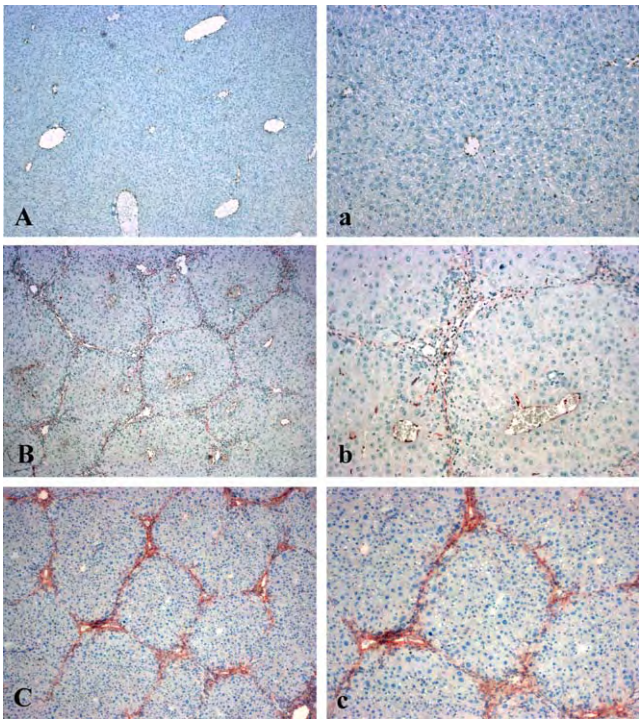

Fig. 5. Hepatic vascular proliferation in C3H/He mice and ICAM-1 expression detected by immunolabeling. Vascular sections were detected by vWF immunolabeling on liver sections (A/a and B/b) and hepatic ICAM expression was detected by anti-ICAM-1 immunolabeling (C/c). (A/a) Untreated liver, vWF expression was restricted to the endothelium of central veins and of portal veins; (B/b) 15th week of TAA i.p and EtOH feeding, vWF-labeled endothelial cells were observed within most of the septa in fibrotic liver samples. (C/c) ICAM-1 was dominantly expressed in fibrotic septa area and not in the liver parenchyma at week 15 (TAA/EtOH). Original magnification 40× (A/B/C) or 100× (a/b/c).

To characterize features of fibrosis induction in this model, we quantified MMP-2 and TIMP-1 showing 2.7-fold increased MMP-2 levels during fibrosis development (control: 9 ng/mL, 15th week TAA/EtOH: 24.5 ng/mL, $p < 0.0001$; Fig. 6A). In contrast to these data, TIMP-1 was only slightly elevated in fibrotic mice stage F4 (control 0.476 ng/mL vs. TAA/EtOH 0.751 ng/mL, $p < 0.0001$ at week 15), while peak levels were seen 10 weeks after treatment initiation (control 0.476 ng/mL vs. TAA/EtOH 8.87 ng/mL, $p < 0.0001$; Fig. 6A). Alpha 1 procollagen (I) was measured in fibrotic livers mRNA transcript levels were 3.9- and 2.2-fold higher at weeks 10 and 15, respectively, in fibrotic mice as compared to untreated controls (Fig. 6B).

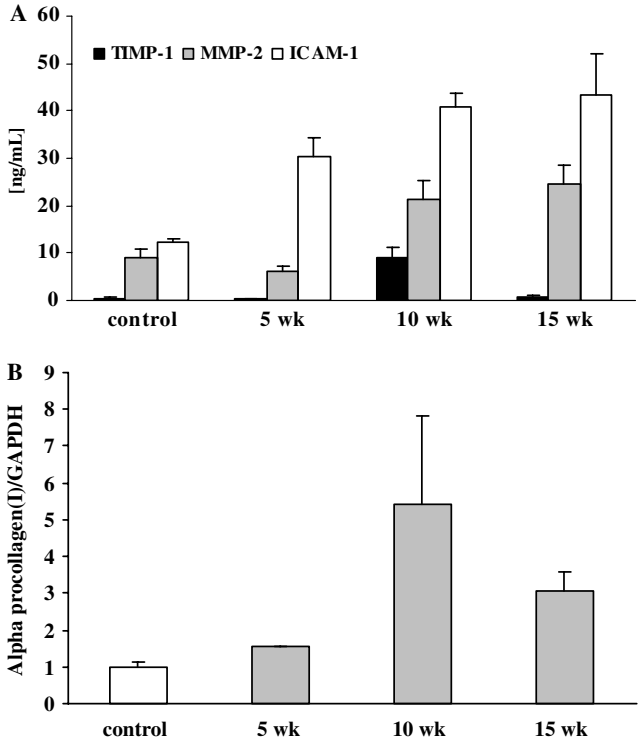

Fig. 6. Hepatic MMP-2, hepatic TIMP-1 and ICAM-1 ELISA results (A), and transcript levels of alpha 1 procollagen (I) were determined relative to GAPDH mRNA levels by quantitative real-time PCR (B), before and after combined TAA/EtOH treatment at week 5, 10 and 15: (A) MMP-2 levels were 2.7-fold increased during fibrosis development. At week 10 we monitored a high peak of TIMP-1 expression, $18\frac{1}{2}$-fold higher than in control mice, otherwise no significant elevation was observed. ICAM values were 3.5-fold higher as compared to control C3H/He mice. Progression of fibrosis was paralleled by increased ICAM values; (B) Alpha 1 procollagen (I) mRNA transcript levels were 3.9- and 2.2-fold higher in fibrotic mice as compared to controls at week 10 and 15.

4. Discussion

Treatment of HCC is challenging and improved animal models are needed to allow testing of innovative therapies. Hepa129 hepatoma cells have been demonstrated to be suitable for orthotopic tumor growth [15] and therapeutic intervention studies in C3H mice [4]. To further improve transferability and relevance of this tumor cell implantation model to the clinic, tumor growth occurring in a pre-damaged fibrotic liver is of interest. For this purpose we intended to improve fibrosis induction, because CCl_4 application is known to be associated with high mortality in this mouse strain [7]. Thus, we tested the fibrotic potential of TAA injections alone and combined with ethanol (EtOH) feeding for fibrosis induction and characterized fibrosis by histology and molecular fibrosis markers.

Although mortality was lower than in the CCl_4 fibrosis models in mice [7], it still was considerably high in the combination group (TAA/EtOH), although the TAA dose for i.p. injection (0.15 mg/g body weight) was lower than in previous publications. Then, TAA was administered at three different dosages of 0.2 mg/g body weight, 0.4 mg/g body weight or 0.6 mg/g body weight twice a week resulting in 30%, 70% or 80% mortality, respectively [16]. Here, we applied TAA 0.15 mg/g body weight three times a week in combination with EtOH inducing 38% mortality. When TAA was injected without additional EtOH feeding mortality was considerably lower (18%), but fibrosis induction was unsatisfactory.

Combination of TAA/EtOH resulted in fibrosis stage F4 after 15 weeks, whereas TAA injection alone was weaker, resulting in mild fibrosis (score F2). Liver fibrosis was characterized by fibrotic expansion of portal areas with marked porto–porto bridging disrupting the liver parenchyma.

Development of liver fibrosis and cirrhosis can be characterized by a large spectrum of bio-markers. Among these, we have chosen MMP-2 and alpha 1 procollagen (I) as two possible markers of fibrosis. Consonant with published data in other models and in man, MMP-2 and alpha 1 procollagen (I) were significantly elevated at fibrosis week 10–15 (F4). A similar observation was done in an experimental rat fibrosis model, showing increased expression levels of alpha 1 procollagen (I) mRNA in advanced fibrosis [17]. The present findings about elevated MMP-2 and alpha 1 procollagen (I) levels are supported by previous publications indicating a correlation between progression of liver fibrosis and progelatinase A and gelatinase A (MMP-2) in a CCL_4 rat liver fibrosis model [8,9,17].

In contrast, the tissue protective proteinase inhibitor TIMP-1 was strongly increased only at week 10. At this time point liver damage was pre-dominated by a dense mixed lymphocytic periportal infiltrate. Presumably, TIMP-1 up regulation was secondary to the inflammatory reaction. Unexpectedly, TIMP-1 concentrations fully normalized until week 15 accomplished by an almost complete disappearance of any inflammatory periportal infiltrate. Collagenase activities were described to initially raise with liver injury and fall with continuous progression to cirrhosis [18–22]. Thus, TIMP-1 possibly bears regulatory functions in collagen degradation and in hepatic fibrosis in our model which corresponds well to observations in human and rat liver fibrosis [23–25].

Corresponding to data about vWF and VEGF [10,11], formation of fibrotic septa was also characterized by increased staining against von Willebrand factor (vWF) along septal areas in this model. Since anti-vWF staining was paralleled by up regulated VEGF expression, it is intriguing to assume that septal angiogenesis, at least partly, was VEGF dependent. Additionally, liver inflammation might have the potency to increase VEGF expression, because VEGF itself is capable to significantly increase alpha procollagen mRNA levels

in activated hepatic stellate cells [26]. Corresponding to this we observed highest alpha 1 procollagen (I)/GAPDH ratio values in the fibrotic liver samples at week 10, which might be partly attributed to elevated VEGF values at this time point.

The interplay between inflammation and angiogenesis affects extracellular matrix and various adhesive interactions on the level of endothelial cells and matrix substances. To this respect, up regulation of ICAM-1 was found in liver biopsies obtained from patients suffering from alcoholic hepatitis and cirrhosis [27–29]. Interestingly, this trait of liver fibrosis was also reflected as shown by a 3.5-fold incline in ICAM-1. ICAM-1 expression is known to be driven by VEGF via nuclear factor-κB activation in endothelial cells [30]. Septal ICAM-1 up regulation strikingly fell in line with septal VEGF up regulation as shown by other groups [10,11]. A similar correlation between fibrosis and ICAM expression had been found in immuno-histochemistry of fibrotic rat livers [31].

In summary we conclude that the potency of TAA alone to induce liver fibrosis was unsatisfactory, whereas the combination of TAA/EtOH resulted in a considerably accelerated fibrosis induction in C3H/He mice. The induction of liver fibrosis using the combination of TAA and EtOH was characterized by typical histological changes, MMP-2, alpha 1 procollagen (I), VEGF and septal ICAM-1 up regulation. Taken together, the established model bears critical aspects of known fibrosis in man and therefore appears suitable to be used for future tumor cell implantation experiments.

Acknowledgements

This work was supported by a Deutsche Krebshilfe grant to V.S. We thank I. Höschler, U. Becker and M. Klöckner for their expert assistance. We also thank Prof. P.A. Knolle, Head of the Institute of Molecular Medicine and Experimental Immunology (IMMEI, Bonn/Germany,) for continuous support of the project.

References

[1] Colombo M. Hepatocellular carcinoma in cirrhotics. Semin Liver Dis 1993;13:374–383.
[2] Friedman SL. Molecular regulation of hepatic fibrosis, an integrated cellular response to tissue injury. J Biol Chem 2000;275:2247–2250.
[3] Schmitz V, Wang L, Barajas M, Gomar C, Prieto J, Qian C. Treatment of colorectal and hepatocellular carcinomas by adenoviral mediated gene transfer of endostatin and angiostatin-like molecule in mice. Gut 2004;53:561–567.
[4] Raskopf E, Dzienisowicz C, Hilbert T, Rabe C, Leifeld L, Wernert N, et al. Effective angiostatic treatment in a murine metastatic and orthotopic hepatoma model. Hepatology 2005;41:1233–1240.
[5] Li L, Huang JL, Liu QC, Wu PH, Liu RY, Zeng YX, et al. Endostatin gene therapy for liver cancer by a recombinant adenovirus delivery. World J Gastroenterol 2004;10:1867–1871.
[6] Hong SY, Lee MH, Kim KS, Jung HC, Roh JK, Hyung WJ, et al. Adeno-associated virus mediated endostatin gene therapy in combination with topoisomerase inhibitor effectively controls liver tumor in mouse model. World J Gastroenterol 2004;10:1191–1197.
[7] Hillebrandt S, Goos C, Matern S, Lammert F. Genome-wide analysis of hepatic fibrosis in inbred mice identifies the susceptibility locus Hfib1 on chromosome 15. Gastroenterology 2002;123:2041–2051.
[8] Takahara T, Furui K, Funaki J, Nakayama Y, Itoh H, Miyabayashi C, et al. Increased expression of matrix metalloproteinase-II in experimental liver fibrosis in rats. Hepatology 1995;21:787–795.
[9] Zheng WD, Zhang LJ, Shi MN, Chen ZX, Chen YX, Huang YH, et al. Expression of matrix metalloproteinase-2 and tissue inhibitor of metalloproteinase-1 in hepatic stellate cells during rat hepatic fibrosis and its intervention by IL-10. World J Gastroenterol 2005;11:1753–1758.
[10] Corpechot C, Barbu V, Wendum D, Kinnman N, Rey C, Poupon R, et al. Hypoxia-induced VEGF and collagen I expressions are associated with angiogenesis and fibrogenesis in experimental cirrhosis. Hepatology 2002;35:1010–1021.
[11] Rosmorduc O, Wendum D, Corpechot C, Galy B, Sebbagh N, Raleigh J, et al. Hepatocellular hypoxia-induced vascular endothelial growth factor expression and angiogenesis in experimental biliary cirrhosis. Am J Pathol 1999;155:1065–1073.
[12] Radisavljevic Z, Avraham H, Avraham S. Vascular endothelial growth factor up-regulates ICAM-1 expression via the phosphatidylinositol 3 OH-kinase/AKT/Nitric oxide pathway and modulates migration of brain microvascular endothelial cells. J Biol Chem 2000;275:20770–20774.
[13] Ishak K, Baptista A, Bianchi L, Callea F, De Groote J, Gudat F, et al. Histological grading and staging of chronic hepatitis. J Hepatol 1995;22:696–699.
[14] Ocker M, Neureiter D, Lueders M, Zopf S, Ganslmayer M, Hahn EG, et al. Variants of bcl-2 specific siRNA for silencing antiapoptotic bcl-2 in pancreatic cancer. Gut 2005;54:1298–1308.
[15] Schmitz V, Tirado-Ledo L, Tiemann K, Raskopf E, Heinicke T, Ziske C, et al. Establishment of an orthotopic tumour model for hepatocellular carcinoma and non-invasive in vivo tumour imaging by high resolution ultrasound in mice. J Hepatol 2004;40:787–791.
[16] Kuriyama S, Yamazaki M, Mitoro A, Tsujimoto T, Kikukawa M, Tsujinoue H, et al. Hepatocellular carcinoma in an orthotopic mouse model metastasizes intrahepatically in cirrhotic but not in normal liver. Int J Cancer 1999;80:471–476.
[17] Du W, Zhang Y, Zhai W. A study on type I, III and IV collagen production in CCl_4 induced rat liver fibrosis. Zhonghua Bing Li Xue Za Zhi 1997;26:74–77.
[18] Perez-Tamayo R, Montfort I, Gonzalez E. Collagenolytic activity in experimental cirrhosis of the liver. Exp Mol Pathol 1987;47:300–308.
[19] Maruyama K, Feinman L, Fainsilber Z, Nakano M, Okazaki I, Lieber CS. Mammalian collagenase increases in early alcoholic liver disease and decreases with cirrhosis. Life Sci 1982;30:1379–1384.
[20] Carter EA, McCarron MJ, Alpert E, Isselbacher KJ. Lysyl oxidase and collagenase in experimental acute and chronic liver injury. Gastroenterology 1982;82:526–534.
[21] Montfort I, Perez-Tamayo R, Alvizouri AM, Tello E. Collagenase of hepatocytes and sinusoidal liver cells in the reversibility of experimental cirrhosis of the liver. Virchows Arch B Cell Pathol Incl Mol Pathol 1990;59:281–289.
[22] Murawaki Y, Yamada S, Koda M, Hirayama C. Collagenase and collagenolytic cathepsin in normal and fibrotic rat liver. J Biochem (Tokyo) 1990;108:241–244.

[23] Benyon RC, Iredale JP, Goddard S, Winwood PJ, Arthur MJ. Expression of tissue inhibitor of metalloproteinases 1 and 2 is increased in fibrotic human liver. Gastroenterology 1996;110:821–831.

[24] Iredale JP, Benyon RC, Arthur MJ, Ferris WF, Alcolado R, Winwood PJ, et al. Tissue inhibitor of metalloproteinase-1 messenger RNA expression is enhanced relative to interstitial collagenase messenger RNA in experimental liver injury and fibrosis. Hepatology 1996;24:176–184.

[25] Iredale JP, Goddard S, Murphy G, Benyon RC, Arthur MJ. Tissue inhibitor of metalloproteinase-I and interstitial collagenase expression in autoimmune chronic active hepatitis and activated human hepatic lipocytes. Clin Sci (Lond) 1995;89:75–81.

[26] Yoshiji H, Kuriyama S, Yoshii J, Ikenaka Y, Noguchi R, Hicklin DJ, et al. Vascular endothelial growth factor and receptor interaction is a prerequisite for murine hepatic fibrogenesis. Gut 2003;52:1347–1354.

[27] Gimbrone Jr MA. Vascular endothelium: an integrator of pathophysiologic stimuli in atherosclerosis. Am J Cardiol 1995;75:67B–70B.

[28] Gimbrone Jr MA, Nagel T, Topper JN. Biomechanical activation: an emerging paradigm in endothelial adhesion biology. J Clin Invest 1997;99:1809–1813.

[29] Sacanella E, Estruch R. The effect of alcohol consumption on endothelial adhesion molecule expression. Addict Biol 2003;8:371–378.

[30] Kim I, Moon SO, Kim SH, Kim HJ, Koh YS, Koh GY. Vascular endothelial growth factor expression of intercellular adhesion molecule 1 (ICAM-1), vascular cell adhesion molecule 1 (VCAM-1), and E-selectin through nuclear factor-kappa B activation in endothelial cells. J Biol Chem 2001;276 :7614–7620.

[31] Lu L, Zeng M, Fan J, Li J, Liu Y, Ren W, Dai N. Intercellular adhesion molecule-1 expression in experimental liver fibrosis. Zhonghua Nei Ke Za Zhi 1999;38:37–39.